University of Alberta

Stochastic and deterministic models of cellular p53 regulation and drug response

by

Gerald Brendan Leenders

A thesis submitted to the Faculty of Graduate Studies and Research
in partial fulfillment of the requirements for the degree of

Master of Science

Department of Physics

Fall 2012
Edmonton, Alberta

Abstract

The protein p53 is a key regulator of cellular response to a wide variety of stresses. In cancerous cells inhibitory regulators of the p53 protein such as MDM2 and MDMX are often overexpressed. *In silico* techniques could be used to inform the selection of interactions to target with novel drug molecules to make the drug development process more efficient. This work furthers these efforts in two ways. Firstly by investigating some of the roles of stochasticity in determining system behavior, and secondly by developing a model of p53 MDM2 and MDMX interactions and attempting to use it to predict the best targets for future drugs. Stochasticity is shown to be able to effect system behavior profoundly, with implications for future work in both theory and experiment. Lack of experimental data is found to limit the effectiveness of attempts to theoretically determine good drug targets.

Acknowledgements
I would like to thank my supervisor, Dr. Jack Tuszynski for his advice throughout the project, Marion Poirel for her assistance with the deterministic ARF model, Brian Dupuis for his advice on statistics and programing in R, and my group members who provided advice and support throughout.

Table of contents

1 Introduction	1
2 Background	2
2.1 Cell Cycle	2
2.2 p53	2
2.3 MDM2	2
2.4 MDMX	3
2.5 Upstream regulators	3
2.6 Other feedbacks	4
2.7 Oscillations?	4
2.8 Previous modeling work	4
3 A model with ARF	7
3.1 Goals and modeling considerations	7
3.2 Model description	7
3.3 Stochastic simulation	11
3.4 Desynchronization in general	13
3.5 Desynchronization in the ARF model	14
3.6 Changes from nonlinear effects	17
3.7 Excursions from the mean	19
4 A model with MDMX	23
4.1 Goals and modeling considerations	23
4.2 Description of the model with MDMX	23
4.3 Limitations and approximations	28
4.4 Fitting parameters	28
4.5 Oscillations	31
4.6 Parameter sensitivity	33
4.7 Drugged models	35
5 Concluding remarks	38
5.1 Stochasticity	38
5.2 Modeling drug response	38
Bibliography	40
Appendix A: Reactions and chemicals in drugged models	44
Appendix B: Plots of drug effects on various cell models	56

List of tables

2.1 Key features of various models of p53 behavior.	6
3.1 Parameters used in the model with ARF.	9
3.2 Bifurcation points in the deterministic model with ARF.	10
3.3 Comparisons of the parameters found when fitting the deterministic model's p53 levels to the function $f(t) = a_0 + a_1\sin(\omega t + \varphi_1) + a_2\sin(2\omega t + \varphi_2)$ and the stochastic model's p53 levels to the function $f(t) = a_0 + e^{-\frac{\alpha^2 t}{2}}a_1\sin(\omega t + \varphi_1) + e^{-\frac{4\alpha^2 t}{2}}a_2\sin(2\omega t + \varphi_2)$.	15
3.4 Comparisons of the parameters found when fitting the deterministic model's nuclear MDM2 levels to the function $f(t) = a_0 + a_1\sin(\omega t + \varphi_1) + a_2\sin(2\omega t + \varphi_2)$ and the stochastic model's nuclear MDM2 levels to the function $f(t) = a_0 + e^{-\frac{\alpha^2 t}{2}}a_1\sin(\omega t + \varphi_1) + e^{-\frac{4\alpha^2 t}{2}}a_2\sin(2\omega t + \varphi_2)$.	16
4.1: List of chemical species used in the model with MDMX.	25
4.2 List of reactions and the constants used for them in the model with MDMX.	25
4.3 Parameters from the best of the evolutionary algorithm runs.	31
4.4 Percent change in average nuclear p53 levels in response to changes in parameters.	34
A.1 Chemical species added in the MDM2 MDMX dual inhibitor model.	44
A.2 Additional reactions needed in the MDM2/MDMX dual inhibitor model.	44
A.3 Chemical species added in the MDMX inhibitor model.	48
A.4 Additional reactions needed in the MDMX inhibitor model.	49
A.5 Chemical species added in the MDM2 inhibitor model.	51
A.6 Additional reactions needed in the MDM2 inhibitor model.	51
A.7 Chemical species added in the MDMX MDM2 interaction inhibitor model.	53
A.8 Additional reactions needed in the MDMX MDM2 interaction inhibitor model.	54

List of figures

2.1 Relationships between MDMX, MDM2, and p53	3
3.1 A schematic of the model of p53 including MDM2 sequestration by ARF.	8
3.2 p53 and MDM2 oscillating in the ARF model.	10
3.3 Examples of time courses in the stochastic model.	12
3.4 A comparison of the stochastic and deterministic models.	13
3.5 Comparison of the mean of 5000 runs of the stochastic model with the deterministic model.	14
3.6 A: Comparison of p53 levels in the deterministic model to a curve fitted to it from the function $f(t) = a_0 + a_1\sin(\omega t + \varphi_1) + a_2\sin(2\omega t + \varphi_2)$. B: Comparison of p53 levels in the stochastic model to a curve fitted to it from the function $f(t) = a_0 + e^{-\frac{\alpha^2 t}{2}}a_1\sin(\omega t + \varphi_1) + e^{-\frac{4\alpha^2 t}{2}}a_2\sin(2\omega t + \varphi_2)$.	16
3.7 Comparison of nuclear MDM2 levels in the stochastic model to a curve fitted to it from the function $f(t) = a_0 + e^{-\frac{\alpha^2 t}{2}}a_1\sin(\omega t + \varphi_1) + e^{-\frac{4\alpha^2 t}{2}}a_2\sin(2\omega t + \varphi_2)$.	17
3.8 A comparison of the function $\frac{[p53]^{1.8}}{K_d^{1.8}+[p53]^{1.8}}$ between the function applied to mean p53 values and the mean of the function when applied to the distribution of p53 values.	18
3.9 Comparison of stochastic and deterministic models when p53 production is near the lower bifurcation point.	19
3.10 Comparison of stochastic and deterministic models when p53 production is near the upper bifurcation point.	19
3.11 Comparison of stochastic and deterministic models when p53 production is past the upper bifurcation point.	20
3.12 Comparison of the function $\frac{[p53]^{1.8}}{K_d^{1.8}+[p53]^{1.8}}$ between the function applied to mean p53 values in black and the mean of the function when applied to the distribution of p53 values in red.	21
3.13 Examples of individual stochastic realizations when p53 production is past the upper bifurcation point.	22
4.1 Visual representation of the model with MDMX.	24
4.2 Total number of proteins in the cell.	29
4.3 Total number of proteins in the nucleus.	30
4.4 Extended graph of cytoplasmic protein quantity.	32
4.5 Extended graph of nuclear protein quantity.	33
4.6 Behaviour of drugged cells.	36
4.7 Response of cells with 10 times over expressed MDMX to hypothetical drugs.	37
B.1 Behaviour of all models of drugged cells.	56

Definitions

Apoptosis: Apoptosis is a program of cell death that allows a cell to die without damaging surrounding tissue.

Cryptic localization signal: A cryptic localization signal is a localization signal that does not work until some for of precondition is met which changes the state of the protein that has it. For example a protein with a cryptic nuclear localization signal may not be localized to the nucleus unless it is bound to another protein that causes its conformation to change.

Dimer: A dimer is a complex formed by the binding of two similar proteins or chemicals.

Heterozygous: An organism is heterozygous for a genetic variant if one copy of its chromosomes possesses the variant but the other copy does not.

Homozygous: An organism is homozygous for a genetic variant if both copies of its chromosomes possess the variant.

Immunoprecipitation: Immunoprecipitation is a method for using an antibody to get a protein to precipitate out of a solution.

Intron: A section of DNA which encodes information about when the cell should transcribe subsequent stretches of DNA.

Localization signal: A localization signal is a structure on a protein that lets the cell know that it should be moved to a specific location. For example it may flag the protein for import into the nucleus.

mRNA: mRNA stands for messenger ribonucleic acid. mRNA is the RNA that carries instructions for protein production from a cell's genes in the nucleus to the cytoplasm to help with protein production.

Polymorphism: There are several definitions of polymorphism. The one used here is that a polymorphism is a common variant of a protein such that some portion of the population will poses the variant form and some people will have the more common form.

Proteasome: The proteasome is a structure in the cell with the primary function of disassembling proteins.

Senescent: A senescent cell is a cell that is alive but no longer able to divide.

siRNA: siRNA stands for small interfering ribonucleic acid. siRNA blocks other RNA from performing its function.

Transcription: Transcription is the process by which a DNA sequence is copied into an RNA sequence.

Translation: Translation is the process by which an RNA sequence is converted into an amino acid sequence to form a protein.

Ubiquitin ligase: A ubiquitin ligase is a protein that attaches ubiquitin to other proteins.

Protein nomenclature

ARF: ARF stands for alternate reading frame. In humans it is also called p14ARF and in mice it is sometimes called p19ARF.

ATM: ATM stands for ataxia telangiectasia mutated.

ATR: ATR stands for ataxia telangiectasia and Rad3-related protein. It is also sometimes called FRP1 which stands for FRAP-related protein 1.

Chk1: Is short for checkpoint kinase 1.

Chk2: Is short for checkpoint kinase 2.

COP1: COP1 stands for constitutive morphogenetic protein 1. COP1 is also known as RFWD2.

cyclin G: Cyclin G is also called CCNG or CCNG1.

MDM2: MDM2 stands for murine double minute 2. Technically the human version is called HDM2, but this is ignored in most publications.

MDMX: MDMX stands for murine double minute X. It is also sometimes called MDM4. The human version would be called HDMX or HDM4, but most publications will use MDMX to refer to ether version.

HBx protein: HBx protein is the X protein from the hepatitis B virus.

p53: p53 is sometimes also called Tp53 or tumoursuppressor p53.

Pirh2: Pirh2 means p53 induced RING-H2 protein.

PP2A phosphatase: PP2A phosphatase is sometimes also called PR65. PP2A is an abbreviation of protein phosphatase 2A.

Ubiquitin: Ubiquitin is a common small protein that is often used by a cell to mark other proteins for degradation by the proteasome.

Wip1: Wip1 is also called PPM1D, which means protein phosphatase 1D.

1 Introduction

The protein p53 responds to a wide variety of forms of genotoxic stress, from radiation[1] to infection by influenza[2]. Indeed it seems that whenever the integrity of a cells genetic code is threatened p53 is there. This tendency has lead many to call p53 the guardian of the genome. When stress is detected by the cell p53 can respond in several different ways depending on the severity and nature of the stress. p53 is post translationally modified in more than 50 different ways to help determine its response[3]. If the damage is minor p53 can induce cell cycle arrest. For more sever damage p53 may permanently block a cells ability to divide, in other words p53 will cause the cell to become senescent. In the worst case p53 may cause a cell to self destruct through apoptosis[4,5]. Given that all of these effects block uncontrolled replication it is not surprising that p53 is commonly mutated in cancerous cells. It has been found that p53 is mutated in approximately 50% of all human tumours[6]. Furthermore proteins that have a part in down regulating p53, such as MDM2 and MDMX, are commonly over expressed in human tumours[7,8]. It has even been demonstrated that restoration of p53 function can result in tumours to regressing *in vivo*[9]. This has naturally resulted in p53 being a prime area of research. At the time of this writing searching for p53 on PubMed returns over 63000 papers. A search for p53 regulation returns over 17000 papers.

With the cost of drug development on the scale of hundreds of millions to billions of dollars and rising, there is good cause to look for any possible improvement to the efficiency and efficacy of the development process[10]. With the ever increasing computing power available to researchers it is becoming ever more practical to attempt to use *in silico* models to improve the development process. One way to do this is to improve the ability of researchers to select appropriate proteins or interactions between proteins as targets for drug development. The purpose of the work presented here is to work towards improved target selection for new drugs. Although a direct attempt at modeling the effects of drugging several different targets is made, much of the research here is of a more basic nature.

Firstly a simple model of p53 oscillations in response to ionizing radiation is presented. Past work with similar models has been focused on demonstrating that oscillations could plausibly be caused by a feedback loop between p53 and a key regulator of p53 called MDM2. The work presented here, in contrast, is focused on an analysis of the effects of stochasticity on the model systems behaviour, and how the behaviour compares to a deterministic realization of the model. Other past work on stochasticity has focused on sources of noise and the contribution of stochastic effects to sorting populations of cells in to one of several possible stable states.

Secondly a more complex deterministic model is developed and parameters for it are fit to experimental data. This model is then used to investigate the potential of targeting various interactions with drug compounds. Unlike most previous models this model includes the protein MDMX. This allows it to be used to compare the possible relative effects of drugs targeting MDM2 and MDMX. Also unlike previous models this model has interacting MDM2, MDMX, and p53 in both the nuclear and cytosolic portions of a simulated cell. Unfortunately, the sparse nature of the experimental data limits the accuracy and effectiveness of this model.

2 Background

2.1 Cell cycle

The protein p53 is a well-known regulator of the cell cycle and cell fate. If all goes well, a cell will normally go through several stages in sequence. In the G1 phase (first gap phase) the cell grows in size to prepare for DNA synthesis. After G1 the cell moves into S phase (synthesis phase), during which new DNA is synthesized. Cells that are not replicating can also leave G1 and enter G0 phase, a state in which they do not grow, and can remain indefinitely. Next comes G2 phase, (second gap phase) where cells grow further and complete their final preparations for mitosis. Mitosis then occurs and the cycle can begin anew[4]. Of course, in practice things can go wrong, and a cell may need to halt its cycle or even self-destruct in a process called apoptosis. Apoptosis may be a desirable outcome of, for example, cancer chemotherapy.

In order to ensure that all is going well during the process of cell division the cell has a number of checkpoints. These checkpoints are conditions that a cell must meet in order to move on in the cell cycle. For example a checkpoint in G1 will ensure that a cell has gained enough size to move into S phase and replicate its DNA. Another checkpoint that occurs in G1 is mediated by the protein p53. When DNA is damaged p53 halts the cell cycle until the damage is repaired. This prevents the cell from trying to duplicate the damaged DNA. When p53 is inactivated this checkpoint no longer functions. A cell attempting to duplicate damaged DNA is likely to accumulate mutations[11].

Simply removing the limitations on a cell imposed by p53 is not enough for it to become cancerous. Mammalian cells do not normally grow on there own, rather they need to detect a variety of growth factors in order to stimulate cell growth and division. Mutations to the cells genetic code may remove these restrictions however. As such as mutations accumulate in a cell lacking functional p53, the probability of a cell becoming cancerous rises[11].

2.2 p53

The p53 tumour suppressor protein is a well-known regulator of cell fate in response to genotoxic stress. p53 responds to many forms of stress including ultraviolet light[12], ionizing radiation[1], hypoxia[13], heat[13], improper cell adhesion[14], ribonucleotide depletion[15], and infection by influenza[2]. Some viral proteins are known to interact with p53, for example hepatitis B virus HBx protein[16] and the large T antigen of simian virus 40[17]. p53 has been demonstrated to induce cell cycle arrest, senescence, and apoptosis, as such p53 levels are tightly regulated by the cell[4,5]. In order to help it execute its various functions p53 is post translationally modified at many sites[18]. p53 transcriptionally regulates numerous other genes, with a pattern that varies depending on the stress it is responding to and the cell type it is in[19]. In addition to its transcriptional activity p53 plays a transcription independent role in apoptosis by binding to several anti-apoptotic proteins[20]. p53 is known to be mutated in approximately 50% of human tumours[6]. In addition to this, in tumours with wild type p53 it is common for p53 to be misregulated. For example, MDM2, a protein which is involved with p53 degradation forming a bound complex, is commonly upregulated in cancer cells[7]. Furthermore, it has been demonstrated that the restoration of p53 function can cause tumours to regress *in vivo*[9].

2.3 MDM2

The protein MDM2 is a key player in the regulation of p53[21] and it has been found that MDM2 is commonly amplified in human cancers[7]. MDM2 has been shown to be an E3 ubiquitin ligase for p53[22]. This means that MDM2 can mark p53 for degradation by the proteasome. As such, amplification of MDM2 leads to reduced p53 levels[23,24]. MDM2 production is also induced by p53, forming a feedback loop[25]. Additionally MDM2 helps to regulate itself by auto-ubiquitination, meaning it marks itself for degradation by the proteasome[26]. MDM2 possess a nuclear localization signal, which is a structure on the protein that lets the cell know to import the

protein into the cell nucleus[27]. MDM2 also has a cryptic nucleolar localization signal, which flags the protein for localization to the nucleolus, but only when MDM2 binding to another molecule changes the conformation of the signalling region[28].

In 2004 several small molecule inhibitors for the p53 MDM2 interaction were discovered[29]. As of 2011 one of these inhibitors, nutlin-3, was in phase 1 clinical trials for retinoblastoma[30]. Nutlin may also have some p53 independent effects, and these may or may not be related to MDM2. It has been shown in some cell lines that MDM2 is upregulated by hypoxia independently of p53[31]. Furthermore it has been shown that Nutlin may radio-sensitize hypoxic cells that are p53 null, although it has a greater effect on cells with wild type p53[32]. Additionally Nutlin has been shown to bind to several anti apoptotic proteins other than MDM2, further complicating any analysis of its effects[33].

2.4 MDMX

Another important regulator of p53 is MDMX, a homolog of MDM2[34,35]. MDMX is commonly over-expressed in tumours, and its upregulation has been shown to promote tumour formation[8]. Unlike MDM2, however, MDMX expression is not induced by DNA damage[34]. MDMX binds to both MDM2[36] and p53[34]. MDMX binding to MDM2 inhibits MDM2 auto-ubiquitination[37]. Furthermore MDM2 ubiquitinates MDMX[38]. The interaction of MDMX and p53 has been shown to inhibit p53 activity[39]. Figure 2.1 outlines the relationships between p53 MDM2 and MDMX. MDMX possesses a cryptic nuclear localization signal[40], so it can only reach the nucleus while bound to other proteins. MDMX is normally located primarily in the cytoplasm[41].

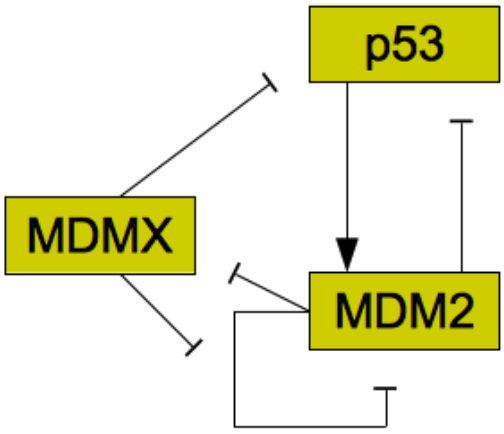

Figure 2.1: Relationships between MDMX, MDM2, and p53. MDM2 inhibits p53 and is promoted by it. MDM2 inhibits itself and this effect is reduced by MDMX. MDMX inhibits p53 directly, and is itself inhibited by MDM2.

Small molecule inhibitors of MDMX have only recently been discovered[42]. Although initial results show some efficacy against cancers with upregulated MDMX in cell culture[43], more work will need to be done to show whether or not they will work *in vivo*, as well as whether or not it is the MDMX interaction or some off target interaction that is causing the effect.

2.5 Upstream regulators

There are many feedback loops known to affect p53 and the behaviour of the p53 system is mediated by a number of upstream regulators[44]. The protein ATM is activated in response to ionizing radiation[45]. Active ATM phosphorylates p53[46] MDM2[47], and Chk2[48]. A related protein ATR also phosphorylates p53 in response to single strand breaks in DNA[49]. Chk2 along with Chk1 phosphorylate p53[50]. These phosphorylations disrupt the ability of MDM2 to affect p53[47,51,52].

2.6 Other feedbacks

There are more feedbacks affecting p53 then just the MDM2 loop, although many of them involve MDM2. The ARF protein is known to bind to MDM2 and promote its degradation[52]. ARF causes both MDM2 and MDMX to be localized to the nucleolus[53,54]. ARF is negatively regulated by p53 in a complex manner, thus forming a feedback loop[55,56]. MDM2 activity gets enhanced by a feedback in which p53 upregulates cyclin G, which then forms a complex with PP2A phosphatase. This complex then dephosphorylates MDM2, removing the inhibition caused by the phosphorylation[44]. The Wip1 protein is induced by p53 and is able to modify ATM and Chk2, deactivating them and thus allowing more interaction between p53 and MDM2[57-59]. Pirh2 has a more direct feedback with p53. Like MDM2 Pirh2 ubiquitinates p53 and is itself upregulated by p53[60]. COP1 is also upregulated by p53 and can ubiquitinate p53[61].

2.7 Oscillations?

G. Lahav et al 2004[62], N. Geva-Zatorsky et al 2006[63] and N. Geva-Zatorsky et al 2010[64] all directly observed sustained oscillations of p53 and MDM2 levels in the nuclei of individual cells. It is worth noting, however, that these single cell studies used MCF-7 cells. MCF-7 cells were initially used to study p53 because they have wild type p53[62]. Unfortunately the MCF-7 cell line has a mutation of an MDM2 intron causing upregulation[65], lack ARF[55], and they possesses amplified MDMX[8]. Because of this, any assumption that any wild type cell would behave similarly to an MCF-7 cell with respect to p53 regulation is questionable at best. Unfortunately, similar single cell studies of non-tumorigenic cell lines cannot be found in the literature at this time. Also of note is the finding in E. Batchelor et al 2011[66] that MCF-7 cells respond differently to damage induced by ultraviolet light than they do to double strand breaks induced by gamma radiation or radiomimetic drugs. N. Geva-Zatorsky et al 2006[63] also point out that undamped oscillations of p53 may appear damped in studies of cell populations due to the individual cells falling out of sync with each other. Damped oscillations have been observed in populations of non tumorigenic cell lines, for example in entire mice[67].

2.8 Previous modeling work

A number of models of p53 response to DNA damage have been proposed in the past. These models are based on a variety of approaches and serve a number of functions. Some basic models use built-in time delays on p53 induction of MDM2 transcription, such as some of the models in N. Geva-Zatorsky et al 2006[63]. In contrast the model presented in Ruth Lev Bar-Or et al 2000[68] used coupled differential equations to create delayed effects. There are advantages and disadvantages to each of these approaches. In a real cell proteins are not produced instantly in response to a promoter. Both transcription and translation take time, and getting the mRNA and the protein to where they need to be does not happen instantaneously ether. An explicit time delay deals with this problem directly, but may be more difficult to analyse then coupled equations. It also adds to the complexity of any program made for stochastic simulations. A set of coupled equations, on the other hand, will start to show effects of induced protein production in the protein levels instantaneously, but the effect will be very small until some time has passed. In a stochastic system the protein levels are quantised and instead of instantaneous effects there is simply a small but non-zero possibility of instantaneous effects. In both the stochastic and deterministic cases adding more steps in the form of more coupled equations makes the system both more realistic and more computationally intensive. In the stochastic model presented in this work there are 3 steps between induced transcription of MDM2 by p53 and the arrival of MDM2 proteins in the cell nucleus. Another factor to consider is that p53 is inducing the transcription of MDM2 mRNA, and that mRNA sticks around for a while. Because of this the actual rate of MDM2 production is dependant on a weighted average of past p53 levels rather that p53 levels at some specific time in the past. Using a single delayed p53 term to describe MDM2 production is therefor problematic. Of course one way around this is to include MDM2 mRNA use a delay term for the production of

the MDM2 mRNA rather than the MDM2 protein, as was done in Xiaodong Cai and Zhi-Min Yuan 2009[69].

L. Ma et al 2005[70] investigated the number of p53 pulses that occur in response to DNA double strand brakes using a model made from three linked modules, simulating DNA repair, ATM activation and the p53 MDM2 feedback loop. Linking together multiple systems like this, in particular linking to systems that can be easily perturbed experimentally, may be a good way to make models that are easy to test.

E. Batchelor et al 2008[71] proposed a model based on abstracted signal and inhibitor systems interacting with MDM2 as well as active and inactive p53. This model was created to investigate the possible effects of ATM, CHK-2 and WIP-1 on p53 behaviour. They included an equation for an input signal that converted p53 from an inactive form to an active form, and a p53 induced inhibitor that reduced the effects of the signal.

There have also been past efforts to look at stochastic models of the p53 regulatory system. Xiaodong Cai and Zhi-Min Yuan 2009[69] model p53 MDM2 and MDMX interactions and analyse some of the effects of intrinsic noise. Their model has MDM2 mRNA being produced with a time delay. It also includes ubiquitinated states of proteins and a deubiquitination term, rather than just assuming all ubiquitinated proteins are degraded. K. Puszynski et al. 2008[72] developed a complex stochastic model of p53 behaviour aimed at showing how stochastic effects lead to variability of cell fate in a bi-stable model. This model includes a cytoplasmic compartment and a nuclear compartment although they do not p53 included in their cytoplasmic compartment. In addition to the negative feedback of MDM2 and p53 they include a positive feedback involving a series of events that lead to MDM2 being sequestered in the cytoplasm where it can no longer degrade p53.

Table 2.1 summarizes some of the key differences between the different models. Ultimately the differences in the models have as much if not more to do with what the researchers were trying to investigate then they do in differing assumptions about p53 behaviour. The stochastic work in Section 3 differs from previous modeling efforts in that its goal is primarily to compare the behaviour of stochastic and deterministic realizations of the same model. This requires only a simple model; therefore much of the complexity of the p53 system can be ignored. The work presented in Section 4 is aimed at comparing the effects of hypothetical inhibitors acting on the p53 regulatory system rather then on exploring the intrinsic behaviours of the system. Since the inhibitors of interest target both MDM2 and MDMX this leads to needing a more complex model that includes both proteins. Furthermore since the available experimental data was a combination of whole cell protein levels and protein levels in the nucleus, it made sense to take the step of making a fully compartmental model. Since it was assumed in this model that reaction kinetics are the same in each compartment this results in a model that looks more complicated then it is, with most reactions being duplicated across the compartments. Since both the models in this work have no intention of addressing DNA repair, or dealing with the problem of variable damage being done nether of them include such systems.

Model	Stochasticity	MDMX	Compartments	Time delayed equations	Stress signal	Other notes
N. Geva-Zatorsky 2006[63]						These models do not have saturable MDM2 production
Model 1	Limited noise	No	No	No	No	Linear Model
Model 2	Limited noise	No	No	No	No	
Model 3	Limited noise	No	No	Yes	No	Linear Model
Model 4	Limited noise	No	No	No	No	
Model 5	Limited noise	No	No	No	No	Linear Model
Model 6	Limited noise	No	No	Yes	Yes	
R. L. Bar-Or et al 2010[68]	None	No	No	No	Yes	Stress is abstract and gets repaired.
L. Ma et al 2005[70]	In the stress and repair modules only	No	No	Yes	Yes	Complex stress and repair modules.
E. Batchelor et al 2008[71]	No	No	No	Yes	Yes	p53 promotes an inhibitor of the stress signal
Xiaodong Cai and Zhi-Min Yuan 2009[69]	Yes	Yes	No	Yes	No	Includes phosphorylated proteins
K. Puszynski et al. 2008[72]	Yes	No	Yes, but not for p53.	No	Yes	Includes many other proteins
Model with ARF	Stochastic and non-stochastic versions were made	No	Only for MDM2	No	No	Details in section 3
Model with MDMX	No	Yes	Yes	No	No	Details in section 4

Table 2.1: Key features of various models of p53 behavior. The last 2 rows are for the models presented in this work.

The models presented here also differ from previous models in a few other ways. Unlike in other models, MDM2 auto-ubiquitination was assumed to happen at a rate proportional to the square of MDM2 concentration. Given that MDM2 forms heterodimers with MDMX[36], and that MDMX inhibits MDM2 auto-ubiquitination[37], and that MDM2 ubiquitinates MDMX[38], it seems likely that one MDM2 molecule is ubiquitinating a second MDM2 molecule. Also, the binding properties of p53 and the MDM2 promoter were investigated experimentally in R. L. Weinberg et al 2005[73], who showed that the appropriate hill coefficient for this process is actually 1.8. The models here use this coefficient, where as the other models do not.

3 A Model with ARF

3.1 Goals and modeling considerations

Since it has been observed that stochastic effects can cause a population of cells that are undergoing undamped oscillations to appear to be undergoing damped oscillations, it is interesting to compare a stochastic model of cell behaviour to a deterministic one. By using stochastic and deterministic versions of the same model it will be possible to look at the process of desynchronization between cells and to search for any other effects by which stochasticity could influence the system. As we shall see later, further investigation also revealed several unexpected ways in which stochasticity influenced the system.

For this work a simple model will suffice. It would have been sufficient in this case to construct a model with only p53 and MDM2, while leaving out ARF. However the goals of the model as used here are not quite the same as the goals when the model was being constructed. One thing that was desired during model construction was to look at bifurcation points of the system in response to various changes. One of the changes of interest was ARF levels, hence the need to include ARF. Knowing something about the bifurcation points is useful however, and removing ARF and finding new parameters would have been time consuming. Hence the model was reused ARF and all, even though at this point ARFs primary function is to give the model a property that makes it easy to refer to.

3.2 Model description

In this model p53 induces the transcription of MDM2 mRNA in the nucleus. Induced transcription is assumed to be proportional to $[p53]^{1.8}/(K_D^{1.8}+[p53]^{1.8})$, as was seen in the binding properties found by R. L. Weinberg et al 2005[73]. MDM2 mRNA is also produced at a basal rate. After being produced in the nucleus the MDM2 mRNA proceeds to the cytoplasm, where it is translated and eventually decays. Even though mRNA from MDM2's different promoter regions are translated at different rates they are treated as one species. Because the two types of mRNA are assumed to decay at the same rate this amounts to absorbing the difference in translation rates into the mRNA production rates. Cytoplasmic MDM2 moves to the nucleus at a constant rate, and all other behaviours that cytoplasmic MDM2 could exhibit is ignored in this model. ARF was given constant production and degradation rates. Once in the nucleus MDM2 can become bound to ARF, which removes both proteins from the system. Additionally, MDM2 auto-ubiquitinates, which is a process that also removes it from the system. Figure 3.1 provides a diagram of this system.

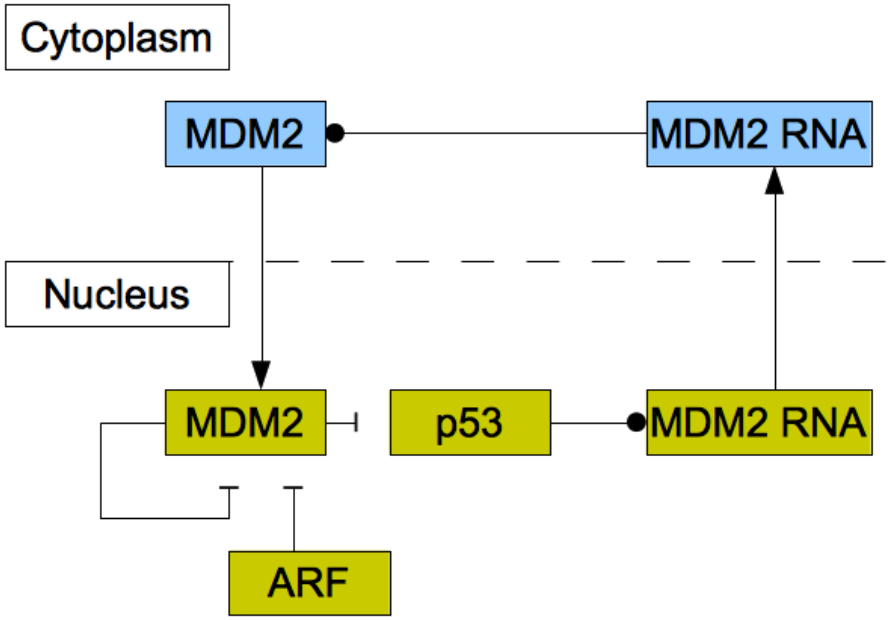

Figure 3.1: A schematic of the model of p53 including MDM2 sequestration by ARF. Arrows denote movement between compartments, barred lines indicate degradation and circles indicate inducing production.

Using mass-action principles and the saturable transcription kinetics mentioned above, the system can be written out in terms of differential equations as follows:

$$\frac{dp53}{dt} = k_p - k_1 p53 MDM2_{nuclear} - d_p p53$$

$$\frac{dMDM2_{nuclear\ rna}}{dt} = k_m + k_2 \frac{p53^{1.8}}{K_D^{1.8} + p53^{1.8}} - k_0 MDM2_{nuclear\ rna}$$

$$\frac{dMDM2_{cytoplasmic\ rna}}{dt} = k_0 MDM2_{nuclear\ rna} - d_{rc} MDM2_{cytoplasmic\ rna}$$

$$\frac{dMDM2_{cytoplasmic}}{dt} = k_T MDM2_{cytoplasmic\ rna} - k_i MDM2_{cytoplasmic}$$

$$\frac{dMDM2_{nuclear}}{dt} = k_i MDM2_{cytoplasmic} - d_{mn} MDM2_{nuclear}^2 - k_3 MDM2_{nuclear} ARF$$

$$\frac{dARF}{dt} = k_a - d_a ARF - k_3 MDM2_{nuclear} ARF$$

with k_p being the production rate of p53, k_1 being the rate at which MDM2 ubiquitinates p53 and d_p being the rate of MDM2 independent p53 degradation. Here, k_m is the rate of p53 independent MDM2 mRNA production, k_2 is the maximum rate of p53 dependant MDM2 mRNA production, K_D is the dissociation constant for p53 on the MDM2 promoter region, and k_0 is the rate of MDM2 mRNA transport to the nucleus. In the equations above, d_{rc} is the decay rate of MDM2 mRNA in the cytoplasm, k_T is the translation rate for MDM2 mRNA and k_i is the rate of nuclear localization for MDM2. MDM2 auto-ubiquitination happens at the rate d_{mn} and MDM2 binds to ARF at the rate k_3. Lastly, ARF is produced at the rate k_a and degraded at the rate d_a. A list of the values used for these parameters can be found in Table 3.1. The initial conditions were chosen by letting the system run until it settled into a stable limit cycle and then by using the values for when nuclear MDM2 levels were at a maximum.

Parameter	Description	Value	Alternate expresion
k_p	p53 production	0.5proteins/s	$8.30*10^{-3}$/nMs
k_1	MDM2 dependant p53 degradation	$9.963*10^{-6}$/s	$6*10^{-4}$/nMs
d_p	p53 decay	$1.925*10^{-5}$/s	10 hour half life
k_m	p53 independent MDM2 production	$1.5*10^{-3}$RNA/s	1 rna per 666s
k_2	p53 dependant MDM2 production	$1.5*10^{-2}$/s	Maximum of 1 rna per 66s
K_D	Dissociation constant	740 proteins	12.3nM
k_0	RNA transport from nucleus to cytoplasm	$8.0*10^{-4}$/s	14.4 min for half the proteins to move
d_{rc}	MDM2 mRNA decay in cytoplasm	$1.444*10^{-4}$/s	1h20min half life
k_T	Transcription rate	$1.66*10^{-2}$ proteins/s	1 protean per RNA per min
k_i	Protein transport from cytoplasm to nucleus	$9.0*10^{-4}$/s	12.4 min for half the proteins to move
d_{mn}	MDM2 autoubiquitination	$1.66*10^{-7}$/s	$2.76*10^{-9}$/nMs
k_a	ARF production	0.5proteins/s	$8.30*10^{-3}$/nMs
d_a	ARF decay	$3.209*10^{-5}$/s	6 hour half life
k_3	MDM2-ARF complex formation rate	$9.963*10^{-6}$/s	$6*10^{-4}$/nMs

Table 3.1: Parameters used in the model with ARF.

Experimental observations of the p53 MDM2 feedback loop have found periods of oscillations between 4 hours and 7 hours[63,64]. Due to scarcity of experimentally verified data, most of parameters in the model were chosen by hand in order to produce oscillations with a similar period. Selecting parameters for the model was done in collaboration with Marion Poirel. Some of the parameters were constrained by experimental data. K_D was found to be 12.3nM by R. L. Weinberg et al 2005[73]. Some experimental results suggested that the half life for MDM2 mRNA should be in the range of 1-2 hours[74,75], so this constrained our choice of the decay rate. The MDM2 translation rate, k_T, was assumed to be 1 protein per mRNA molecule per minute, approximately the value estimated by Xiaodong Cai and Zhi-Min Yuan 2009[69]. The transport rate for MDM2 mRNA was constrained to be in the range of 5-40min, based on A. Mor et al 2010[76]. The half life of the ARF protein, d_a, was chosen to be 6 hours based on M-L. Kuo et al 2004[77]. Complex formation rates were assumed to be $6*10^{-4}$/nMs, a reasonable rate for protein-protein interactions[78]. It was further assumed that p53 MDM2 interaction would always result in p53 degradation. MDM2 independent p53 turnover was assumed to give a half-life of 10h for the p53 protein. This is essentially negligible in this model, the terms was included in the model so that a bifurcation value could be calculated for it. Cytoplasmic volume was assumed to be $1000\mu m^3$ with a nuclear volume of $100\mu m^3$. The values for p53 production, ARF production, basal MDM2 mRNA production, p53 induced MDM2 mRNA production, MDM2 nuclear import, and MDM2 auto-ubiquitination were unknown. These unknown parameters were chosen manually in order to produce oscillations similar to the ones observed in experiments on single cells. Although only one set of parameters was produced for this model the choice is certainly not unique given the loose selection criteria.

The model produces oscillations with a period of 6.4 hours as can be seen in Figure 3.2. Bifurcation points for the model were determined by Marion Poirel (unpublished work) and are listed in Table 3.2.

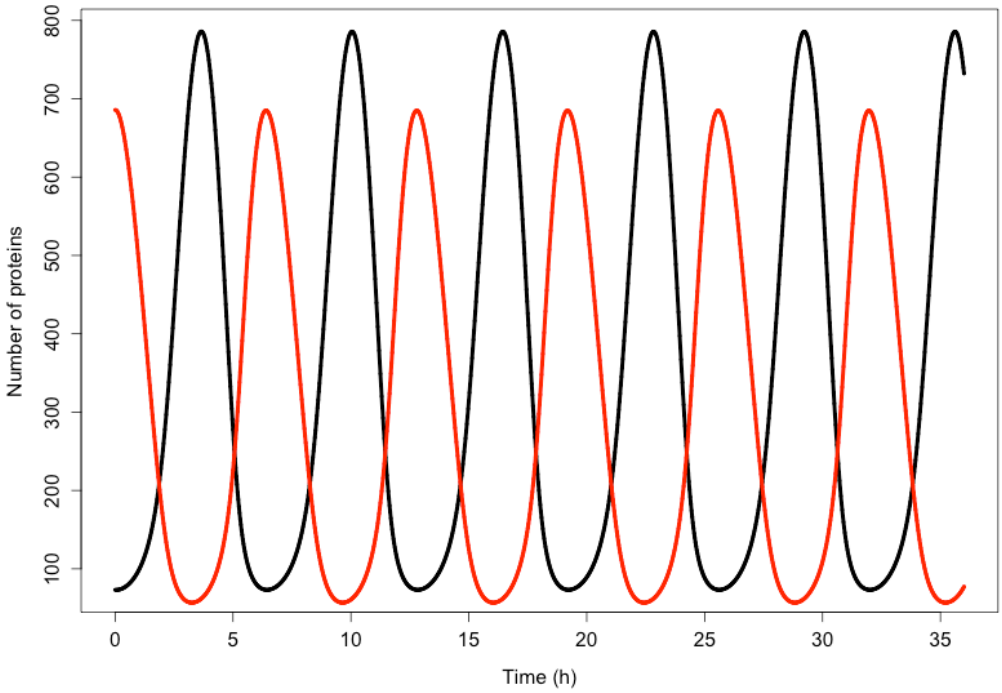

Figure 3.2: p53 and MDM2 oscillating in the ARF model. p53 is in black, MDM2 is in red.

Parameter	Bifurcation value	Oscillatory behavior
k_p	0.215/s	undamped : $0.215 \leq k_p \leq 1.462$
k_p	1.462/s	damped:$k_p \leq 0.215 \cup k_p \geq 1.462$
k_1	$2.903*10^{-6}$/s	undamped : $2.903*10^{-6} \leq k_1 \leq 1.834*10^{-5}$
k_1	$1.834*10^{-5}$/s	damped : $k_1 \leq 2.903*10^{-6} \cup k_1 \geq 1.834*10^{-5}$
d_p	$4.237*10^{-4}$/s	undamped : $d_p \leq 4.237*10^{-4}$
k_m	$2.788*10^{-3}$/s	undamped : $k_m \leq 2.788*10^{-3}$
k_2	$7.501*10^{-3}$/s	undamped : $7.501*10^{-3} \leq k_2 \leq 0.118$
k_2	0.118/s	damped : $k_2 \leq 7.501*10^{-3} \cup k_2 \geq 0.118$
K_D	253.083	undamped : $253.083 \leq K_D \leq 1723.058$
K_D	1723.058	damped : $K_D \leq 253.083 \cup K_D \geq 1723.058$
k_0	$7.010*10^{-6}$/s	undamped : $7.010*10^{-6} \leq k_0 \leq 6.160*10^{-3}$
k_0	$6.160*10^{-3}$/s	damped : $k_0 \leq 7.010*10^{-6} \cup k_0 \geq 6.160*10^{-3}$
d_{rc}	$8.714*10^{-5}$/s	undamped : $8.714*10^{-5} \leq d_{rc} \leq 2.704*10^{-4}$
d_{rc}	$2.704*10^{-4}$/s	damped : $d_{rc} \leq 8.714*10^{-5} \cup d_{rc} \geq 2.704*10^{-4}$
k_T	$8.760*10^{-3}$/s	undamped : $8.760*10^{-3} \leq k_T \leq 2.936*10^{-2}$
k_T	$2.936*10^{-2}$/s	damped:kT $\leq 8.760*10^{-3} \cup k_T \geq 2.936*10^{-2}$
k_i	$6.845*10^{-6}$/s	undamped : $6.845*10^{-6} \leq k_i \leq 1.559*10^{-2}$
k_i	$1.559*10^{-2}$/s	damped : $k_i \leq 6.845*10^{-6} \cup k_i \geq 1.559*10^{-2}$
d_{mn}	$1.251*10^{-6}$/s	undamped : $d_{mn} \leq 1.251*10^{-6}$
k_a	0.324/s	undamped : $0.324 \leq k_a \leq 0.963$
k_a	0.963/s	damped : $k_a \leq 0.324 \cup k_a \geq 0.963$
d_a	$2.088*10^{-3}$/s	undamped : $d_a \leq 2.088*10^{-3}$
k_3	$5.866*10^{-6}$/s	undamped : $k_3 \geq 5.866*10^{-6}$

Table 3.2: Bifurcation points in the deterministic model with ARF.

3.3 Stochastic simulation

At its heart the stochastic simulation used bears a strong resemblance to a finite difference integrator. Rather then being evaluated as a single set of derivatives, however, each chemical reaction is evaluated separately. When the simulation evaluates a chemical reaction the first step is to use the law of mass action and the average of the current chemical concentrations and their concentrations after the last time the reaction was evaluated to find an expectation value for the number of times the reaction will occur this time step. After this the expectation value for the number of times the reaction will occur is set as the expectation value for a Poisson random number generator and the result is the number of times the reaction will actually occur during that time step. In order to improve efficiency while preserving accuracy an adaptive time step is used. The program evaluates each reaction 0.5^N times per simulated second, with N chosen such that the expectation value for a particular evaluation of a reaction is lower then a pre-set threshold multiplied by the quantity of the chemical molecules involved. In this way parts of the system that are changing rapidly are evaluated with a low enough time step to prevent numerical errors without needing to waste additional computations on the slower reactions.

Figure 3.3 shows some examples of individual simulation runs for this model. In order to make comparisons with the deterministic model it is helpful to look at the average of protein levels across many runs, such as is displayed in Figure 3.4. The stochastic nature of the simulation leads to a number of interesting differences arising from the desynchronization of the individual model runs as well as from applying a distribution of p53 values into the nonlinear function for MDM2 production.

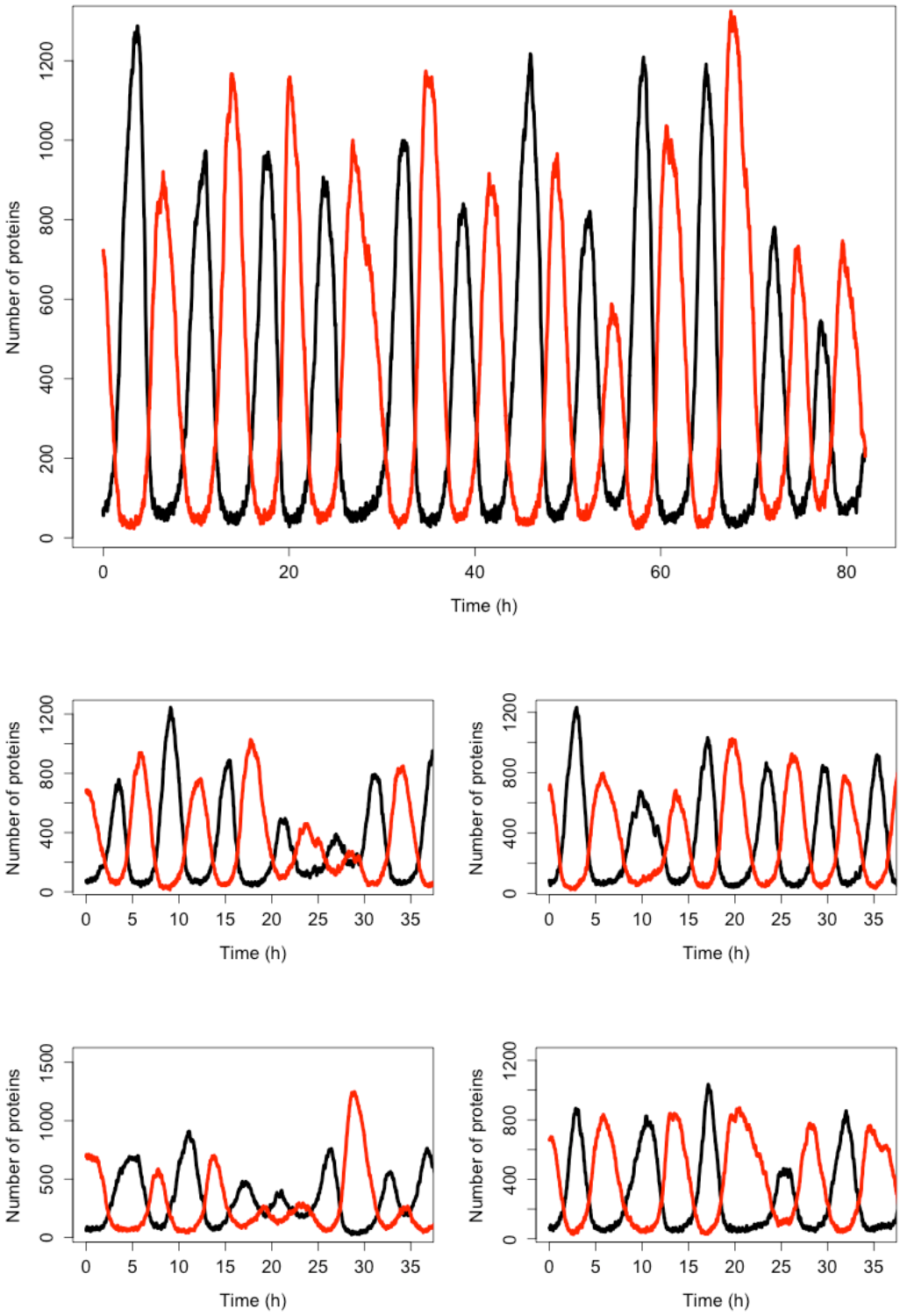

Figure 3.3: Examples of time courses in the stochastic model. p53 is in black and MDM2 is in red.

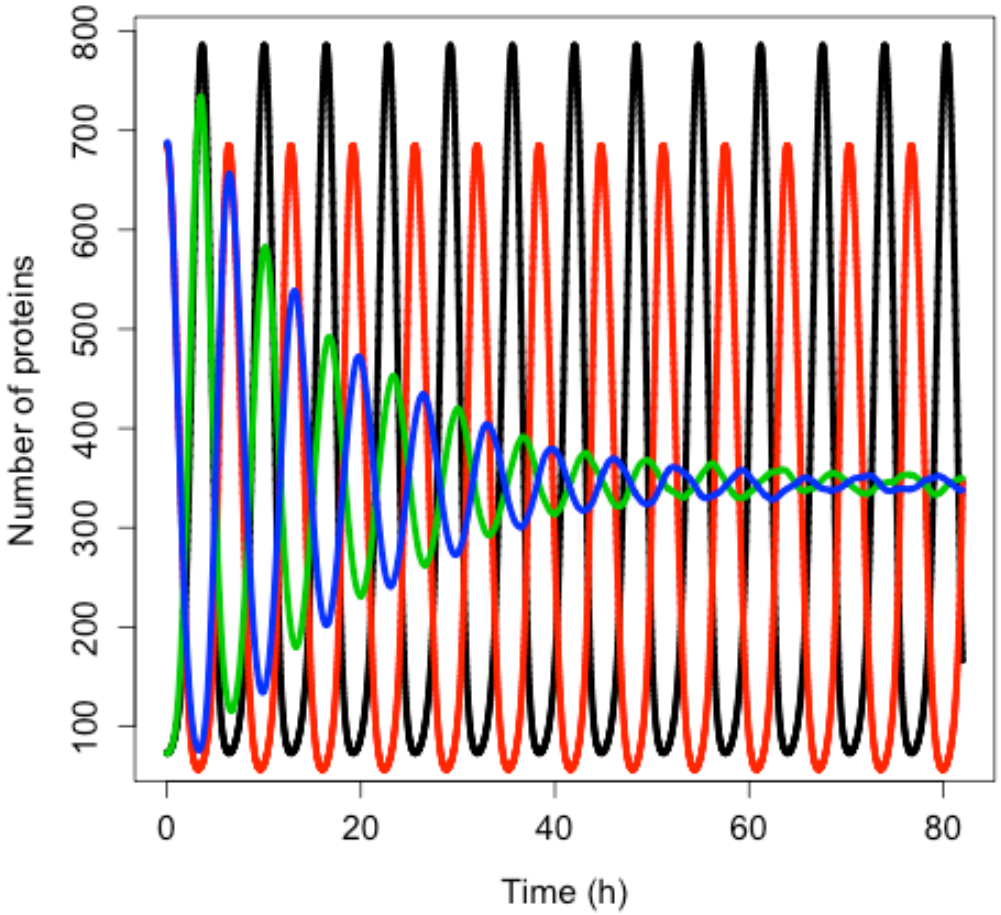

Figure 3.4: A comparison of the stochastic and deterministic models. p53 is in black in the deterministic model and in green for the stochastic one. MDM2 is in red for the deterministic model and blue for the stochastic one.

3.4 Desynchronization in general

An experiment averaging protein levels across many cells is like looking at the average of many runs of a stochastic system. As such it is interesting to consider how aggregate average behaviour differs from the behaviour of individual model runs. A given run of the stochastic model will not necessarily just be equal to the deterministic model plus noise. At any given step the stochastic model's variables depend on the values of the variables at the previous time step. For a periodic model this will result not only in noise moving variables up and down but also in random stepping forwards and backwards of the models phase. As such an ensemble of model runs will fall out of synchronization over time. Imagine for simplicity a stochastic model based on a deterministic model with a variable given by $Asin(\omega t + \varphi)$. In the stochastic model random chance continuously moves each run in the ensemble towards or away from the next peak. Considering the central limit theorem applied over a large number of runs, one would then expect the distribution of timing of the peak in individual runs to approach a normal distribution. If all the runs are initialized from the same starting point then the amplitude of the mean will not be $Asin(\omega t + \varphi)$ but rather it will be

$$A\int_{-\infty}^{\infty}\frac{1}{\sigma\sqrt{2\pi}}e^{-\frac{1t'^2}{2\sigma^2}}\sin(\omega t+\varphi+\omega t')\,dt'$$

because the timing of each run will be shifted with a Gaussian weighting given to the shift. Since the width of the distribution will increase proportionally to the square root of time, the standard deviation σ can be expanded as $\alpha\sqrt{t}$. This integral then works out to be

$$Ae^{-\frac{\omega^2\alpha^2 t}{2}}\sin(\omega t+\varphi)$$

Consider a 2π periodic function that is integrable on $-\pi$ to π. This function could be expressed as a Fourier series such that

$$f(t)=\frac{a_0}{2}+\sum_{n=1}^{\infty}[a_n\cos(nt)+b_n\sin(nt)]$$

or equivalently

$$f(t)=\frac{a_0}{2}+\sum_{n=1}^{\infty}\left[a_n\sin\left(nt+\frac{\pi}{2}\right)+b_n\sin(nt)\right]$$

Applying the result above we find that the function will be changed by desynchronization to become

$$f'(t)=\frac{a_0}{2}+\sum_{n=1}^{\infty}\left[a_n\sin\left(nt+\frac{\pi}{2}\right)+b_n\sin(nt)\right]e^{-\frac{n^2\alpha^2 t}{2}}$$

Since the decay is proportional to the square of the frequency, any function will rapidly take on the appearance of a single decaying sin curve as time progresses.

3.5 Desynchronization in the ARF model

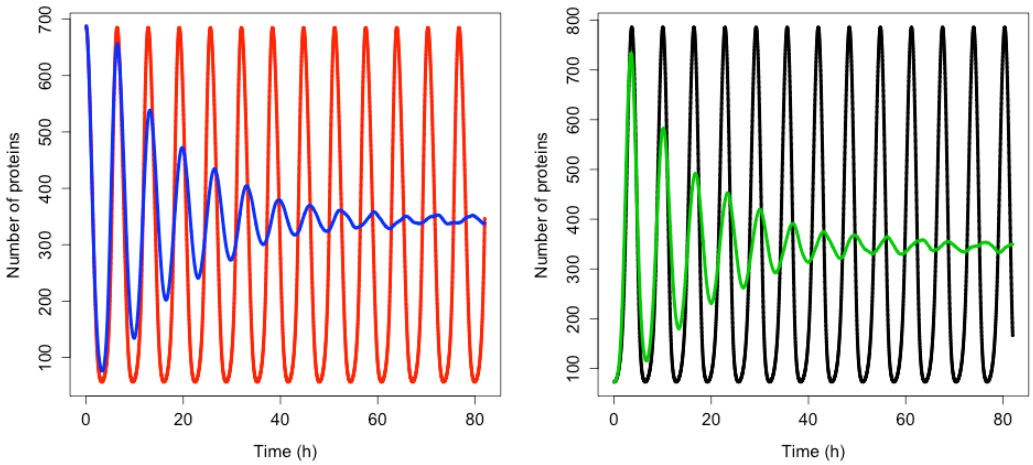

A **B**

Figure 3.5: Comparison of stochastic and deterministic models. Graph A shows the comparison for MDM2 with MDM2 from the deterministic model in red and from the mean of 5,000 runs of the stochastic model in blue. Graph B shows the comparison for p53 with the deterministic model in black and from the mean of 5,000 runs of the stochastic model in green.

The effects of desynchronization in the ARF model can be seen in Figure 3.5. The deterministic and stochastic systems can be compared by fitting a curve to the time series for p53. Specifically:

$$f(t) = a_0 + a_1 \sin(\omega t + \varphi_1) + a_2 \sin(2\omega t + \varphi_2)$$

for the deterministic model, and

$$f(t) = a_0 + e^{-\frac{\alpha^2 t}{2}} a_1 \sin(\omega t + \varphi_1) + e^{-\frac{4\alpha^2 t}{2}} a_2 \sin(2\omega t + \varphi_2)$$

for the stochastic model. Table 3.3 lists the parameter estimates for the deterministic model as well as 95% confidence intervals for the stochastic model. Figure 3.6 shows graphs of the functions and their fits. The best fit was determined by using least squares regression on the mean p53 values from 5,000 instances of the stochastic model. The upper and lower bounds were found by using bootstrapping on the 5,000 instances that were used to compute the best fit. The 95% confidence intervals for the amplitude and phase of the second sign curve ended up being very large due to the curve fitting function jumping between local minima. To ensure that the algorithm was being run at a high enough numerical precision, an additional 5,000 instances were generated with the acceptable error parameter in the code set to at 10 times the value used in this analysis. The resulting new confidence intervals were compared to the ones from the higher accuracy runs. In all cases there was significant overlap of the intervals, suggesting that the acceptable error was set low enough in the high accuracy runs to result in only negligible deviations from an exact solution.

	Deterministic model	Best fit to stochastic model	Lower bound	Upper bound
α	NA	$21.8/s^{1/2}$	$21.2/s^{1/2}$	$22.5/s^{1/2}$
ω	$2.73*10^{-4}/s$	$2.63*10^{-4}/s$	$2.62*10^{-4}/s$	$2.64*10^{-4}/s$
A_0	332	346	345	347
A_1	-348	-396	-406	-388
ϕ_1	1.21	1.40	1.38	1.43
A_2	105	136	-136	144
ϕ_2	0.633	-1.16	-36.6	13.6

Table 3.3: Comparisons of the parameters found when fitting the deterministic model's p53 levels to the function $f(t) = a_0 + a_1 \sin(\omega t + \varphi_1) + a_2 \sin(2\omega t + \varphi_2)$ and the stochastic model's p53 levels to the function $f(t) = a_0 + e^{-\frac{\alpha^2 t}{2}} a_1 \sin(\omega t + \varphi_1) + e^{-\frac{4\alpha^2 t}{2}} a_2 \sin(2\omega t + \varphi_2)$.

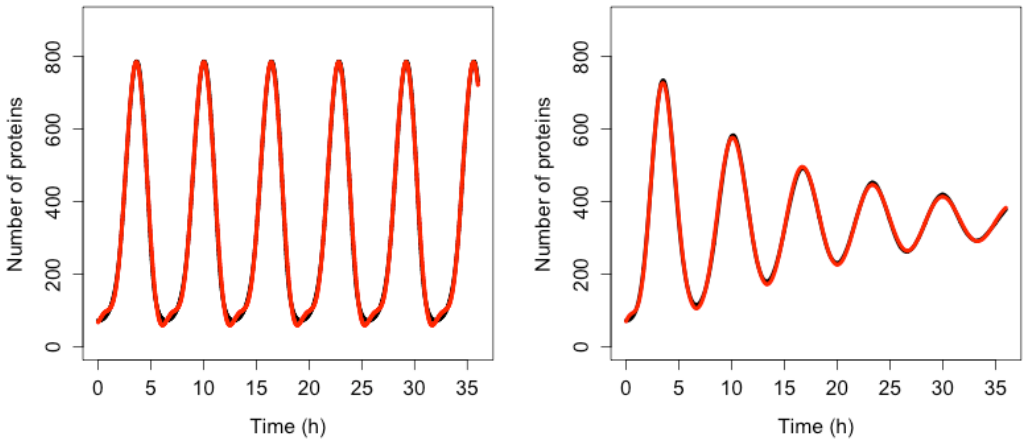

A B

Figure 3.6 A: Comparison of p53 levels in the deterministic model in black to a curve fitted to it from the function $f(t) = a_0 + a_1 \sin(\omega t + \varphi_1) + a_2 \sin(2\omega t + \varphi_2)$ in red. B: Comparison of p53 levels in the stochastic model in black to a curve fitted to it from the function $f(t) = a_0 + e^{-\frac{\alpha^2 t}{2}} a_1 \sin(\omega t + \varphi_1) + e^{-\frac{4\alpha^2 t}{2}} a_2 \sin(2\omega t + \varphi_2)$ in red.

The differences between the stochastic model's behaviour and the deterministic model's behaviour are statistically significant. Most striking is that the frequency of the oscillations was changed by stochastic effects. The same analysis can be done on nuclear MDM2 levels, and can be seen in Figure 3.7 and Table 3.4. The discrepancy between the fitted curve for MDM2 levels and the levels from the simulation hints at another difference between stochastic and deterministic systems, which will be discussed in the next section. It is also worth noting that this stochastic model only considers the differences between cells due to noise in a few chemical reactions. In a real cell there would be many more factors contributing to desynchronization. Even simply adding mRNA for the p53 and ARF included in this model raises the desynchronization parameter α from $21.8 s^{-1/2}$ to $23.5 s^{-1/2}$ (a mean of 30 mRNA molecules was used for this simulation). Additionally, differences in cell volume would increase desynchronization by altering protein concentrations between cells.

	Deterministic model	Best fit to stochastic model	Lower bound	Upper bound
α	NA	$20.7/s^{1/2}$	$20.2/s^{1/2}$	$21.3/s^{1/2}$
ω	$2.73*10^{-4}$/s	$2.63*10^{-4}$/s	$2.62*10^{-4}$/s	$2.63*10^{-4}$/s
A_0	302	345	343	346
A_1	-314	-372	-379	-365
ϕ_1	-1.72	-1.49	-1.51	-1.47
A_2	-71	-78.5	-82.8	-74.6
ϕ_2	-1.73	-0.80	-0.87	-0.73

Table 3.4: Comparisons of the parameters found when fitting the deterministic model's nuclear MDM2 levels to the function $f(t) = a_0 + a_1 \sin(\omega t + \varphi_1) + a_2 \sin(2\omega t + \varphi_2)$ and the stochastic model's nuclear MDM2 levels to the function $f(t) = a_0 + e^{-\frac{\alpha^2 t}{2}} a_1 \sin(\omega t + \varphi_1) + e^{-\frac{4\alpha^2 t}{2}} a_2 \sin(2\omega t + \varphi_2)$.

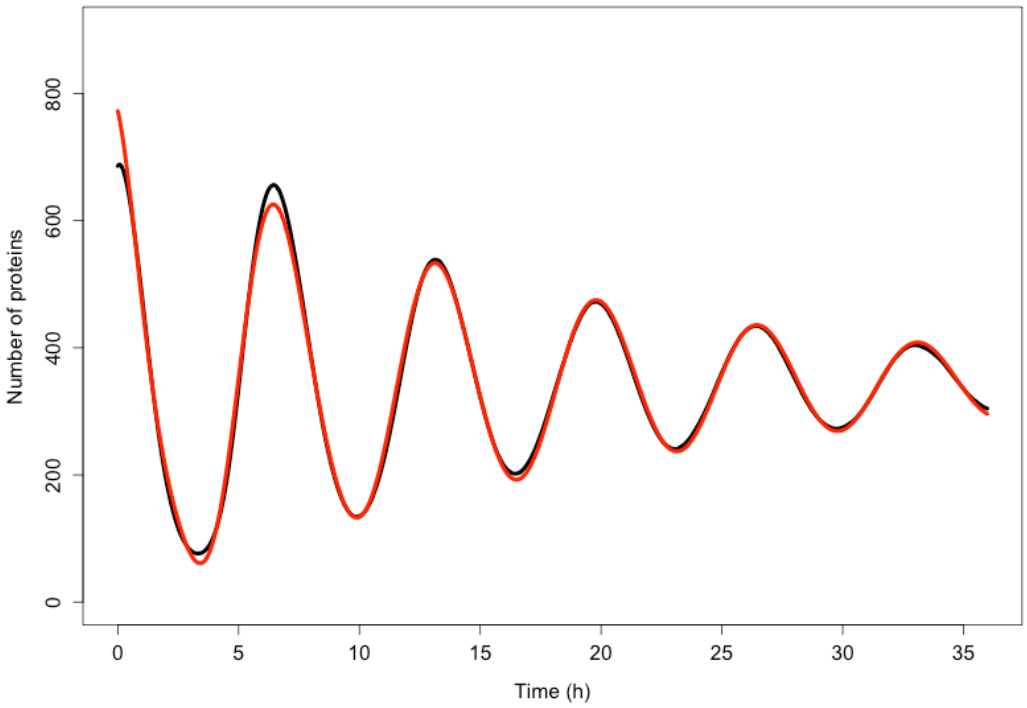

Figure 3.7: Comparison of nuclear MDM2 levels in the stochastic model in black to a curve fitted to it from the function $f(t) = a_0 + e^{-\frac{\alpha^2 t}{2}} a_1 \sin(\omega t + \varphi_1) + e^{-\frac{4\alpha^2 t}{2}} a_2 \sin(2\omega t + \varphi_2)$ in red.

3.6 Changes from nonlinear effects

The mean of a stochastic ensemble for the ARF model deviates from the deterministic model not just from desynchronization but also due to nonlinear effects. For a nonlinear function applied to a distribution of inputs the mean of the function will not necessarily be equal to the function of the mean. In other words, as is well know, the following is usually true: <f(x)>≠f(<x>), unless f is a linear function of x. Production of MDM2 mRNA in this model is clearly nonlinear because it is proportional to f(p53)= $\frac{[p53]^{1.8}}{K_d^{1.8}+[p53]^{1.8}}$. Figure 3.8 compares the function of the mean to the mean of the function for this case. Mean MDM2 values in the stochastic model are determined by <f(p53)> (the red curve in Figure 3.8) which has a different amplitude then f(<p53>) (the black curve in Figure 3.8). This discrepancy causes the behaviour of the system to change relative to the deterministic case, which only has mean p53 values. This is also the most likely source of the discrepancy between the fitted curve in Figure 3.7 and the actual levels of MDM2. With production that behaves differently, the initial conditions in the simulation would not have been a point on the limit cycle for MDM2 levels. As a consequence, the system would have been moving towards the limit cycle at the same time as it was desynchronizing. The simple fitted curve cannot possibly account for this, which is why it did not fit well. p53 levels would also have been affected by this but it does not seem to have been a large enough effect to be obvious on the graph.

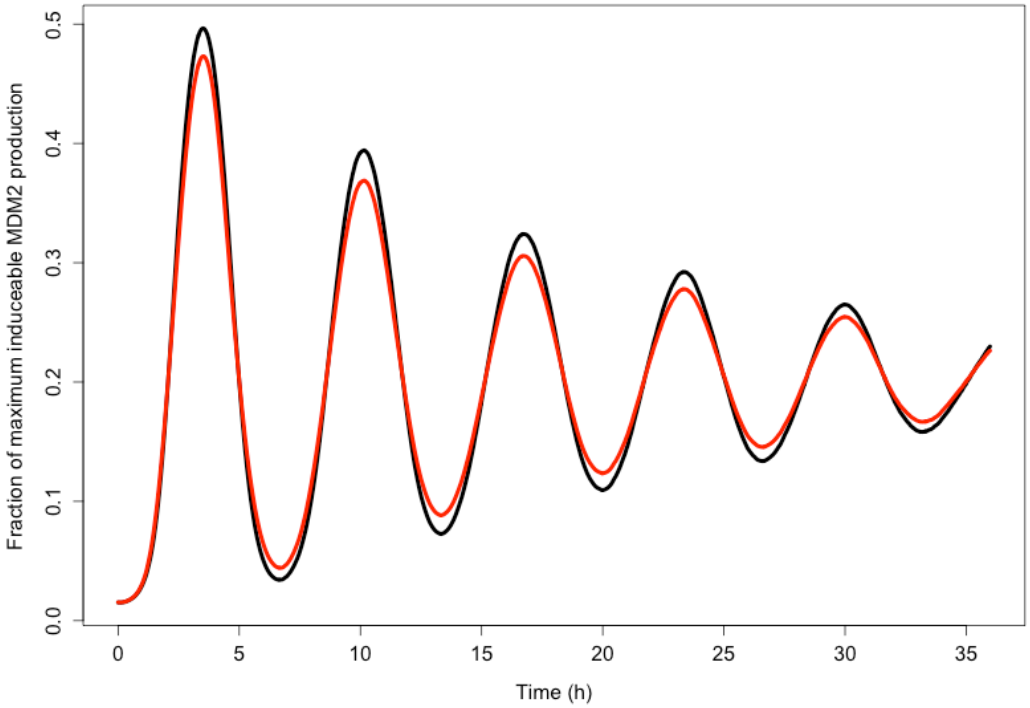

Figure 3.8: A comparison of the function $\frac{[p53]^{1.8}}{K_d^{1.8}+[p53]^{1.8}}$ between the function applied to mean p53 values in black and the mean of the function when applied to the distribution of p53 values in red.

Although the effect on the amplitude of the oscillations with the original parameters was relatively small, approximately 5%, the nonlinear effects can be a lot larger in other situations. Consider the case when the p53 production rate is set near to the lower bifurcation point, as shown in Figure 3.9. In this case the mean level of MDM2 from the stochastic model ends up being higher then the maximum amplitude of the oscillations in the deterministic model. A similar phenomenon occurs when p53 production is near the upper bifurcation point as shown in Figure 3.10.

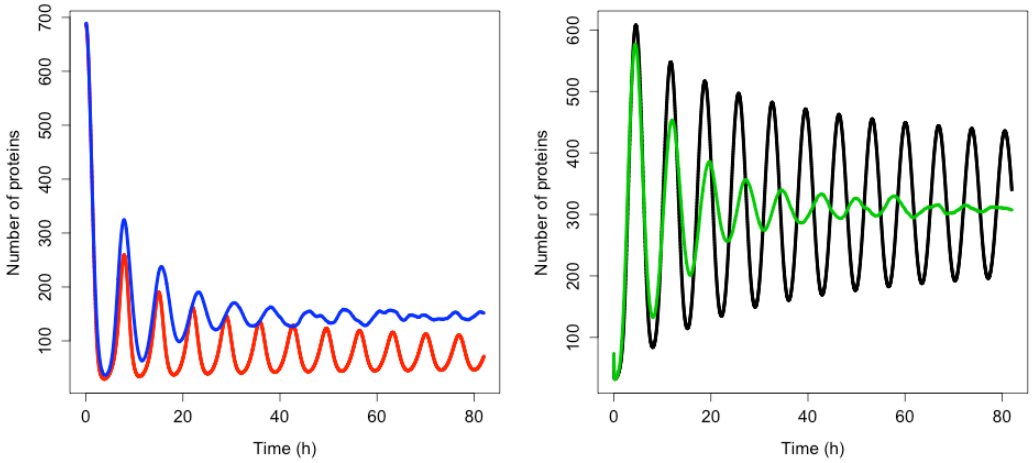

A B

Figure 3.9: Comparison of stochastic and deterministic models when p53 production is near the lower bifurcation point. Graph A shows the comparison for MDM2 with MDM2 from the deterministic model in red and from the mean of 5,000 runs of the stochastic model in blue. Graph B shows the comparison for p53 with the deterministic model in black and from the mean of 5,000 runs of the stochastic model in green.

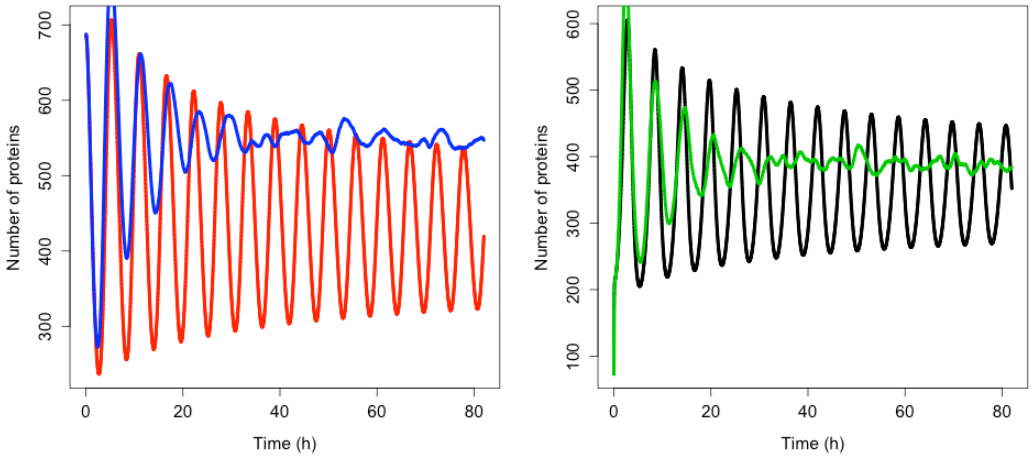

A B

Figure 3.10: Comparison of stochastic and deterministic models when p53 production is near the upper bifurcation point. Graph A shows the comparison for MDM2 with MDM2 from the deterministic model in red and from the mean of 5,000 runs of the stochastic model in blue. Graph B shows the comparison for p53 with the deterministic model in black and from the mean of 5,000 runs of the stochastic model in green.

3.7 Excursions from the mean

Stochastic effects continue to play an interesting role in the systems behaviour even as we move past the upper bifurcation point, so that the deterministic model exhibits damped oscillations. For Figures 3.11-3.13 p53 production was set to 1.6, putting the system into the realm of damped oscillations. In Figure 3.11 we can see that as the oscillations decay the MDM2 levels settle in at a value significantly higher in the stochastic model than the deterministic one. From

Figure 3.12 we can see that the nonlinear effects of variable p53 levels are still altering behaviour, but something more is occurring this time. In Figure 3.11 B we see that mean p53 levels are settling in at a level higher in the stochastic model than in the deterministic one. This seems strange in light of the higher MDM2 levels but Figure 3.13 shows the reason. The stochastic nature of the system is sufficient to cause significant excursions from the mean even though the oscillations should be decaying. Some of the oscillations that occur later on are even larger then the initial pulse.

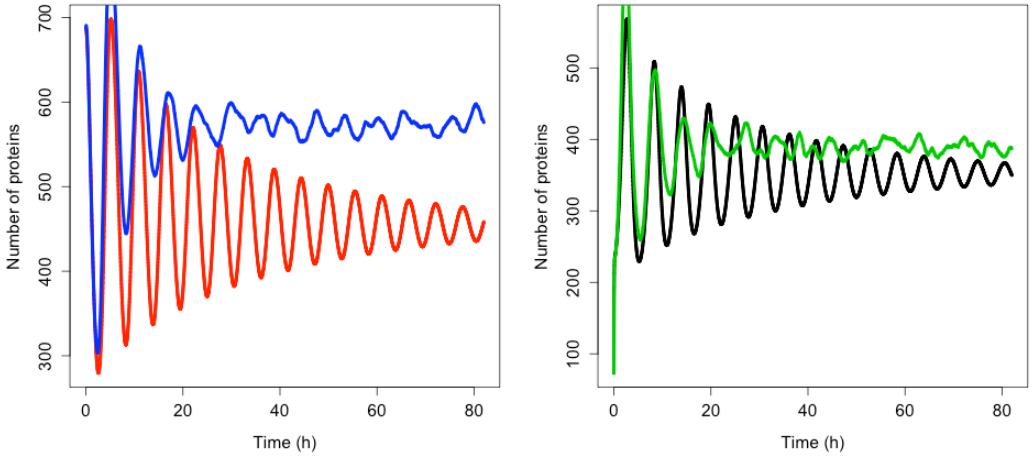

A B

Figure 3.11: Comparison of stochastic and deterministic models when p53 production is past the upper bifurcation point. Graph A shows the comparison for MDM2 with MDM2 from the deterministic model in red and from the mean of 5,000 runs of the stochastic model in blue. Graph B shows the comparison for p53 with the deterministic model in black and from the mean of 5,000 runs of the stochastic model in green.

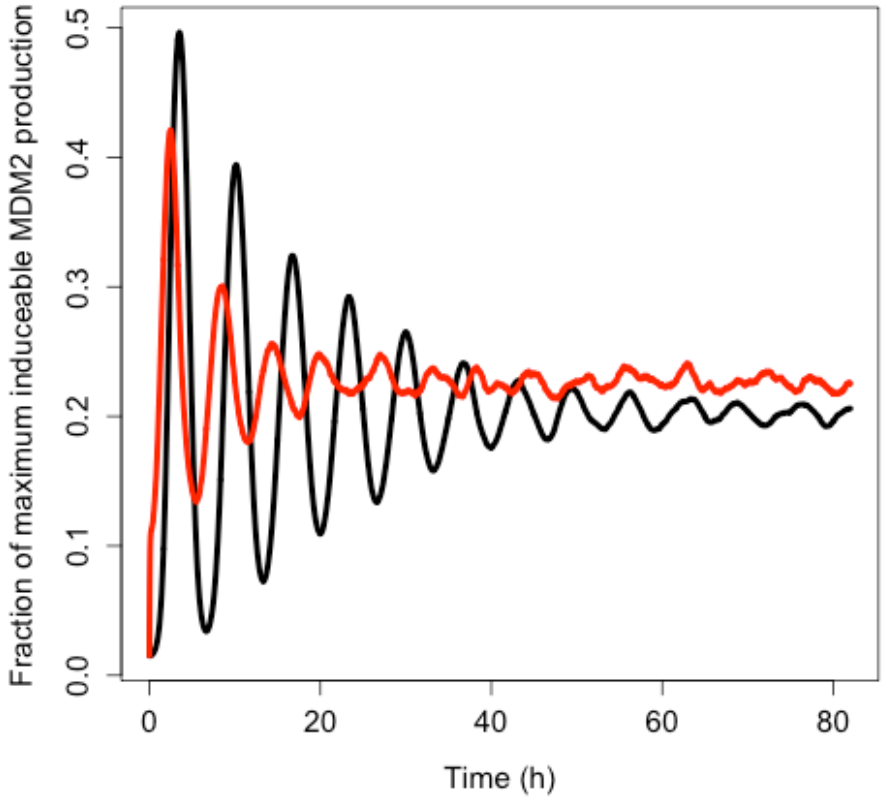

Figure 3.12 Comparison of the function $\frac{[p53]^{1.8}}{K_d^{1.8}+[p53]^{1.8}}$ between the function applied to mean p53 values in black and the mean of the function when applied to the distribution of p53 values in red.

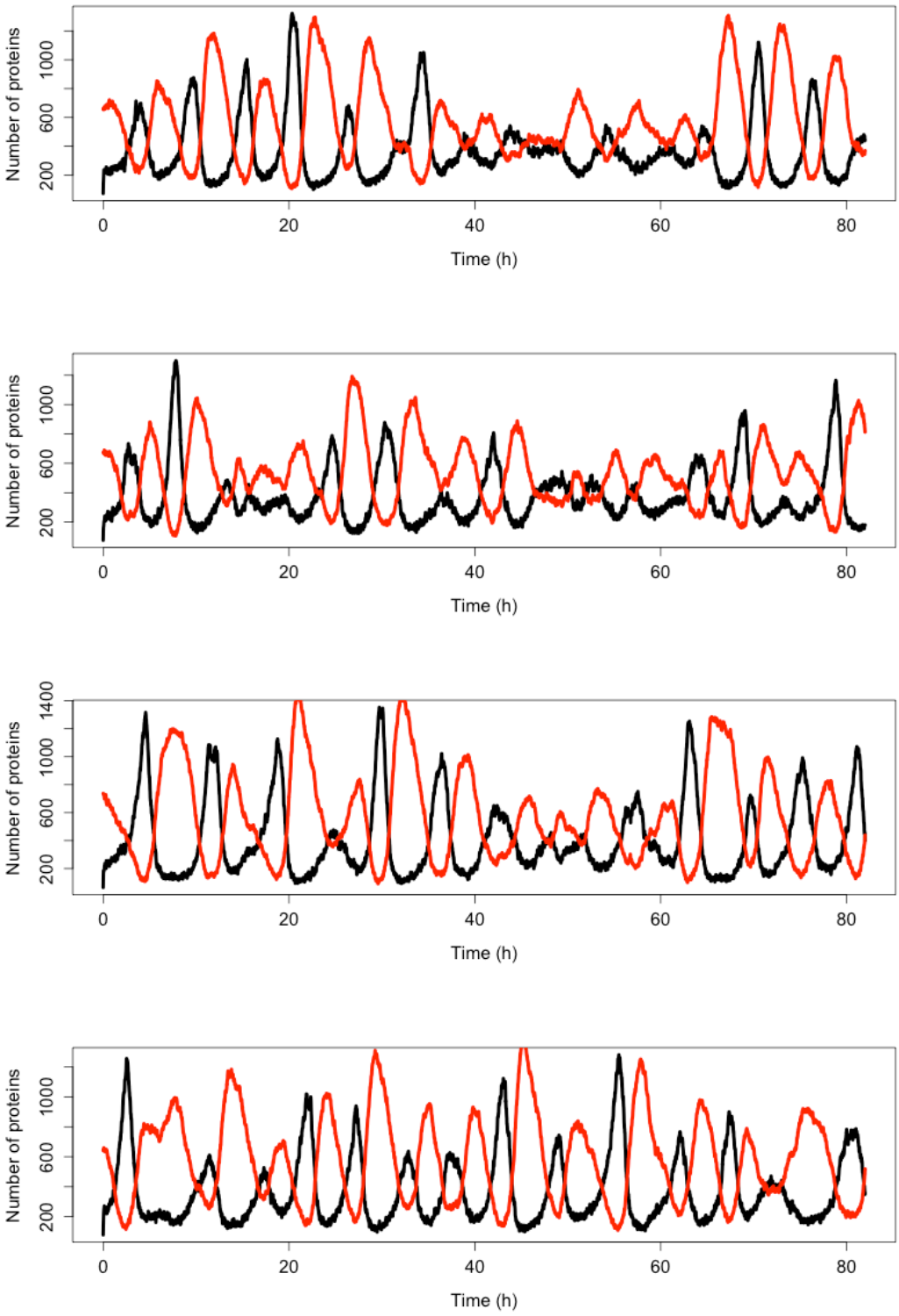

Figure 3.13: Examples of individual stochastic realizations when p53 production is past the upper bifurcation point. p53 is in black MDM2 is in red.

4 A model with MDMX

4.1 Goals and modeling considerations

Given the large amount of resources needed to develop a drug targeting a specific interaction, it is important to choose targets wisely. Unfortunately, determining the effects of targeting an interaction with a drug is itself a challenging task. Although there is not enough experimental data to determine the effects of hypothetical drugs with confidence, it is nonetheless interesting to see what information can be gained, as well as what would be needed for a more precise estimation.

The possible drugs being considered here target the MDM2 p53 interaction, the MDMX p53 interaction, and the MDM2 MDMX interaction, so the model must necessarily include these interactions. The experimental data to which the model was fitted gave information about protein levels in the whole cell as well as in the nucleus. Nuclear protein levels are the most relevant ones because of p53's transcriptional activity. Unfortunately the bulk of the data is for whole cell protein levels, not nuclear protein levels. Furthermore given that MDMX inhibits MDM2 auto-ubiquitination[37], localization of MDMX could be important for determining nuclear MDM2 levels. These factors suggested that adding compartments to fully take advantage of the available data would be a good option. Adding cytoplasmic and nuclear compartments however also required dealing with nucleolar sequestration in some way. This is because some fraction of the nuclear proteins has been sequestered where as the cytoplasmic proteins have not. The alternative to a nucleolar compartment would be to have different interaction constants in the nucleus and cytoplasm. On the other hand, including ARF as a mediator of nucleolar sequestration would add more complexity then necessary since the details of ARF behaviour are not of interest here. Likewise, adding to the model the specific phosphorylation states of the proteins involved would be excessive, since none of the drugs will affect them, and doing so would at minimum more then triple the number of parameters.

4.2 Description of the model with MDMX

In this model, as in the simpler MDM2/ARF model, p53 induces the transcription of MDM2 mRNA according to the formula $(f*[p53])^{1.8}/(k_d^{1.8}+(f*[p53])^{1.8})$. The form of this equation is based on the findings of L. Weinberg et al 2005[73]. The constant f in this equation represents the fraction of the nuclear p53 in the model that is available to bind to DNA. In other words, f is the fraction of p53 not bound to other proteins not explicitly included in the model or otherwise prevented from binding, say by being inappropriately phosphorylated. The MDM2 mRNA is also produced at a basal transcription rate from another promoter. After production, the mRNA proceeds into the cytoplasm where it gets translated and eventually broken down. In contrast, since MDMX transcription is not induced by p53[34] its mRNA is not included in the model, instead it is simply produced at a constant rate in the cytoplasm. This model also includes cytoplasmic p53. Like MDMX p53's mRNA is not included in the model. After being produced in the cytoplasm p53, MDM2, and MDMX, can be imported to the nucleus. Although ubiquitination by Mdm2 is known to be involved in exporting p53 from the nucleus[79] this is part of the degradation process for p53[80], therefore it is assumed that any exported p53 exists for a negligible amount of time so p53 export is ignored (p53 bound to MDMX, on the other hand, can be exported in the model). Likewise, because p53 was found not to co-immunoprecipitate with MDM2[81], it is assumed that p53 and MDM2 spend a negligible fraction of their lifetimes bound to each other so no term is included for a bound p53 MDM2 state. Since it is known that elevated MDMX levels can inhibit p53's ability to promote transcription[82] and this is a relevant effect for studying the possible action of a MDMX inhibitor, a bound p53 MDMX state is included. In this model MDM2 and MDMX can form hetero-dimers in the cytoplasm, the nucleus, and the nucleolus. Ubiquitination of MDMX occurs while it is in a hetero-dimer with MDM2. As with ubiquitinated p53, it is assumed that the ubiquitinated MDMX exists for a negligible amount of time and so it is immediately removed from the model. MDM2 and MDM2/MDMX hetero-dimers are allowed to

move back and forth between the nucleus and the cytoplasm and do so at the same rate. Because MDMX has a cryptic nuclear localization signal[40] and needs to bind with another protein to get into the nucleus, it is imported at a different rate then MDM2. p53 also acquires its own import rate. Bound p53 MDMX complexes are assumed to be imported at the average of the p53 and MDMX import rates. In this model free MDM2 ubiquitinates other free MDM2 molecules, as with the other proteins, ubiquitination is assumed to lead to rapid degradation. Figure 4.1 provides a visual representation of the pathway. Table 4.1 lists all the chemical species needed in the model and table 4.2 provides a list of all the reactions in the model.

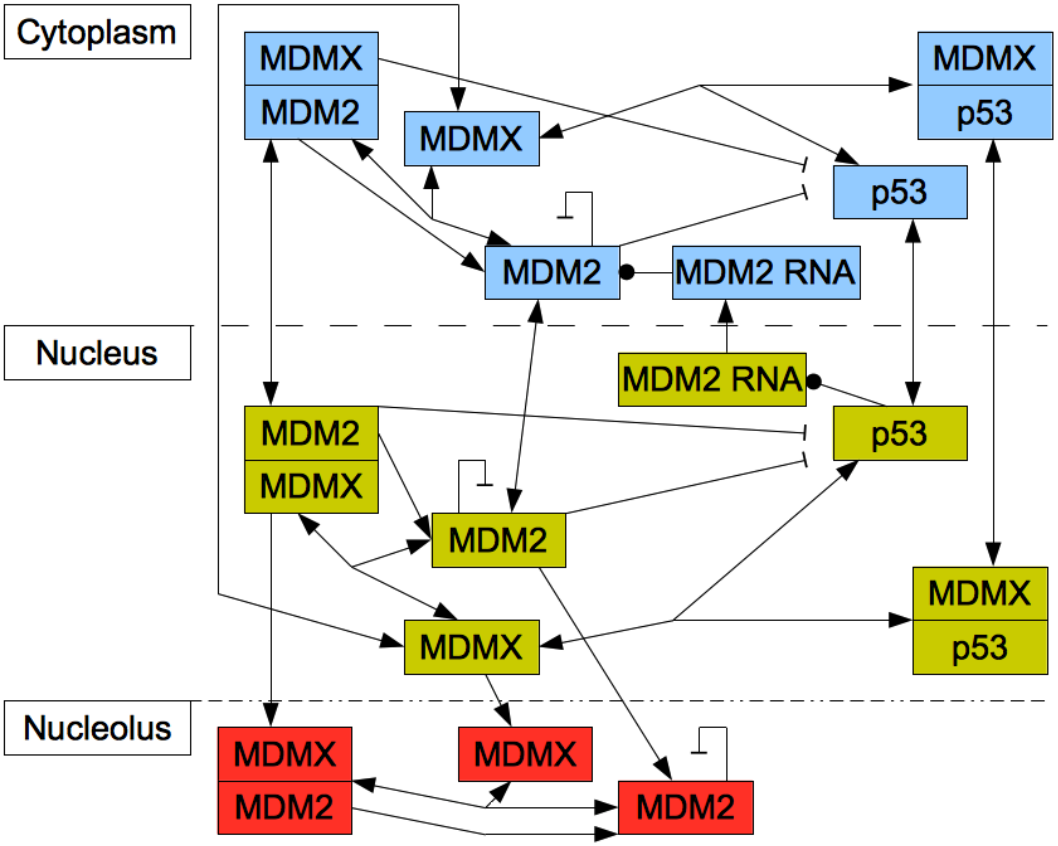

Figure 4.1: Visual representation of the model with MDMX. Arrows denote conversion of one species into another or movement between compartments, and lines with a bar on the end denote ubiquitination of a target protein. Note that the MDM2 MDMX complexes can break down ether by dissociation or the ubiquitination of MDMX, which is denoted as a single arrow from the complex to the MDM2.

Chemical	Description
[MDM2c]	Cytoplasmic MDM2
[MDM2n]	Nuclear MDM2
[MDM2o]	MDM2 sequestered in the nucleolus
[MDMXc]	Cytoplasmic MDMX
[MDMXn]	Nuclear MDMX
[MDMXo]	MDMX sequestered in the nucleolus
[MDM2:MDMXc]	Cytoplasmic MDM2/MDMX heterodimer
[MDM2:MDMXn]	Nuclear MDM2/MDMX heterodimer
[MDM2:MDMXo]	MDM2/MDMX heterodimer sequestered in the nucleolus
[p53c]	Cytoplasmic p53
[p53n]	Nuclear p53
[MDMX:p53c]	Cytoplasmic MDMX/p53 complex
[MDMX:p53n]	Nuclear MDMX/p53 complex
[MDM2rnac]	Cytoplasmic MDM2 mRNA
[MDM2rnan]	Nuclear MDM2 mRNA

Table 4.1: List of chemical species used in the model with MDMX.

Reaction	Constant	Description	Value
-> [p53c]	T_{p53}	p53 production	7.15/s
-> [MDM2rnan]	B	Basal transcription of MDM2 mRNA	0.0175/s
[MDM2rnac] -> [MDM2rnac]+[MDM2c]	T_{MDM2}	Translation of MDM2 mRNA	0.001/s
-> [MDMXc]	T_{MDMX}	MDMX production	1.32/s
[MDM2rnan] -> [MDM2rnac]	E_{rna}	Export of MDM2 mRNA from the nucleus	5.78e-4/s
[MDM2n] -> [MDM2c]	$E_{protein}$	Export of MDM2 from the nucleus	0.0136/s
[MDMXn] -> [MDMXc]	$E_{protein}$	Export of MDMX from the nucleus	0.0136/s
[MDM2:MDMXn] -> [MDM2:MDMXc]	$E_{protein}$	Export of MDM2:MDMX from the nucleus	0.0136/s
[MDMX:p53n] -> [MDMX:p53c]	$E_{protein}$	Export of MDMX:p53 from the nucleus	0.0136/s
[MDM2c] -> [MDM2n]	I_{MDM2}	Import of MDM2 to the nucleus	0.00323/s
[MDM2:MDMXc] -> [MDM2:MDMXn]	I_{MDM2}	Import of MDM2:MDMX to the nucleus	0.00323/s

Reaction	Constant	Description	Value
[MDMXc] -> [MDMXn]	I_{MDMX}	Import of MDMX to the nucleus	1.73e-7/s
[p53c] -> [p53n]	I_{p53}	Import of p53 to the nucleus	0.000215/s
[MDMX:p53c] -> [MDMX:p53n]	$0.5*I_{MDMX}+0.5*I_{p53}$	Import of MDMX:p53 to the nucleus	0.000107/s
[MDM2n] -> [MDM2o]	No	Nucleolar sequestration of MDM2	0.00480/s
[MDMXn] -> [MDMXo]	No	Nucleolar sequestration of MDMX	0.00480/s
[MDM2:MDMXn] -> [MDM2:MDMXo]	No	Nucleolar sequestration of MDM2:MDMX	0.00480/s
[MDMXc]+[p53c] -> [MDMX:p53c]	k_+	MDMX binding to p53	6e-4/nMs
[MDMXn]+[p53n] -> [MDMX:p53n]	k_+	MDMX binding to p53	6e-4/nMs
[MDM2c]+[MDMXc] -> [MDM2:MDMXc]	k_+	MDM2 MDMX binding	6e-4/nMs
[MDM2n]+[MDMXn] -> [MDM2:MDMXn]	k_+	MDM2 MDMX binding	6e-4/nMs
[MDM2o]+[MDMXo] -> [MDM2:MDMXo]	k_+	MDM2 MDMX binding	6e-4/nMs
[MDM2:MDMXc] -> [MDM2c]+[MDMXc]	k_{-2x}	MDM2:MDMX dissociation	0.0506/s
[MDM2:MDMXn] -> [MDM2n]+[MDMXn]	k_{-2x}	MDM2:MDMX dissociation	0.0506/s
[MDM2:MDMXo] -> [MDM2o]+[MDMXo]	k_{-2x}	MDM2:MDMX dissociation	0.0506/s
[MDMX:p53c] -> [MDMXc]+[p53c]	k_{-xp}	MDMX:p53 dissociation	41.6/s
[MDMX:p53n] -> [MDMXn]+[p53n]	k_{-xp}	MDMX:p53 dissociation	41.6/s
[MDM2n]+[p53n] -> [MDM2n]	U_{p53}	p53 ubiquitination	4.86e-6/nMs
[MDM2c]+[p53c] -> [MDM2c]	U_{p53}	p53 ubiquitination	4.86e-6/nMs
[MDM2:MDMXn]+[p53n] -> [MDM2:MDMXn]	U_{p53}	p53 ubiquitination	4.86e-6/nMs
[MDM2:MDMXc]+[p53c] -> [MDM2:MDMXc]	U_{p53}	p53 ubiquitination	4.86e-6/nMs

Reaction	Constant	Description	Value
[MDM2:MDMXc] -> [MDM2c]	U_{MDMX}	MDM2 bound MDMX ubiquitination	0.000487/s
[MDM2:MDMXn] -> [MDM2n]	U_{MDMX}	MDM2 bound MDMX ubiquitination	0.000487/s
[MDM2:MDMXo] -> [MDM2o]	U_{MDMX}	MDM2 bound MDMX ubiquitination	0.000487/s
[MDM2c]+[MDM2c] -> [MDM2c]	U_{MDM2}	MDM2 auto ubiquitination	2.38e-6/nMs
[MDM2n]+[MDM2n] -> [MDM2n]	U_{MDM2}	MDM2 auto ubiquitination	2.38e-6/nMs
[MDM2o]+[MDM2o] -> [MDM2o]	U_{MDM2}	MDM2 auto ubiquitination	2.38e-6/nMs
[p53c]->	H	protein decay	1.925e-5/s
[p53n]->	H	protein decay	1.925e-5/s
[MDMX:p53c]->	H	protein decay	1.925e-5/s
[MDMX:p53n]->	H	protein decay	1.925e-5/s
[MDM2c]->	H	protein decay	1.925e-5/s
[MDM2n]->	H	protein decay	1.925e-5/s
[MDM2o]->	H	protein decay	1.925e-5/s
[MDMXc]->	H	protein decay	1.925e-5/s
[MDMXn]->	H	protein decay	1.925e-5/s
[MDMXo]->	H	protein decay	1.925e-5/s
[MDM2:MDMXc]->	H	protein decay	1.925e-5/s
[MDM2:MDMXn]->	H	protein decay	1.925e-5/s
[MDM2:MDMXo]->	H	protein decay	1.925e-5/s
[MDM2rnac]->	H_{rna}	decay of MDM2 mRNA	1.444e-4/s
Additional MDM2mRNA is produced according to the formula:			
$I*(f*[p53n])^{1.8}/(k_d^{1.8}+(f*[p53n])^{1.8})$	I	Induced transcription of MDM2 mRNA	71.7/s
	f	Fraction of p53 available for DNA binding	0.0928
	k_d	Dissociation constant for DNA bound p53	12.3nM

Table 4.2: List of reactions and the constants used for them in the model with MDMX.

4.3 Limitations and approximations

When considering models of the sort presented here, there are some aspects worth keeping in mind about the constant parameters in the model. The production rate of p53 or the binding constants between MDM2 and MDMX, for example, are treated as constants in this model. In the real world, however, these numbers could vary with time for any number of reasons. For example, it is possible that p53 is translationally regulated by proteins that have time varying concentrations. Other interacting proteins may also regulate binding between proteins as part of a larger complex, or by having different proportions of the total amount of protein in different phosphorylation states as the result of time varying processes. As such, the constants used should be viewed as approximate parameterizations of more complicated processes rather than estimates of some real value.

Another assumption in the model is that the MDM2 and MDMX system is the primary regulator of p53 levels. Given the existence of other proteins with some similar behaviours to MDM2, such as COP1, it this is not guarantied. It may be the case that different regulators are the most important in different cell types. Obviously in a cell type where other regulators play the dominant role this model would fail.

Finally, it is worth noting that this model does not include phosphorylation states or other post translational modifications to the proteins. This amounts to the assumption that the modifications to these proteins which are induced by DNA damage affect a proportion of the proteins which is constant in time. The most likely way for this to be the case is for some step of the modification process to be sufficiently efficient that all of the target proteins become modified. This is certainly plausible, particularly given the observation in N. Geva-Zatorsky et al 2006[63] that the amount of DNA damage affects the number of p53 pulses but not the amplitude or timing of the pulses. Of course plausible is not the same as having experimental confirmation, and it may be the case that post translational modifications do need to be directly modeled.

4.4 Fitting parameters

Experimental data on the concentrations of p53 MDM2 and MDMX were obtained from Y. Wang et al 2007[83]. Some of the parameters used in the model were chosen by hand, the rest were fit to the data for protein concentrations in WS1 cells using an evolutionary algorithm. The fitting function for the algorithm was minimizing the square of the difference between the natural logarithms of model and experimental protein concentrations. The algorithm was run 75 times for 1,000,000 iterations each time. The parameter set with the smallest difference between the squares of the natural logs of experimental and computed protein levels is used in the reaction list in Table 4.2. The chemical species in the model are listed in Table 4.1. Figures 4.2 and 4.3 show the model and experimental behaviours of the system.

The parameters used here come with the caveat that there is not enough data to confer any real confidence in fitting them. They are superior to the parameters used in the simpler ARF model only in that they have been chosen to approximately reproduce actual quantitative data; they are probably not accurate estimates. The reason for running the algorithm 75 times was that not every run produced model parameters that were consistent with the experimental data. The parameters found for the best five runs of the evolutionary algorithm are displayed in table 4.3. Five was chosen as the cut off here because the range of the fitness function for the first five is 0.205-0.236 and then jumps to 0.305 for the next best run. It is worth noting that the 4^{th} and 5^{th} best runs did not reproduce cytoplasmic MDMX behaviour very well. The fact that there is significant variation in similarly scored parameter sets implies that small variations in the experiment the model was fit to could have significant impact on the best parameters. If the experiment were performed a second time, and the model fit again to the new results some of the model parameters would likely have substantial differences, just because of noise in the experimental results. This is why the final parameterization is not something worth placing a lot of confidence in.

Not every parameter in the model was chosen with the genetic algorithm. MDM2 mRNA translation was assumed to be 0.001/s. This number is totally irrelevant to the model however, since MRM2 mRNA production was tuned and the data does not say anything about MDM2

mRNA levels. MDM2 mRNA was given the same 1 hour 20 minute half-life as in the simpler model. The nuclear export rate of the mRNA was assumed to be 0.000578/s, corresponding to a time of 20 minutes for half the mRNA to move. This is within the range of possibility based on the 5-40 minute time frame for mRNA transport found by A. Mor et al 2010[76]. Since the WS1 cell line is a line of fibroblasts a volume of 500μm^3 was assumed for the nucleus[84], and the nucleolus was given a volume one tenth of that size. The cytoplasmic compartment was assumed to have a volume of 2000μm^3. Unfortunately things like mean or median cell volumes can differ a lot between cell lines as well as within lines due to differing growth conditions, and are not the sort of things that normally get measured. As such experimental values for this volume were not available. The association constants for protein binding were assumed to be $6*10^{-4}$/nMs, a reasonable value based on ranges discussed in S. H. Northrup et al 1992[78]. The genetic algorithm determined protein binding properties by altering dissociation rates. The 10 hour half-life for the proteins was a hold over from the simpler model. In hindsight it would have made more sense to tune this term with the genetic algorithm or else drop it entirely. The dissociation constant for p53 binding to the MDM2 promoter region was set to 12.3nM, the same value that was found experimentally in R. L. Weinberg et al 2005[73].

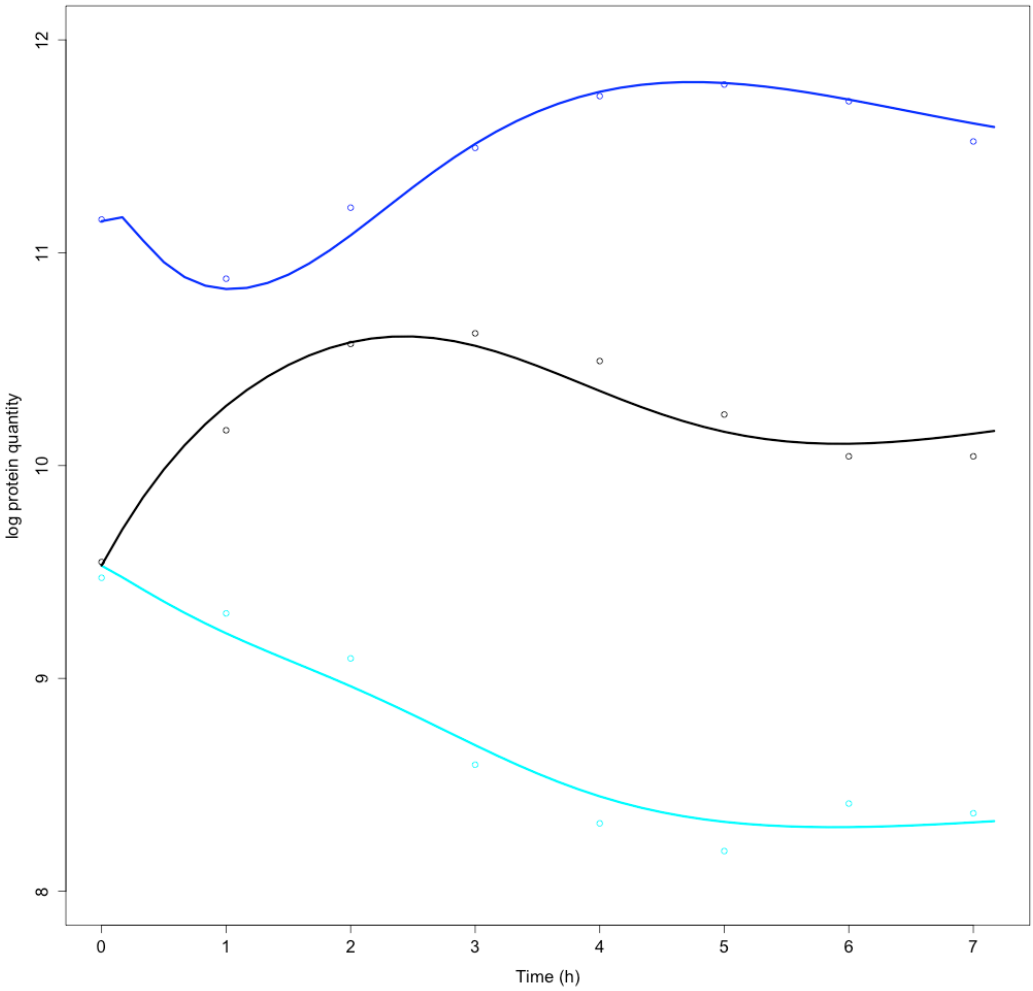

Figure 4.2: Total number of proteins in the cell. Black is p53, dark blue is MDM2 and light blue is MDMX. Points represent the experimental data. The vertical axis uses a natural logarithm. For reference when the natural log of protein quantity is 10 there are 22000 proteins in the cell, corresponding to an average concentration of 15nM.

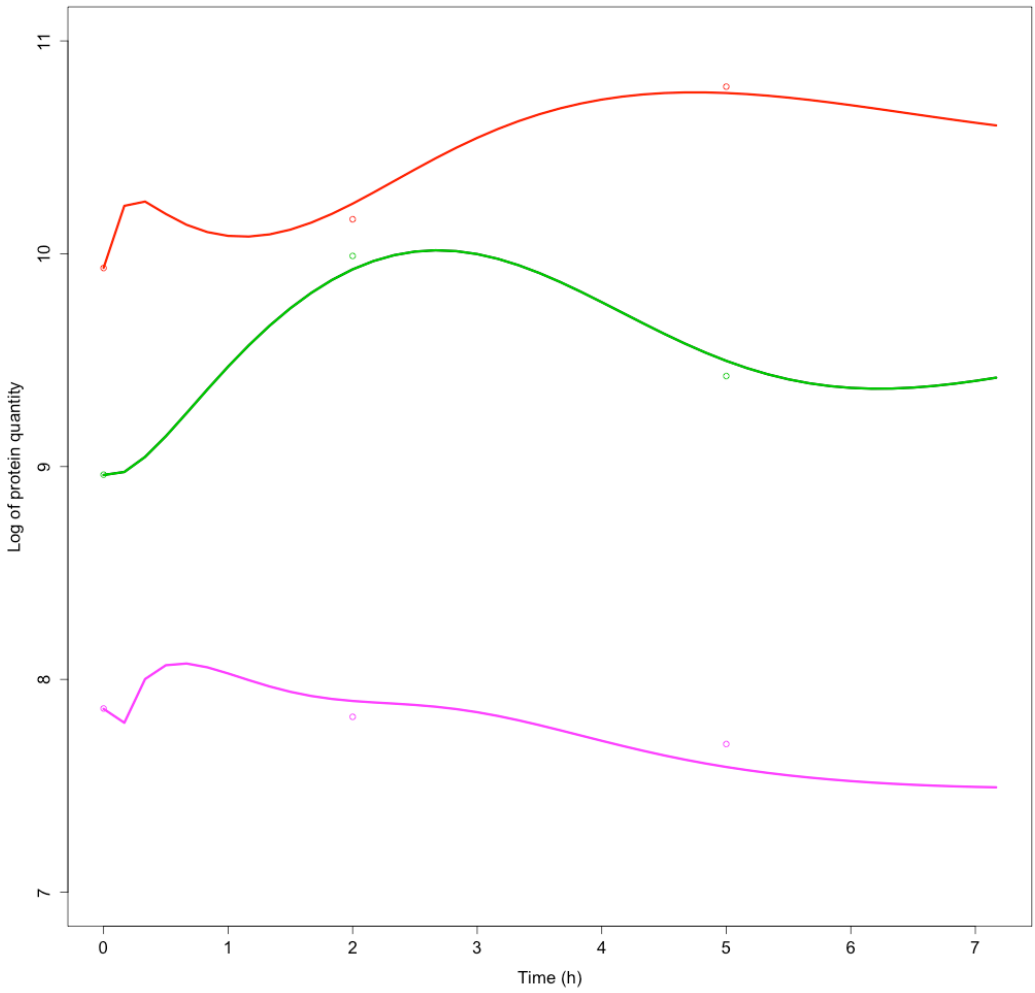

Figure 4.3: Total number of proteins in the nucleus. Red is MDM2, green is p53, and purple is MDMX. Points represent the experimental data. The vertical axis uses a natural logarithm. For reference when the natural log of protein quantity is 10 there are 22000 proteins in the nucleus, corresponding to a concentration of 73nM.

Parameter	Run rank					Min	Max
	1	2	3	4	5		
$\mathbf{T_{p53}}$	7.16	7.19	6.75	6.23	6.64	6.23	7.19
B	0.0175	0.0297	0.00913	0.0142	0.0204	0.00913	0.0297
$\mathbf{I_{MDM2}}$	0.00323	0.00168	0.00252	0.0399	0.0260	0.00168	0.0399
No	0.00480	0.00407	0.0161	0.458	0.295	0.00407	0.458
$\mathbf{k_{-xp}}$	41.6	49.4	2.99	0.00206	0.00216	0.00206	49.4
$\mathbf{U_{MDMX}}$	0.000487	0.000461	0.000779	0.00684	0.00563	0.000461	0.00684
$\mathbf{k_{-2x}}$	0.0506	0.0470	0.108	0.0239	0.0249	0.0239	0.108
$\mathbf{E_{protein}}$	0.0136	0.00462	0.00235	$3.05*10^{-6}$	$4.73*10^{-6}$	$3.05*10^{-6}$	0.0136
$\mathbf{T_{MDMX}}$	1.32	1.27	1.78	15.2	12.9	1.27	15.2
$\mathbf{I_{MDMX}}$	$1.73*10^{-7}$	$3.31*10^{-7}$	$4.37*10^{-8}$	0.000118	0.000100	$4.37*10^{-8}$	0.000100
$\mathbf{U_{p53}}$	$4.86*10^{-6}$	$4.74*10^{-6}$	$5.02*10^{-6}$	$6.60*10^{-6}$	$6.58*10^{-6}$	$4.74*10^{-6}$	$6.60*10^{-6}$
$\mathbf{U_{MDM2}}$	$2.38*10^{-6}$	$2.20*10^{-6}$	$5.30*10^{-6}$	$8.01*10^{-5}$	$5.21*10^{-5}$	$2.20*10^{-6}$	$8.01*10^{-5}$
I	71.7	56.4	676	5625	3079	56.4	5625
$\mathbf{I_{p53}}$	0.000215	0.000220	0.000184	0.000168	0.000171	0.000168	0.000220
f	0.0928	0.102	0.0405	0.0636	0.0711	0.0405	0.0928

Table 4.3: Parameters from the best of the evolutionary algorithm runs. Note that runs 4 and 5 had a significant problem with modeling MDMX levels in the cytoplasm.

4.5 Oscillations

None of the parameter sets out of the 75 produced by the evolutionary algorithm produced sustained oscillations. Since experiments have not shown whether or not WS1 cells exhibit oscillations, this cannot be convincingly compared to reality. Figures 4.4 and 4.5 show the system behaviour when it is run for an extended period of time.

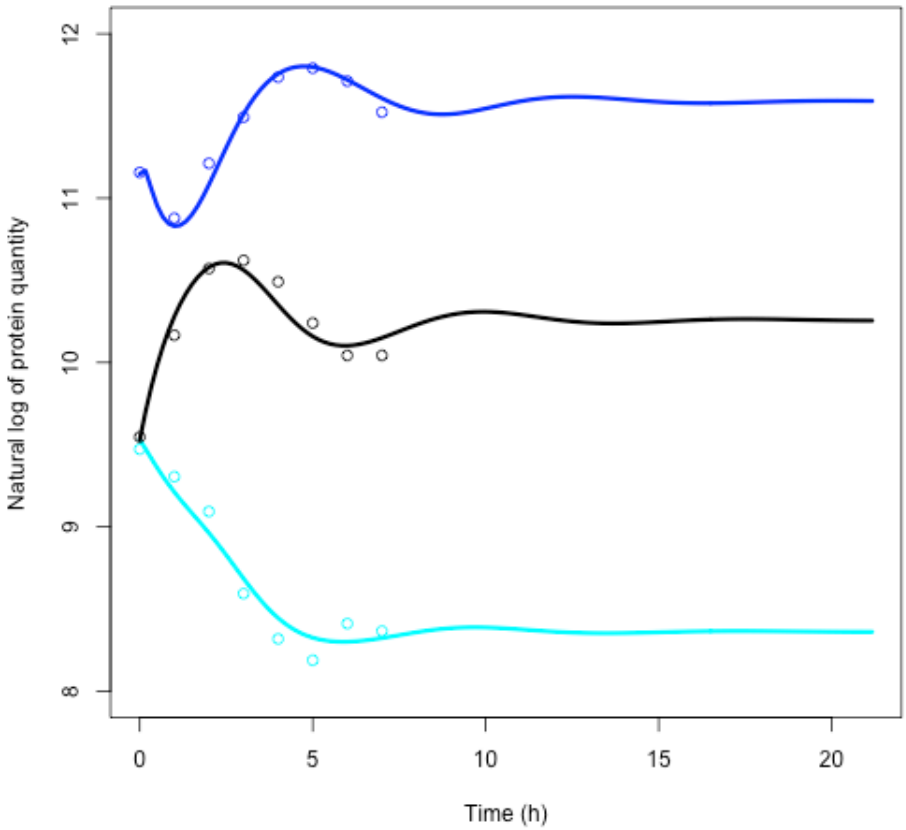

Figure 4.4: Extended graph of cytoplasmic protein quantity. Black is p53, dark blue is MDM2 and light blue is MDMX. Points represent the experimental data. For reference when the natural log of protein quantity is 10 there are 22000 proteins in the cell, corresponding to an average concentration of 15nM.

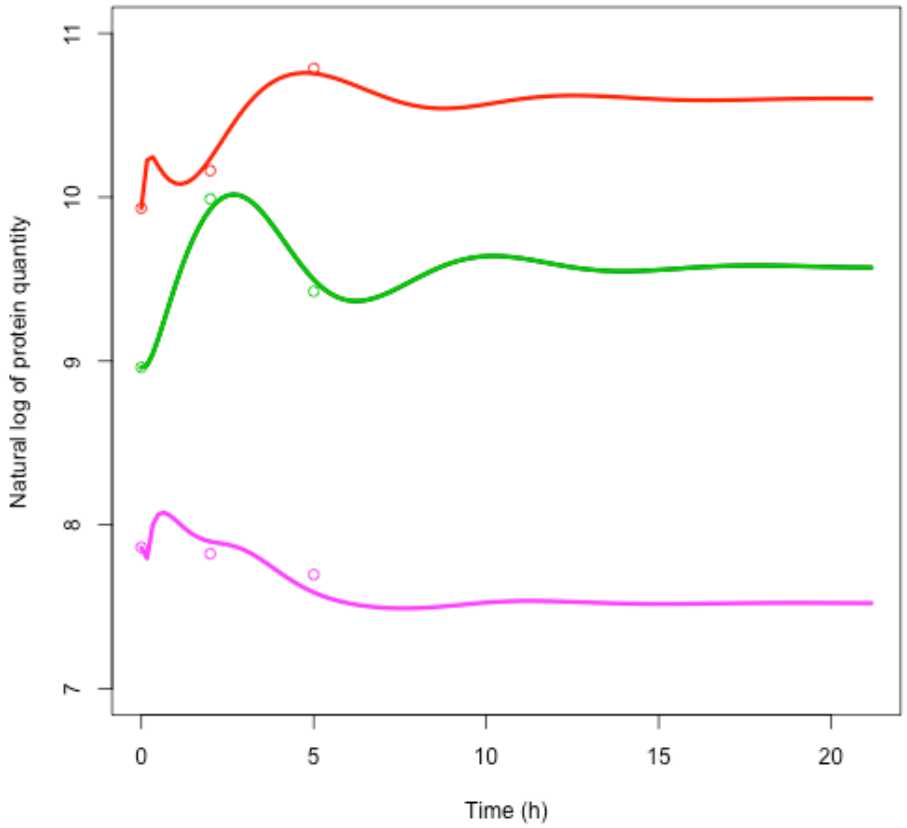

Figure 4.5: Extended graph of nuclear protein quantity. Red is MDM2, green is p53, and purple is MDMX. Points represent the experimental data. For reference when the natural log of protein quantity is 10 there are 22000 proteins in the nucleus, corresponding to a concentration of 73nM.

4.6 Parameter sensitivity

One question that can be asked of this model is how sensitive its behaviour is to changes in the parameters used. Table 4.4 shows the percentage change in free nuclear p53 averaged over 7 hours in response to a change in any of the parameters, other than initial conditions, that were fit using the evolutionary algorithm. Interestingly, changes in any of the parameters result in proportionally smaller changes in p53 levels. This shows that even in this simple model p53 is fairly robust to perturbations in its regulatory system.

Parameter	Description	Percent change in free nuclear p53 when multiplying parameter by:			
		0.5	1.01	1.1	2
f	Fraction of p53 available to bind to DNA	50.0	-0.586	-5.46	-32.8
U_{p53}	Ubiquitination of p53	45.9	-0.535	-5.00	-30.5
I	Maximum inducible MDM2 mrna transcription	33.0	-0.407	-3.82	-24.2
T_{p53}	Production rate of p53	-21.9	0.364	3.56	31.0
No	Nucleolar sequestration rate	-21.0	0.363	3.55	30.0
I_{p53}	Nuclear import of p53	-14.5	0.216	2.07	15.2
U_{MDM2}	MDM2 auto-ubiquitination rate	-3.47	0.0658	0.652	6.03
I_{MDM2}	Nuclear import of MDM2 and MDM2 MDMX heterodimers	1.17	0.0343	0.376	4.53
$E_{protein}$	Export of proteins other then p53 from the nucleus	2.61	-0.0246	-0.211	0.256
T_{MDMX}	Production of MDMX	0.0891	-0.00171	-0.0177	-0.177
U_{MDMX}	Ubiquitination of MDMX that is bound to MDM2	-0.0501	$8.80*10^{-4}$	0.00788	0.0590
B	Basal MDM2 mRNA transcription	0.0294	$-5.74*10^{-4}$	-0.00586	-0.0585
k_{-xp}	Dissociation of p53 and MDMX	-0.00728	$8.60*10^{-5}$	$6.92*10^{-4}$	0.00368
k_{-2x}	Dissociation of MDM2 with MDMX	0.00376	$-4.79*10^{-5}$	$-6.98*10^{-4}$	-0.00437
I_{MDMX}	Import of MDMX to the nucleus	$4.97*10^{-5}$	$1.18*10^{-5}$	$1.31*10^{-5}$	$5.44*10^{-5}$

Table 4.4: Percent change in average nuclear p53 levels in response to changes in parameters.

It is worth considering the implications of parameter sensitivity for drug development. The parameter the system is most sensitive to is the fraction of p53 available for DNA binding. Blocking p53 binding to DNA would not be helpful, since this would also prevent p53 from carrying out its desirable functions. The maximum amount of inducible MDM2 transcription also has a high sensitivity. This could theoretically be blocked by a sequence specific DNA binding agent but probably not by a conventional drug molecule. Ubiquitination of p53 is also a high sensitivity parameter. Since this is caused by MDM2 it suggests drugging MDM2. As shall be seen in the next section targeting MDM2 is effective *in silico*. The production rate of p53 is also a relatively sensitive parameter. Increasing p53 production with drugs, however, would require targeting something outside the scope of this model, assuming it is even possible. Attempting to manipulate the nucleolar sequestration rate may also be viable, but the proteins responsible for nucleolar sequestration are outside the scope of this model.

As it happened in the best parameter set free MDMX transport into the nucleus was essentially non-existent. As such its low parameter sensitivity is unsurprising. What was not expected is that the other parameters involving MDMX also have a low sensitivity. This suggests that MDMX will not work as well as a drug target as MDM2 will. This mirrors the results of the drug models in the next section. It may be the case that MDMX is relatively unimportant in the WS1 cell line, given its low concentration relative to MDM2 and p53.

4.7 Drugged models

Four hypothetical drugs were considered, a MDM2 MDMX dual inhibitor, an inhibitor of MDM2/p53 binding, an inhibitor of MDMX/p53 binding, and an inhibitor of MDM2 MDMX dimerization. It was assumed that these drugs do not interfere with MDM2 auto-ubiquitination, which is plausible based on the results of Z. Lai et al 2001[82], and also desirable because inhibition of this process would likely lead to increased MDM2 levels counteracting the effects of the drug. Since ARF binds to a different site than p53 and the dimerization point between MDM2 and MDMX[85], it is assumed that none of the drugs interfere with nucleolar sequestration. The drug molecules were initialised to an equal concentration in all three cellular compartments. The additional chemical species and reactions needed for the drugged models can be found in Appendix A. Adding the drugs required the addition of several parameters to the model. The drug molecules were assumed to rapidly come to equilibrium between the cellular compartments. Since small molecules can freely pass through the nuclear pores between the cytoplasm and the nucleus[86], this assumption seems reasonable. The specific parameters used were a nuclear import rate of 0.1/s and an export rate of 0.4/s. For transport into and out of the nucleolus the import rate was considered to be 0.01/s and the export rate to be 0.1/s. Keeping the concentration of drug molecules constant in each compartment means that choosing either the import or the export rate fixes the value of the other rate. Because import and export form both the cytoplasm and the nucleolus are happening quickly relative to the other changes in the system, the specific numbers do not really matter as long as the import and export rates have the right ratio. Drug binding was assumed to occur at a rate of 0.0001/nMs and dissociation at a rate of 0.1/s. This represents a dissociation constant of 1μM. For comparison Y. Lu et al 2006[87] found a dissociation constant of 36nM for Nutlin-3, so drugs with a 1μM dissociation constant are certainly achievable. Also for comparison, the association and dissociation rates for MDM2 MAMX heterodimers in this model was 0.0006/nMs and 0.05/s, corresponding to a dissociation constant of 83nM.

Each of the hypothetical drugs was tested on each of 16 different kinds of cell models. The first test was done on the WS1 model as described above. The other fifteen were variants on the WS1 cells having every combination of 2, 5, and 10 times over-expressed MDM2 and MDMX. Initial levels of these proteins were also increased by a corresponding amount. It is doubtful that a real cell with those over-expression levels would actually have a linear dependence between protein over-expression and protein concentration. Since determining the actual initial levels for these hypothetical cells is not practical, a linear dependence was assumed anyway. Also, initial p53 levels were assumed to be the same for all cell variants, which is almost certainly not how real mutated cells would behave. Improving on the modeling of the initial steady state protein levels in the cells would be an interesting and important area for further work.

Nuclear p53 levels of drugged cells were compared to nuclear p53 levels in non-drugged cells of the same type. Figure 4.6 shows the comparison for wild type cells.

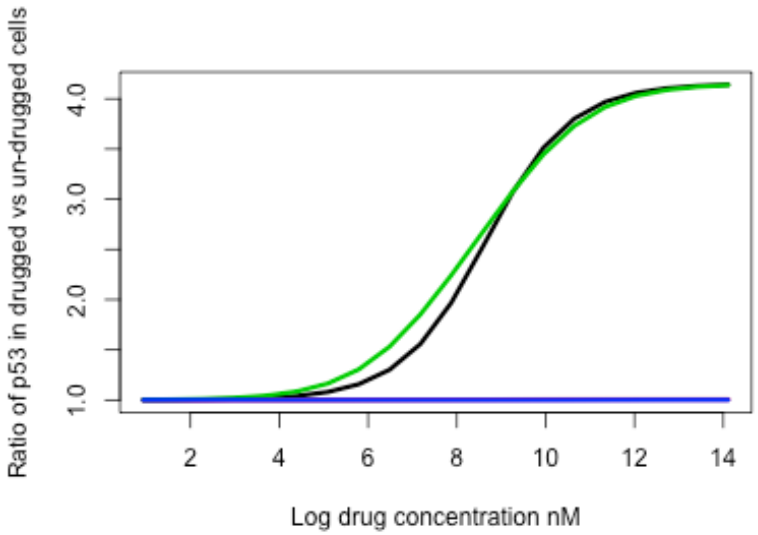

Figure 4.6: Response of wild type cells to hypothetical drugs. The ratio on the vertical axis is based on an average of p53 concentrations over a 7 hour period. The horizontal axis is the natural logarithm of drug concentration in nM. For reference this means that a value of 2 represents a concentration of 7.4nM, a value of 8 means a 3.0μM concentration, and a value of 14 means a 1.2mM concentration. The MDM2 MDMX dual inhibitor is in black, the MDMX p53 binding inhibitor is in red, the MDM2 p53 binding inhibitor is in green and the inhibitor of MDMX binding to MDM2 is in blue.

It is clear from Figure 4.6 that the drugs with the greatest effect on wild type cells in this model are the MDM2 inhibitor and the MDM2/MDMX dual inhibitor. The MDMX and the dimerization inhibitors, on the other hand, appear to be useless. As figure 4.7 shows the MDMX and dimerization inhibitors continue to be useless even when MDMX is over expressed by a factor of 10.

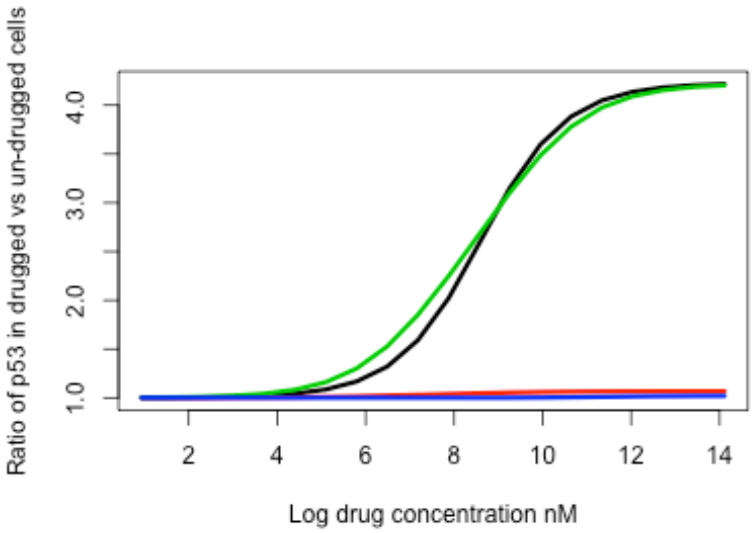

Figure 4.7: Response of cells with 10 times over expressed MDMX to hypothetical drugs. The ratio on the vertical axis is based on an average of p53 concentrations over a 7 hour period. The horizontal axis is the natural logarithm of drug concentration in nM. For reference this means that a value of 2 represents a concentration of 7.4nM, a value of 8 means a 3.0μM concentration, and a value of 14 means a 1.2mM concentration. The MDM2 MDMX dual inhibitor is in black, the MDMX p53 binding inhibitor is in red, the MDM2 p53 binding inhibitor is in green and the inhibitor of MDMX binding to MDM2 is in blue.

The MDM2 inhibitor and the dual inhibitor both increased p53 levels proportionally more in cells with overexpressed MDM2 then in wild type cells. However there was little difference between the performances of the two inhibitors in any cell type. Figure B.1 shows graphs from all cell models. Overall the MDM2 inhibitor and the MDM2 MDMX dual inhibitor performed about equally well, and the MDMX and dimerization inhibitors appear to be useless. This model therefor predicts that targeting MDM2 is far more effective at increasing p53 levels in the WS1 cell line then targeting MDMX. If an experiment showed significant changes in p53 levels as a result of MDMX inhibition in WS1 cells, then that experiment would demonstrate this model to be, at best, seriously flawed.

5 Concluding remarks

5.1 Stochasticity

The work on the ARF model demonstrates that the effects of stochasticity on the behaviour of genetic regulatory networks cannot be dismissed without consideration. In the system presented here, stochastic effects altered every aspect of system behaviour. In addition to desynchronization leading to the appearance of decaying oscillations, the amount of MDM2 in the system increased and the period of the oscillations changed. The changes in MDM2 levels became more obvious when p53 production was near bifurcation points. When the system was put into a state with decaying oscillations, the quantity of MDM2 still remained above that in the deterministic model, showing that stochasticity still alters behaviour as a system is near a steady state. Furthermore, stochastic systems will not necessarily undergo damped oscillations even when given parameters that would cause damped oscillations in a deterministic system. Instead they may show sporadic oscillation like excursions from the mean behaviour. It would seem then that even for cells in a steady state, the distribution of protein levels across a population and over time could wreak havoc with attempts to model cell behaviour. This has implications for anyone wishing to model cell-level processes as systemic errors could occur in deterministic models with no obvious way to compensate for them. As computers and algorithms improve, it may be the case that simply moving to stochastic modeling of cell populations will become the most practical solution.

The demonstration that stochasticity can be relevant is very general, but it was also shown that the magnitude of the effects could vary significantly between systems. The effect on mean protein levels could be around 5% as in the original parameter set, or around 50% as in some of the parameter sets with differing p53 levels. The obvious way to experimentally test the relevance of stochasticity on any given system is by comparing data from cell populations to data from individual cells. Such experimental comparisons were, after all, the inspiration for investigating stochasticity in this system in the first place. The difference between a stochastic model and a deterministic one with different parameters are not likely to be obvious from just population data, even if the effects of stochasticity are expected to be large. Testing the details of stochastic models will require looking at the behaviour of individual cells. Of course stochasticity is not the only factor that could drive individual cells to different behaviours. Factors such as differences in cell size, different cell cycle stages, and anisotropies in cell culture medium could all alter behaviour on the scale of single cells. Untangling these effects is an area for future research.

5.2 Modeling drug response

Modeling of p53 drug responses is problematic at the current time. Lack of experimental data means that it is hard to construct a quantitative model with information gleaned from a single species, let alone a single cell type. As such, even though MDM2 inhibitors and the MDM2 MDMX dual inhibitors were clearly far more effective on the model system than the others, it cannot be said with any confidence that this would carry over into the real world, i.e. there may not be a correlation between *in silico*, *in vitro* and *in vivo* effects. Future efforts in modeling would be greatly helped by an effort to gather data systematically on a single cell type, preferably one without known abnormalities in the p53 pathway. Variables such as protein production and degradation rates are generally not constant over time, so time-dependent measurements of these values would greatly reduce the number of assumptions and better constrain the parameters in the models. Furthermore there may be changes in the volume of cellular compartments as a result of stress or the p53 stress response. Knowing mean volumes of cell compartments in the experiments would be helpful for modeling. Measurements of import and export rates of the proteins from the nucleus would also be very helpful for future work.

If the drug response model could be improved sufficiently a great deal more could be accomplished with it. With a proper scripting system set up, altering drug behaviour and generating new results becomes a simple task. For example by making the drugs get metabolized

over time would only require a few additional terms in the model. If one wanted to account for a polymorphism in one of the proteins that alters that protein's interactions in some known way, the constants in the model could be altered and the drug model rerun to make new predictions. In the case of a cell that is heterozygous for the relevant polymorphism this could be time consuming however, since it may require adding a second set of reactions to account for the discrepancy between the proteins. Of course once that is done the first time other heterozygous polymorphisms of the same protein would be much faster, because the code could be reused.

Another way of expanding the utility of the model would be to link it to other models of related processes. The DNA repair and damage detection modules in L. Ma et al 2005[70] would be a good example of this. Once one system is sufficiently well understood it would be possible to begin looking at how altering it changes connected systems, or conversely, how changing connected systems alters it. This could allow one to find out about down stream drug effects. For that kind of work it would likely be best to start as far upstream as possible, in order to facilitate the experimental control of inputs. For example for the p53 system it would make sense to start with a model of how much damage ionizing radiation causes to DNA and other cellular systems, because the level of radiation a cell is exposed to can be controlled in the lab. Then, once that is modeled well, move on to the DNA damage detection systems, and finally on to the p53 response. Repeating this process for other forms of damage, like for example ultraviolet light, could bring a lot of insight into the systems behaviour.

Other altered cell scenarios could provide a good experimental test for the model. For example removing MDMX production using siRNA. This would enable a comparison between experimental data taken from siRNA exposed cells and the model predictions. The same thing could be done with MDM2 and ARF. Although marginal results are possible, the effect of experimental uncertainty on data from knock outs of key proteins is likely to be small enough to allow for model validation or refutation. Of course given the current lack of data to fit the model in the first place it may be better to use some of the experiments to refit the model parameters and test the new model in other ways. The most significant way this model could be tested would be to replace the binding properties of the hypothetical drugs with the properties of an actual inhibitor such as Nutlin-3, or something as yet undiscovered, since predicting drug response was the primary reason for constructing this model.

Bibliography

[1] Participation of p53 Protein in the Cellular Response to DNA Damage, M. B. Kastan, O. Onyekwere, D. Sidransky, B. Vogelstein, R. W. Craig, Cancer Res. **51**, 6304 (1991)
[2] Influenza Virus Infection Increases p53 Activity: Role of p53 in Cell Death and Viral Replication, E. Turpin, K. Luke, J. Jones, T. Tumpey, K. Konan, S. Schultz-Cherry, J. Virol. **79** (14), 8802 (2005)
[3] Posttranslational Modification of p53: Cooperative Integrators of Function, D. W. Meek, C. W. Anderson, Cold Spring Harb. Perspect. Biol. (2009)
[4] H. Lodish, A. Berk, C. A. Kaiser, M. Kriger, M. P. Scott, A. Bretscher, H. Ploegh, P. Matsudaira, *Molecular Cell Biology* 6th ed. (W. H. Freeman and Company, New York, 2008)
[5] Wild-type p53 triggers a rapid senescence program in human tumor cells lacking functional p53, M. M. Sugrue, D. Y. Shin, S. W. Lee, S. A. Aaronson, Proc. Natl. Acad. Sci. U.S.A. **94** (18), 9648 (1997)
[6] Shaping Genetic Alterations in Human Cancer: The p53 Mutation Paradigm, T. Soussi, K. G. Wiman, Cancer Cell **12** (4), 303 (2007)
[7] The MDM2 gene amplification database, J. Momand, D. Jung, S. Wilczynski, J. Niland, Nucleic Acids Res. **26** (15), 3453 (1998)
[8] Amplification of Mdmx (or Mdm4) Directly Contributes to Tumor Formation by Inhibiting p53 Tumor Suppressor Activity, D. Danovi, E. Meulmeester, D. Pasini, D. Migliorini, M. Capra, R. Frenk, P. de Graaf, S. Francoz, P. Gasparini, A. Gobbi, K. Helin, P. G. Pelicci, A. G. Jochemsen, J. C. Marine, Mol. Cell Biol. **24** (13), 5835 (2004)
[9] Restoration of p53 function leads to tumour regression in vivo, A. Ventura, D. G. Kirsch, M. E. McLaughlin, D. A. Tuveson, J. Grimm, L. Lintault, J. Newman, E. E. Reczek, R. Weissleder, T. Jacks, Nature **445**, 661 (2007)
[10] How to improve R&D productivity: the pharmaceutical industry's grand challenge S. M. Paul, D. S. Mytelka, C. T. Dunwiddie, C. C. Persinger, B. H. Munos, S. R. Lindborg, A. L. Schacht, Nat. Drug Discovery **9** (3), 203 (2010)
[11] B. Alberts, D. Bray, J. Lewis, M. Raff, K. Roberts, J. D. Watson, *Molecular Biology of the Cell* 3rd ed. (Garland Publishing Inc., New York, 1994)
[12] UV irradiation stimulates levels of p53 cellular tumor antigen in nontransformed mouse cells, W. Maltzman, L. Czyzyk, Mol. Cell Biol. **4** (9), 1689 (1984)
[13] Hypoxia induces accumulation of p53 protein, but activation of a G1-phase checkpoint by low-oxygen conditions is independent of p53 status, T. G. Graeber, J. F. Peterson, M. Tsai, K. Monica, A. J. Fornace Jr., A. J. Giaccia, Mol. Cell Biol. **14** (9), 6264 (1994)
[14] Cellular Adhesion Regulates p53 Protein Levels in Primary Human Keratinocytes, J. M. Nigro, K. D. Aldape, S. M. Hess, T. D. Tlsty, Cancer Res. **57**, 3635 (1997)
[15] A reversible, p53-dependent G0/G1 cell cycle arrest induced by ribonucleotide depletion in the absence of detectable DNA damage, S. P. Linke, K. C. Clarkin, A. D. Leonardo, A. Tsou, G. M. Wahl, Genes Dev. **10** (8), 934 (1996)
[16] Direct interaction of the hepatitis B virus HBx protein with p53 leads to inhibition by HBx of p53 response element-directed transactivation, R. Truant, J. Antunovic, J. Greenblatt, C. Prives, J. A. Cromlish, J. Virol. **69** (3), 1851 (1995)
[17] The large T antigen of simian virus 40 binds and inactivates p53 but not p73, M. Dobbelstein, J. Roth, J. Gen. Virol. **79** (12), 3079 (1998)
[18] p53 post-translational modification: deregulated in tumorigenesis, C. Dai, W. Gu, Trends Mol. Med. **16** (11), 528 (2010)
[19] Analysis of p53-regulated gene expression patterns using oligonucleotide arrays, R. Zhao, K. Gish, M. Murphy, Y. Yin, D. Notterman, W. H. Hoffman, E. Tom, D. H. Mack, A. J. Levine, Genes Dev. **14** (8), 981 (2000)
[20] p53 has a direct apoptogenic role at the mitochondria, M. Mihara, S. Erster, A. Zaika, O. Petrenko, T. Chittenden, P. Pancoska, U. M. Moll, Mol. Cell **11** (3), 577 (2003)
[21] MDM2 is a Central Node in the p53 Pathway: 12 Years and Counting, G. L. Bond, W. Hu, A. J. Levine, Curr. Cancer Drug Targets **5** (1), 3 (2005)

[22] Oncoprotein MDM2 is a ubiquitin ligase E3 for tumour suppressor p53, R. Honda, H. Tanaka, H. Yasuda, FEBS Lett. **420** (1), 25 (1997)
[23] Regulation of p53 stability by Mdm2, M. H. G. Kubbutat, S. N. Jones, K. H. Vousden, Nature **387**, 299 (1997)
[24] Mdm2 promotes the rapid degradation of p53, Y. Haupt, R. Maya, A. Kazaz, M. Oren, Nature **387**, 296 (1997)
[25] MDM2 expression is induced by wild type p53 activity, Y. Barak, T. Juven, R. Haffner, M. Oren EMBO J. **12** (2), 461 (1993)
[26] Mdm2 Is a RING Finger-dependent Ubiquitin Protein Ligase for Itself and p53, S. Fang, J. P. Jensen, R. L. Ludwig, K. H. Vousden, A. M. Weissman, J. Biol. Chem. **275** (12), 8945 (2000)
[27] Regulation of Transcription Functions of the p53 Tumor Suppressor by the mdm-2 Oncogene, J. Chen, J. Lin, A. J. Levine, Mol. Med. **1** (2), 142 (1995)
[28] Identification of a cryptic nucleolar-localization signal in MDM2, M. A. E. Lohrum, M. Ashcroft, M. H. G. Kubbutat, K. H. Vousden, Nature Cell Biol. **2**, 179 (2000)
[29] In vivo activation of the p53 pathway by small-molecule antagonists of MDM2, L. T. Vassilev, B. T. Vu, B. Graves, D. Carvajal, F. Podlaski, Z. Filipovic, N. Kong, U. Kammlott, C. Lukacs, C. Klein, N. Fotouhi, E. A. Liu, Science **303** (5659), 844 (2004)
[30] Recent advances in the therapeutic perspectives of Nutlin-3, P. Secchiero, R. Bosco, C. Celeghini, G. Zauli, Curr. Pharm. Des. **17** (6), 567 (2011)
[31] Hypoxia Enhances Metastatic Efficiency by Up-Regulating Mdm2 in KHT Cells and Increasing Resistance to Apoptosis, Li Zhang, Richard P. Hill, Cancer Res. **64** (12), 4180 (2004)
[32] Nutlin-3 radiosensitizes hypoxic prostate cancer cells independent of p53, S. Supiot, R. P. Hill, R. G. Bristow, Mol. Cancer Ther. **7** (4), 993 (2008)
[33] Molecular mimicry-based repositioning of nutlin-3 to anti-apoptotic Bcl-2 family proteins, J. H. Ha, E. Y. Won, J. S. Shin, M. Jang, K. S. Ryu, K. H. Bae, S. G. Park, B. C. Park, H. S. Yoon, S. W. Chi, J. Am. Chem. Soc. **133** (5), 1244 (2011)
[34] MDMX: a novel p53-binding protein with some functional properties of MDM2, A. Shvarts, W. T. Steegenga, N. Riteco, T. van Laar, P. Dekker, M. Bazuine, R. C. van Ham, W. van der Houven van Oordt, G. Hateboer, A. J. van der Eb, A. G. Jochemsen, EMBO J. **15** (19), 5349, (1996)
[35] Mdmx Is a Negative Regulator of p53 Activity in Vivo, R. A. Finch, D. B. Donoviel, D. Potter, M. Shi, A. Fan, D. D. Freed, C. Wang, B. P. Zambrowicz, R. Ramirez-Solis, A. T. Sands, N. Zhang, Cancer Res. **62** (11), 3221 (2002)
[36] Stabilization of the MDM2 Oncoprotein by Interaction with the Structurally Related MDMX Protein, D. A. Sharp, S. A. Kratowicz, M. J. Sank, D. L. George, J. Biol. Chem. **274** (53), 38189 (1999)
[37] Mdmx enhances p53 ubiquitination by altering the substrate preference of the Mdm2 ubiquitin ligase, K. Okamoto, Y. Taya, H. Nakagama, FEBS Lett. **583** (17), 2710 (2009)
[38] Hdmx Protein Stability Is Regulated by the Ubiquitin Ligase Activity of Mdm2, P. de Graaf, N. A. Little, Y. F. M. Ramos, E. Meulmeester, S. J. F. Letteboer, A. G. Jochemsen, J. Biol. Chem. **278** (40), 38315 (2003)
[39] MDMX: from bench to bedside, J-C. W. Marine, M. A. Dyer, A. G. Jochemsen, J. Cell Sci. **120** (3), 371 (2007)
[40] Regulation of MDMX nuclear import and degradation by Chk2 and 14-3-3, C. LeBron, L. Chen, D. M. Gilkes, J. Chen, EMBO J. **25** (6), 1196 (2006)
[41] Mutual Dependence of MDM2 and MDMX in Their Functional Inactivation of p53, J. Gu, H. Kawai, L. Nie, H. Kitao, D. Wiederschain, A. G. Jochemsen, J. Parant, G. Lozano, Z. Yuan, J. Biol. Chem. **277** (22), 19251 (2002)
[42] Identification and Characterization of the First Small Molecule Inhibitor of MDMX, D. Reed, Y. Shen, A. A. Shelat, L. A. Arnold, A. M. Ferreira, F. Zhu, N. Mills, D. C. Smithson, C. A. Regni, D. Bashford, S. A. Cicero, B. A. Schulman, A. G. Jochemsen, R. K. Guy, M. A. Dyer, J. Biol. Chem. **285** (14), 10786 (2010)
[43] A small-molecule inhibitor of MDMX activates p53 and induces apoptosis, H. Wang, X. Ma, S. Ren, J. K. Buolamwini, C. Yan, **10** (1), 69 (2010)
[44] The p53 pathway: positive and negative feedback loops, S. L. Harris, A. J. Levine, Oncogene

24 (17), 2899 (2005)
[45] DNA damage activates ATM through intermolecular autophosphorylation and dimer dissociation, C. J. Bakkenist, M. B. Kastan, Nature **421**, 495 (2003)
[46] Enhanced phosphorylation of p53 by ATM in response to DNA damage, S. Banin, L. Moyal, S.-Y. Shieh, Y. Taya, C. W. Anderson, L. Chessa, N. I. Smorodinsky, C. Prives, Y. Reiss, Y. Shiloh, Y. Ziv Science **281**, 5383 (1998)
[47] ATM-dependent phosphorylation of Mdm2 on serine 395: role in p53 activation by DNA damage, R. Maya, M. Balass, S.-T. Kim, D. Shkedy, J.-F. M. Leal, O. Shifman, M. Moas, T. Buschmann,Z. Ronai, Y. Shiloh, M. B. Kastan, E. Katzir, M. Oren, Genes Dev. **15** (9), (2001)
[48] Ataxia telangiectasia-mutated phosphorylates Chk2 *in vivo* and *in vitro,* S. Matsuoka, G. Rotman, A. Ogawa, Y. Shiloh, K. Tamai, S. J. Elledge, Proc. Natl. Acad. Sci. U.S.A. **97** (19), 10389 (2000)
[49] A role for ATR in the DNA damage-induced phosphorylation of p53, R. S. Tibbetts, K. M. Brumbaugh, J. M. Williams, J. N. Sarkaria, W. A. Cliby, S. Y. Shieh, Y. Taya, C. Prives, R. T. Abraham, Genes Dev. 13 (2), 152 (1999)
[50] The human homologs of checkpoint kinases Chk1 and Cds1 (Chk2) phosphorylate p53 at multiple DNA damage-inducible sites, S.-Y. Shieh, J. Ahn, K. Tamai, Y. Taya, C. Prives, Genes Dev. **14** (3), 289 (2000)
[51] Chk2/hCds1 functions as a DNA damage checkpoint in G_1 by stabilizing p53, N. H. Chehab, A. Malikazay, M. Appel, T. D. Halazonetis, Genes Dev. **14** (3), 278 (2000)
[52] ARF Promotes MDM2 Degradation and Stabilizes p53: ARF-INK4a Locus Deletion Impairs Both the Rb and p53 Tumor Suppression Pathways, Y. Zhang, Y. Xiong, W. G. Yarbrough, Cell **92** (6), 725 (1998)
[53] MdmX Binding to ARF Affects Mdm2 Protein Stability and p53 Transactivation, M. W. Jackson, M. S. Lindstrom, S. J. Berberich, J. Biol. Chem. **276** (27), 25336 (2001)
[54] Nucleolar Arf sequesters Mdm2 and activates p53, J. D. Weber, L. J. Taylor, M. F. Roussel, C. J. Sherr, D. Bar-Sagi, Nat. Cell Biol. **1** (1), 20 (1999)
[55] The alternative product from the human CDKN2A locus, p14ARF, participates in a regulatory feedback loop with p53 and MDM2, F. J. Stott, S. Bates, M. C. James, B. B. McConnell, M. Starborg, S. Brookes, I. Palmero, K. Ryan, E. Hara, K. H. Vousden, G. Peters, EMBO J. **17** (17), 5001 (1998)
[56] Tumor suppression by Ink4a±Arf: progress and puzzles, S. W. Lowe, C. J. Sherr, Curr. Opin. Genet. Dev. **13** (1), 77 (2003)
[57] Wip1, a novel human protein phosphatase that is induced in response to ionizing radiation in a p53-dependent manner, M. Fiscella, H. Zhang, S. Fan, K. Sakaguchi, S. Shen, W. E. Mercer, G. F. Vande Woude, P. M. O'Connor, E. Appella, Proc. Natl. Acad. Sci. U.S.A. **94** (12), 6048 (1997)
[58] Wip1 Phosphatase Modulates ATM-Dependent Signaling Pathways, S. Shreeram, O. N. Demidov, W. K. Hee, H. Yamaguchi, N. Onishi, C. Kek, O. N. Timofeev, C. Dudgeon, A. J. Fornace, C. W. Anderson, Y. Minami, E. Appella, D. V. Bulavin, Mol. Cell **23** (5), 757 (2006)
[59] Regulation of the antioncogenic Chk2 kinase by the oncogenic Wip1 phosphatase, H. Fujimoto, N. Onishi, N. Kato, M. Takekawa, X. Z. Xu, A. Kosugi, T. Kondo, M. Imamura, I. Oishi, A. Yoda, Y. Minami, Cell Death Differ. **13** (7), 1170 (2006)
[60] Pirh2, a p53-Induced Ubiquitin-Protein Ligase, Promotes p53 Degradation, R. P. Leng, Y. Lin, W. Ma, H. Wu, B. Lemmers, S. Chung, J. M. Parant, G. Lozano, R. Hakem, S. Benchimol, Cell **112** (6), 779 (2003)
[61] The ubiquitin ligase COP1 is a critical negative regulator of p53, D. Dornan, I. Wertz, H. Shimizu, D. Arnott, G. D. Frantz, P. Dowd, K. O' Rourke, H. Koeppen, V. M. Dixit, Nature **429**, 86 (2004)
[62] Dynamics of the p53-Mdm2 feedback loop in individual cells, G. Lahav, N. Rosenfeld, A. Sigal, N. Geva-Zatorsky, A. J. Levine, M. B Elowitz, U. Alon, Nat. Genet. **36**, 147 (2004)
[63] Oscillations and variability in the p53 system, N. Geva-Zatorsky, N. Rosenfeld, S. Itzkovitz, R. Milo, A. Sigal, E. Dekel, T. Yarnitzky, Y. Liron, P. Polak, G. Lahav, U. Alon, Mol. Syst. Biol. **2**, 33 (2006)
[64] Fourier analysis and systems identification of the p53 feedback loop, N. Geva-Zatorskya, E. Dekela, E. Batchelor, G. Lahav, U. Alon, Proc. Natl. Acad. Sci. U.S.A. **107** (30), 13550 (2010)

[65] A Single Nucleotide Polymorphism in the MDM2 Gene Disrupts the Oscillation of p53 and MDM2 Levels in Cells, W. Hu, Z. Feng, L. Ma, J. Wagner, J. J. Rice, G. Stolovitzky, A. J. Levine, Cancer Res. **67** (6), 2757 (2007)
[66] Stimulus-dependent dynamics of p53 in single cells, E. Batchelor, A. Loewer, C. Mock, G. Lahav, Mol. Syst. Biol. **7**, 488 (2011)
[67] Real-time Evaluation of p53 Oscillatory Behavior *In vivo* Using Bioluminescent Imaging, D. A. Hamstra, M. S. Bhojani, L. B. Griffin, B. Laxman, B. D. Ross, A. Rehemtulla, Cancer Res. **66** (15), 7482 (2006)
[68] Generation of oscillations by the p53-Mdm2 feedback loop: A theoretical and experimental study, R. L. Bar-Or, R. Maya, L. A. Segel, U. Alon, A. J. Levine, M. Oren, Proc. Natl. Acad. Sci. U.S.A. **97** (21), 11250 (2000)
[69] Stochastic Modeling and Simulation of the p53-MDM2/MDMX Loop, X. Cai Z.-M. Yuan, J. Comput. Biol. **16** (7), 917 2009
[70] A plausible model for the digital response of p53 to DNA damage, L. Ma, J. Wagner, J. J. Rice, W. Hu, A. J. Levine, G. A. Stolovitzky, Proc. Natl. Acad. Sci. U.S.A. **102** (40), 14266 (2005)
[71] Recurrent Initiation: A Mechanism for Triggering p53 Pulses in Response to DNA Damage, E. Batchelor, C. S. Mock, I. Bhan, A. Loewer, G. Lahav, Mol. Cell **30** (3), 277 (2008)
[72] Oscillations and bistability in the stochastic model of p53 regulation, K. Puszyński, B. Hat, T. Lipniacki, J. Theor. Biol. **254** (2), 452 (2008)
[73] Comparative Binding of p53 to its Promoter and DNA Recognition Elements, R. L. Weinberg, D. B. Veprintsev, M. Bycroft, A. R. Fersht, J. Mol. Biol. **348**, 589 (2005)
[74] Characterization of the 50 and 30 untranslated regions in murine mdm2 mRNAs, S. M. Mendrysa, M. K. McElwee, M. E. Perry, Gene **264** (1), 139 (2001)
[75] DNA-damaging Aryl Hydrocarbons Induce Mdm2 Expression via p53-independent Post-transcriptional Mechanisms, A. Hsing, D. V. Faller, C. Vaziri, J. Biol. Chem. **275** (34), 26024 (2000)
[76] Dynamics of single mRNP nucleocytoplasmic transport and export through the nuclear pore in living cells, A. Mor, S. Suliman, R. Ben-Yishay, S. Yunger, Y. Brody, Y. Shav-Tal, Nat. Cell Biol. **12** (6), 543 (2010)
[77] N-terminal polyubiquitination and degradation of the Arf tumor suppressor, M-L. Kuo, W. D. Besten, D. Bertwistle, M. F. Roussel, C. J. Sherr, Genes Dev. **18** (15), 1862 (2004)
[78] Kinetics of protein-protein association explained by Brownian dynamics computer simulations, S. H. Northrup, H. P. Erickson, Proc. Natl Acad. Sci. U.S.A. **89** (8), 3338 (1992)
[79] The MDM2 RING-finger domain is required to promote p53 nuclear export R. K. Geyer, Z. K. Yu, C. G. Maki, Nat. Cell Biol. **2** (9), 569 (2000)
[80] C-Terminal Ubiquitination of p53 Contributes to Nuclear Export, M. A. E. Lohrum, D. B. Woods, R. L. Ludwig, É. Bálint, K. H. Vousden 21 (24), 8521 (2001)
[81] Accelerated MDM2 auto-degradation induced by DNA-damage kinases is required for p53 activation, J. M. Stommel, G. M. Wahl, EMBO J. **23** (7), 1547 (2004)
[82] Differentiation of Hdm2-mediated p53 ubiquitination and Hdm2 autoubiquitination activity by small molecular weight inhibitors, Z. Lai, T. Yang, Y. B. Kim, T. M. Sielecki, M. A. Diamond, P. Strack, M. Rolfe, M. Caligiuri, P. A. Benfield, K. R. Auger, R. A. Copeland, Proc. Natl. Acad. Sci. U.S.A. **99** (23), 14734 (2002)
[83] Quantitative analyses reveal the importance of regulated Hdmx degradation for P53 activation, Y. V. Wang, M. Wade, E. Wong, Y. Li, L. W. Rodewald, G. M. Wahl, Proc. Natl. Acad. Sci. U.S.A. **104** (30), 12365 (2007)
[84] Nuclear substructure and dynamics, A. I. Lamond, J. E. Sleeman, Curr. Biol. **13** (21), R825 (2003)
[85] The Mdm2–p53 relationship evolves: Mdm2 swings both ways as an oncogene and a tumor suppressor, J. J. Manfredi, Genes & Dev. **24**, 1580 (2010)
[86] B. Lewin, *Genes VII* (Oxford University Press Inc., New York, 2000)
[87] Discovery of a nanomolar inhibitor of the human murine double minute 2 (MDM2)-p53 interaction through an integrated, virtual database screening strategy, Y. Lu, Z. Nikolovska-Coleska, X. Fang, W. Gao, S. Shangary, S. Qiu, D. Qin, S. Wang, **49** (13), 3759 (2006)

Appendix A: Reactions and chemical species used in drugged models

Dual inhibitor species	
Chemical	**Description**
[Drugc]	Free drug in the cytoplasm
[Drugn]	Free drug in the nucleus
[Drugo]	Free drug in the nucleolus
[Drug:MDM2c]	MDM2 bound drug in the cytoplasm
[Drug:MDM2n]	MDM2 bound drug in the nucleus
[Drug:MDM2o]	MDM2 bound drug in the nucleolus
[Drug:MDMXc]	MDMX bound drug in the cytoplasm
[Drug:MDMXn]	MDM2 bound drug in the nucleus
[Drug:MDMXo]	MDM2 bound drug in the nucleus
[Drug:MDM2:MDMXc]	drug bound to a MDM2 MDMX heterodimer in the cytoplasm
[Drug:MDM2:MDMXn]	drug bound to a MDM2 MDMX heterodimer in the nucleus
[Drug:MDM2:MDMXo]	drug bound to a MDM2 MDMX heterodimer in the nucleolus
[2Drug:MDM2:MDMXc]	2 drugs bound to a MDM2 MDMX heterodimer in the cytoplasm
[2Drug:MDM2:MDMXn]	2 drugs bound to a MDM2 MDMX heterodimer in the nucleus
[2Drug:MDM2:MDMXo]	2 drugs bound to a MDM2 MDMX heterodimer in the nucleolus

Table A.1: Chemical species added in the MDM2 MDMX dual inhibitor model.

Dual inhibitor reactions			
Reaction	**Constant**	**Description**	**Value**
[Drugn] -> [Drugc]	E_{Drug}	Nuclear export of drug molecules	0.4/s
[Drug:MDM2n] -> [Drug:MDM2c]	$E_{protein}$	Export of drug bound MDM2 from the nucleus	0.0136/s
[Drug:MDMXn] -> [Drug:MDMXc]	$E_{protein}$	Export of drugged MDMX from the nucleus	0.0136/s
[Drug:MDM2:MDMXn] -> [Drug:MDM2:MDMXc]	$E_{protein}$	Nuclear export of drugged MDM2:MDMX	0.0136/s
[2Drug:MDM2:MDMXn] -> [2Drug:MDM2:MDMXc]	$E_{protein}$	Nuclear export of drugged MDM2:MDMX	0.0136/s
[Drug:MDM2n] -> [Drug:MDM2o]	No	Nucleolar sequestration of drugged MDM2	0.00480/s
[Drug:MDMXn] -> [Drug:MDMXo]	No	Nucleolar sequestration of drugged MDMX	0.00480/s
[Drug:MDM2:MDMXn] -> [Drug:MDM2:MDMXo]	No	Nucleolar sequestration of drugged MDM2:MDMX	0.00480/s
[2Drug:MDM2:MDMXn] -> [2Drug:MDM2:MDMXo]	No	Nucleolar sequestration of drugged MDM2:MDMX	0.00480/s

Reaction	Constant	Description	Value
[Drugn] -> [Drugo]	No_{drug}	Nucleolar drug import	0.1/s
[Drugo] -> [Drugn]	Ne_{drug}	Nucleolar drug export	0.01/s
[Drugc] -> [Drugn]	I_{drug}	Nuclear import of drug molecules	0.1/s
[Drug:MDM2c] -> [Drug:MDM2n]	I_{MDM2}	Import of drug bound MDM2 to the nucleus	0.00323/s
[Drug:MDMXc] -> [Drug:MDMXn]	I_{MDMX}	Import of MDMX to the nucleus	1.73e-7/s
[Drug:MDM2:MDMXc] -> [Drug:MDM2:MDMXn]	I_{MDM2}	Nuclear import of drugged MDM2:MDMX	0.00323/s
[2Drug:MDM2:MDMXc] -> [2Drug:MDM2:MDMXn]	I_{MDM2}	Nuclear import of drugged MDM2:MDMX	0.00323/s
[Drugc]+[MDM2c] -> [Drug:MDM2c]	k_{+Drug}	Drug binding to cytoplasmic MDM2	1e-4/nMs
[Drugn]+[MDM2n] -> [Drug:MDM2n]	k_{+Drug}	Drug binding to nuclear MDM2	1e-4/nMs
[Drugo]+[MDM2o] -> [Drug:MDM2o]	k_{+Drug}	Drug binding to nucleolar MDM2	1e-4/nMs
[Drugc]+[MDMXc] -> [Drug:MDMXc]	k_{+Drug}	Drug binding to cytoplasmic MDMX	1e-4/nMs
[Drugn]+[MDMXn] -> [Drug:MDMXn]	k_{+Drug}	Drug binding to nuclear MDMX	1e-4/nMs
[Drugo]+[MDMXo] -> [Drug:MDMXo]	k_{+Drug}	Drug binding to nucleolar MDMX	1e-4/nMs
[Drugc]+[MDM2:MDMXc] -> [Drug:MDM2:MDMXc]	$2*k_{+Drug}$	Drug binding to cytoplasmic MDM2:MDMX	2e-4/nMs
[Drugn]+[MDM2:MDMXn] -> [Drug:MDM2:MDMXn]	$2*k_{+Drug}$	Drug binding to nuclear MDM2:MDMX	2e-4/nMs
[Drugo]+[MDM2:MDMXo] -> [Drug:MDM2:MDMXo]	$2*k_{+Drug}$	Drug binding to nucleolar MDM2:MDMX	2e-4/nMs
[Drugc]+[Drug:MDM2:MDMXc] -> [2Drug:MDM2:MDMXc]	k_{+Drug}	Drug binding to drugged cytoplasmic MDM2:MDMX	1e-4/nMs
[Drugn]+[Drug:MDM2:MDMXn] -> [2Drug:MDM2:MDMXn]	k_{+Drug}	Drug binding to drugged nuclear MDM2:MDMX	1e-4/nMs
[Drugo]+[Drug:MDM2:MDMXo] -> [2Drug:MDM2:MDMXo]	k_{+Drug}	Drug binding to drugged nucleolar MDM2:MDMX	1e-4/nMs
[Drug:MDM2c] -> [Drugc]+[MDM2c]	k_{-Drug}	Drug dissociation from MDM2	0.1/s
[Drug:MDM2n] -> [Drugn]+[MDM2n]	k_{-Drug}	Drug dissociation from MDM2	0.1/s
[Drug:MDM2o] -> [Drugo]+[MDM2o]	k_{-Drug}	Drug dissociation from MDM2	0.1/s
[Drug:MDMXc] -> [Drugc]+[MDMXc]	k_{-Drug}	Drug dissociation from MDMX	0.1/s

Reaction	Constant	Description	Value
[Drug:MDMXn] -> [Drugn]+[MDMXn]	k_{-Drug}	Drug dissociation from MDMX	0.1/s
[Drug:MDMXo] -> [Drugo]+[MDMXo]	k_{-Drug}	Drug dissociation from MDMX	0.1/s
[Drug:MDM2:MDMXc] -> [Drugc]+[MDM2:MDMXc]	k_{-Drug}	Drug dissociation from MDM2:MDMX	0.1/s
[Drug:MDM2:MDMXn] -> [Drugn]+[MDM2:MDMXn]	k_{-Drug}	Drug dissociation from MDM2:MDMX	0.1/s
[Drug:MDM2:MDMXo] -> [Drugo]+[MDM2:MDMXo]	k_{-Drug}	Drug dissociation from MDM2:MDMX	0.1/s
[2Drug:MDM2:MDMXc] -> [Drugc]+[Drug:MDM2:MDMXc]	$2*k_{-Drug}$	Drug dissociation from MDM2:MDMX	0.2/s
[2Drug:MDM2:MDMXn] -> [Drugn]+[Drug:MDM2:MDMXn]	$2*k_{-Drug}$	Drug dissociation from MDM2:MDMX	0.2/s
[2Drug:MDM2:MDMXo] -> [Drugo]+[Drug:MDM2:MDMXo]	$2*k_{-Drug}$	Drug dissociation from MDM2:MDMX	0.2/s
[Drug:MDM2c] -> [Drugc]	H	protein decay, freeing bound drug	1.925e-5/s
[Drug:MDM2n] -> [Drugn]	H	protein decay, freeing bound drug	1.925e-5/s
[Drug:MDM2o] -> [Drugo]	H	protein decay, freeing bound drug	1.925e-5/s
[Drug:MDMXc] -> [Drugc]	H	protein decay, freeing bound drug	1.925e-5/s
[Drug:MDMXn] -> [Drugn]	H	protein decay, freeing bound drug	1.925e-5/s
[Drug:MDMXo] -> [Drugo]	H	protein decay, freeing bound drug	1.925e-5/s
[Drug:MDM2:MDMXc] -> [Drugc]	H	protein decay, freeing bound drug	1.925e-5/s
[Drug:MDM2:MDMXn] -> [Drugn]	H	protein decay, freeing bound drug	1.925e-5/s
[Drug:MDM2:MDMXo] -> [Drugo]	H	protein decay, freeing bound drug	1.925e-5/s
[2Drug:MDM2:MDMXc]->2[Drugc]	H	protein decay, freeing bound drug	1.925e-5/s
[2Drug:MDM2:MDMXn]->2[Drugn]	H	protein decay, freeing bound drug	1.925e-5/s
[2Drug:MDM2:MDMXo]->2[Drugo]	H	protein decay, freeing bound drug	1.925e-5/s
[Drug:MDM2:MDMXc] -> [MDM2c]+[Drugc]	$0.5*U_{MDMX}$	MDM2 bound MDMX ubiquitination	2.43e-4/s
[Drug:MDM2:MDMXn] -> [MDM2n]+[Drugn]	$0.5*U_{MDMX}$	MDM2 bound MDMX ubiquitination	2.43e-4/s
[Drug:MDM2:MDMXo] -> [MDM2o]+[Drugo]	$0.5*U_{MDMX}$	MDM2 bound MDMX ubiquitination	2.43e-4/s
[Drug:MDM2:MDMXc] -> [Drug:MDM2c]	$0.5*U_{MDMX}$	MDM2 bound MDMX ubiquitination	2.43e-4/s
[Drug:MDM2:MDMXn] -> [Drug:MDM2n]	$0.5*U_{MDMX}$	MDM2 bound MDMX ubiquitination	2.43e-4/s

Reaction	Constant	Description	Value
[Drug:MDM2:MDMXo] -> [Drug:MDM2o]	$0.5*U_{MDMX}$	MDM2 bound MDMX ubiquitination	2.43e-4/s
[2Drug:MDM2:MDMXc] -> [Drug:MDM2c]+[Drugc]	U_{MDMX}	MDM2 bound MDMX ubiquitination	4.87e-4/s
[2Drug:MDM2:MDMXn] -> [Drug:MDM2n]+[Drugn]	U_{MDMX}	MDM2 bound MDMX ubiquitination	4.87e-4/s
[2Drug:MDM2:MDMXo] -> [Drug:MDM2o]+[Drugo]	U_{MDMX}	MDM2 bound MDMX ubiquitination	4.87e-4/s
[MDM2c]+[Drug:MDM2c] -> [MDM2c]+[Drugc]	U_{MDM2}	MDM2 auto ubiquitination	2.38e-6/nMs
[MDM2n]+[Drug:MDM2n] -> [MDM2n]+[Drugn]	U_{MDM2}	MDM2 auto ubiquitination	2.38e-6/nMs
[MDM2o]+[Drug:MDM2o] -> [MDM2o]+[Drugo]	U_{MDM2}	MDM2 auto ubiquitination	2.38e-6/nMs
[MDM2c]+[Drug:MDM2c] -> [Drug:MDM2c]	U_{MDM2}	MDM2 auto ubiquitination	2.38e-6/nMs
[MDM2n]+[Drug:MDM2n] -> [Drug:MDM2n]	U_{MDM2}	MDM2 auto ubiquitination	2.38e-6/nMs
[MDM2o]+[Drug:MDM2o] -> [Drug:MDM2o]	U_{MDM2}	MDM2 auto ubiquitination	2.38e-6/nMs
[Drug:MDM2c]+[Drug:MDM2c] -> [Drug:MDM2c]+[Drugc]	U_{MDM2}	MDM2 auto ubiquitination	2.38e-6/nMs
[Drug:MDM2n]+[Drug:MDM2n] -> [Drug:MDM2n]+[Drugn]	U_{MDM2}	MDM2 auto ubiquitination	2.38e-6/nMs
[Drug:MDM2o]+[Drug:MDM2o] -> [Drug:MDM2o]+[Drugo]	U_{MDM2}	MDM2 auto ubiquitination	2.38e-6/nMs
[Drug:MDM2c]+[MDMXc] -> [Drug:MDM2:MDMXc]	k_+	Drugged MDM2 MDMX binding	6e-4/nMs
[Drug:MDM2n]+[MDMXn] -> [Drug:MDM2:MDMXn]	k_+	Drugged MDM2 MDMX binding	6e-4/nMs
[Drug:MDM2o]+[MDMXo] -> [Drug:MDM2:MDMXo]	k_+	Drugged MDM2 MDMX binding	6e-4/nMs
[MDM2c]+[Drug:MDMXc] -> [Drug:MDM2:MDMXc]	k_+	Drugged MDM2 MDMX binding	6e-4/nMs
[MDM2n]+[Drug:MDMXn] -> [Drug:MDM2:MDMXn]	k_+	Drugged MDM2 MDMX binding	6e-4/nMs
[MDM2o]+[Drug:MDMXo] -> [Drug:MDM2:MDMXo]	k_+	Drugged MDM2 MDMX binding	6e-4/nMs
[Drug:MDM2c]+[Drug:MDMXc] -> [2Drug:MDM2:MDMXc]	k_+	Drugged MDM2 MDMX binding	6e-4/nMs
[Drug:MDM2n]+[Drug:MDMXn] -> [2Drug:MDM2:MDMXn]	k_+	Drugged MDM2 MDMX binding	6e-4/nMs
[Drug:MDM2o]+[Drug:MDMXo] -> [2Drug:MDM2:MDMXo]	k_+	Drugged MDM2 MDMX binding	6e-4/nMs
[Drug:MDM2:MDMXc] -> [Drug:MDM2c]+[MDMXc]	$0.5*k_{-2x}$	Drugged MDM2:MDMX dissociation	0.0253/s

Reaction	Constant	Description	Value
[Drug:MDM2:MDMXn] -> [Drug:MDM2n]+[MDMXn]	$0.5*k_{-2x}$	Drugged MDM2:MDMX dissociation	0.0253/s
[Drug:MDM2:MDMXo] -> [Drug:MDM2o]+[MDMXo]	$0.5*k_{-2x}$	Drugged MDM2:MDMX dissociation	0.0253/s
[Drug:MDM2:MDMXc] -> [MDM2c]+[Drug:MDMXc]	$0.5*k_{-2x}$	Drugged MDM2:MDMX dissociation	0.0253/s
[Drug:MDM2:MDMXn] -> [MDM2n]+[Drug:MDMXn]	$0.5*k_{-2x}$	Drugged MDM2:MDMX dissociation	0.0253/s
[Drug:MDM2:MDMXo] -> [MDM2o]+[Drug:MDMXo]	$0.5*k_{-2x}$	Drugged MDM2:MDMX dissociation	0.0253/s
[2Drug:MDM2:MDMXc] -> [Drug:MDM2c]+[Drug:MDMXc]	k_{-2x}	Drugged MDM2:MDMX dissociation	0.0506/s
[2Drug:MDM2:MDMXn] -> [Drug:MDM2n]+[Drug:MDMXn]	k_{-2x}	Drugged MDM2:MDMX dissociation	0.0506/s
[2Drug:MDM2:MDMXo] -> [Drug:MDM2o]+[Drug:MDMXo]	k_{-2x}	Drugged MDM2:MDMX dissociation	0.0506/s

Table A.2: Additional reactions needed in the MDM2/MDMX dual inhibitor model.

MDMX inhibitor species	
Chemical	**Description**
[Drugc]	Free drug in the cytoplasm
[Drugn]	Free drug in the nucleus
[Drugo]	Free drug in the nucleolus
[Drug:MDMXc]	MDMX bound drug in the cytoplasm
[Drug:MDMXn]	MDM2 bound drug in the nucleus
[Drug:MDMXo]	MDM2 bound drug in the nucleolus
[Drug:MDM2:MDMXc]	drug bound to a MDM2 MDMX heterodimer in the cytoplasm
[Drug:MDM2:MDMXn]	drug bound to a MDM2 MDMX heterodimer in the nucleus
[Drug:MDM2:MDMXo]	drug bound to a MDM2 MDMX heterodimer in the nucleolus

Table A.3: Chemical species added in the MDMX inhibitor model.

MDMX inhibitor reactions

Reaction	Constant	Description	Value
[Drugn] -> [Drugc]	E_{Drug}	Nuclear export of drug molecules	0.4/s
[Drug:MDMXn] -> [Drug:MDMXc]	$E_{protein}$	Export of drugged MDMX from the nucleus	0.0136/s
[Drug:MDM2:MDMXn] -> [Drug:MDM2:MDMXc]	$E_{protein}$	Nuclear export of drugged MDM2:MDMX	0.0136/s
[Drug:MDMXn] -> [Drug:MDMXo]	No	Nucleolar sequestration of drugged MDMX	0.00480/s
[Drug:MDM2:MDMXn] -> [Drug:MDM2:MDMXo]	No	Nucleolar sequestration of drugged MDM2:MDMX	0.00480/s
[Drugn] -> [Drugo]	No_{drug}	Nucleolar drug import	0.1/s
[Drugo] -> [Drugn]	Ne_{drug}	Nucleolar drug export	0.01/s
[Drugc] -> [Drugn]	I_{drug}	Nuclear import of drug molecules	0.1/s
[Drug:MDMXc] -> [Drug:MDMXn]	I_{MDMX}	Import of MDMX to the nucleus	1.73e-7/s
[Drug:MDM2:MDMXc] -> [Drug:MDM2:MDMXn]	I_{MDM2}	Nuclear import of drugged MDM2:MDMX	0.00323/s
[Drugc]+[MDMXc] -> [Drug:MDMXc]	k_{+Drug}	Drug binding to cytoplasmic MDMX	1e-4/nMs
[Drugn]+[MDMXn] -> [Drug:MDMXn]	k_{+Drug}	Drug binding to nuclear MDMX	1e-4/nMs
[Drugo]+[MDMXo] -> [Drug:MDMXo]	k_{+Drug}	Drug binding to nucleolar MDMX	1e-4/nMs
[Drugc]+[MDM2:MDMXc] -> [Drug:MDM2:MDMXc]	k_{+Drug}	Drug binding to cytoplasmic MDM2:MDMX	1e-4/nMs
[Drugn]+[MDM2:MDMXn] -> [Drug:MDM2:MDMXn]	k_{+Drug}	Drug binding to nuclear MDM2:MDMX	1e-4/nMs
[Drugo]+[MDM2:MDMXo] -> [Drug:MDM2:MDMXo]	k_{+Drug}	Drug binding to nucleolar MDM2:MDMX	1e-4/nMs
[Drug:MDMXc] -> [Drugc]+[MDMXc]	k_{-Drug}	Drug dissociation from MDMX	0.1/s
[Drug:MDMXn] -> [Drugn]+[MDMXn]	k_{-Drug}	Drug dissociation from MDMX	0.1/s
[Drug:MDMXo] -> [Drugo]+[MDMXo]	k_{-Drug}	Drug dissociation from MDMX	0.1/s
[Drug:MDM2:MDMXc] -> [Drugc]+[MDM2:MDMXc]	k_{-Drug}	Drug dissociation from MDM2:MDMX	0.1/s
[Drug:MDM2:MDMXn] -> [Drugn]+[MDM2:MDMXn]	k_{-Drug}	Drug dissociation from MDM2:MDMX	0.1/s
[Drug:MDM2:MDMXo] -> [Drugo]+[MDM2:MDMXo]	k_{-Drug}	Drug dissociation from MDM2:MDMX	0.1/s

Reaction	Constant	Description	Value
[Drug:MDMXc] -> [Drugc]	H	protein decay, freeing bound drug	1.925e-5/s
[Drug:MDMXn] -> [Drugn]	H	protein decay, freeing bound drug	1.925e-5/s
[Drug:MDMXo] -> [Drugo]	H	protein decay, freeing bound drug	1.925e-5/s
[Drug:MDM2:MDMXc] -> [Drugc]	H	protein decay, freeing bound drug	1.925e-5/s
[Drug:MDM2:MDMXn] -> [Drugn]	H	protein decay, freeing bound drug	1.925e-5/s
[Drug:MDM2:MDMXo] -> [Drugo]	H	protein decay, freeing bound drug	1.925e-5/s
[Drug:MDM2:MDMXc] -> [MDM2c]+[Drugc]	U_{MDMX}	MDM2 bound MDMX ubiquitination	4.87e-4/s
[Drug:MDM2:MDMXn] -> [MDM2n]+[Drugn]	U_{MDMX}	MDM2 bound MDMX ubiquitination	4.87e-4/s
[Drug:MDM2:MDMXo] -> [MDM2o]+[Drugo]	U_{MDMX}	MDM2 bound MDMX ubiquitination	4.87e-4/s
[MDM2c]+[Drug:MDMXc] -> [Drug:MDM2:MDMXc]	k_{+}	Drugged MDM2 MDMX binding	6e-4/nMs
[MDM2n]+[Drug:MDMXn] -> [Drug:MDM2:MDMXn]	k_{+}	Drugged MDM2 MDMX binding	6e-4/nMs
[MDM2o]+[Drug:MDMXo] -> [Drug:MDM2:MDMXo]	k_{+}	Drugged MDM2 MDMX binding	6e-4/nMs
[Drug:MDM2:MDMXc] -> [MDM2c]+[Drug:MDMXc]	k_{-2x}	Drugged MDM2:MDMX dissociation	0.0506/s
[Drug:MDM2:MDMXn] -> [MDM2n]+[Drug:MDMXn]	k_{-2x}	Drugged MDM2:MDMX dissociation	0.0506/s
[Drug:MDM2:MDMXo] -> [MDM2o]+[Drug:MDMXo]	k_{-2x}	Drugged MDM2:MDMX dissociation	0.0506/s

Table A.4: Additional reactions needed in the MDMX inhibitor model.

MDM2 inhibitor species	
Chemical	**Description**
[Drugc]	Free drug in the cytoplasm
[Drugn]	Free drug in the nucleus
[Drugo]	Free drug in the nucleolus
[Drug:MDM2c]	MDM2 bound drug in the cytoplasm
[Drug:MDM2n]	MDM2 bound drug in the nucleus
[Drug:MDM2o]	MDM2 bound drug in the nucleolus
[Drug:MDM2:MDMXc]	drug bound to a MDM2 MDMX heterodimer in the cytoplasm
[Drug:MDM2:MDMXn]	drug bound to a MDM2 MDMX heterodimer in the nucleus
[Drug:MDM2:MDMXo]	drug bound to a MDM2 MDMX heterodimer in the nucleolus

Table A.5: Chemical species added in the MDM2 inhibitor model.

MDM2 inhibitor reactions			
Reaction	**Constant**	**Description**	**Value**
[Drugn] -> [Drugc]	E_{Drug}	Nuclear export of drug molecules	0.4/s
[Drug:MDM2n] -> [Drug:MDM2c]	$E_{protein}$	Export of drug bound MDM2 from the nucleus	0.0136/s
[Drug:MDM2:MDMXn] -> [Drug:MDM2:MDMXc]	$E_{protein}$	Nuclear export of drugged MDM2:MDMX	0.0136/s
[Drug:MDM2n] -> [Drug:MDM2o]	No	Nucleolar sequestration of drugged MDM2	0.00480/s
[Drug:MDM2:MDMXn] -> [Drug:MDM2:MDMXo]	No	Nucleolar sequestration of drugged MDM2:MDMX	0.00480/s
[Drugn] -> [Drugo]	No_{drug}	Nucleolar drug import	0.1/s
[Drugo] -> [Drugn]	Ne_{drug}	Nucleolar drug export	0.01/s
[Drugc] -> [Drugn]	I_{drug}	Nuclear import of drug molecules	0.1/s
[Drug:MDM2c] -> [Drug:MDM2n]	I_{MDM2}	Import of drug bound MDM2 to the nucleus	0.00323/s
[Drug:MDM2:MDMXc] -> [Drug:MDM2:MDMXn]	I_{MDM2}	Nuclear import of drugged MDM2:MDMX	0.00323/s
[Drugc]+[MDM2c] -> [Drug:MDM2c]	k_{+Drug}	Drug binding to cytoplasmic MDM2	1e-4/nMs
[Drugn]+[MDM2n] -> [Drug:MDM2n]	k_{+Drug}	Drug binding to nuclear MDM2	1e-4/nMs
[Drugo]+[MDM2o] -> [Drug:MDM2o]	k_{+Drug}	Drug binding to nucleolar MDM2	1e-4/nMs
[Drugc]+[MDM2:MDMXc] -> [Drug:MDM2:MDMXc]	k_{+Drug}	Drug binding to cytoplasmic MDM2:MDMX	1e-4/nMs

Reaction	Constant	Description	Value
[Drugn]+[MDM2:MDMXn] -> [Drug:MDM2:MDMXn]	k_{+Drug}	Drug binding to nuclear MDM2:MDMX	1e-4/nMs
[Drugo]+[MDM2:MDMXo] -> [Drug:MDM2:MDMXo]	k_{+Drug}	Drug binding to nucleolar MDM2:MDMX	1e-4/nMs
[Drug:MDM2c] -> [Drugc]+[MDM2c]	k_{-Drug}	Drug dissociation from MDM2	0.1/s
[Drug:MDM2n] -> [Drugn]+[MDM2n]	k_{-Drug}	Drug dissociation from MDM2	0.1/s
[Drug:MDM2o] -> [Drugo]+[MDM2o]	k_{-Drug}	Drug dissociation from MDM2	0.1/s
[Drug:MDM2:MDMXc] -> [Drugc]+[MDM2:MDMXc]	k_{-Drug}	Drug dissociation from MDM2:MDMX	0.1/s
[Drug:MDM2:MDMXn] -> [Drugn]+[MDM2:MDMXn]	k_{-Drug}	Drug dissociation from MDM2:MDMX	0.1/s
[Drug:MDM2:MDMXo] -> [Drugo]+[MDM2:MDMXo]	k_{-Drug}	Drug dissociation from MDM2:MDMX	0.1/s
[Drug:MDM2c] -> [Drugc]	H	protein decay, freeing bound drug	1.925e-5/s
[Drug:MDM2n] -> [Drugn]	H	protein decay, freeing bound drug	1.925e-5/s
[Drug:MDM2o] -> [Drugo]	H	protein decay, freeing bound drug	1.925e-5/s
[Drug:MDM2:MDMXc] -> [Drugc]	H	protein decay, freeing bound drug	1.925e-5/s
[Drug:MDM2:MDMXn] -> [Drugn]	H	protein decay, freeing bound drug	1.925e-5/s
[Drug:MDM2:MDMXo] -> [Drugo]	H	protein decay, freeing bound drug	1.925e-5/s
[Drug:MDM2:MDMXc] -> [Drug:MDM2c]	U_{MDMX}	MDM2 bound MDMX ubiquitination	4.87e-4/s
[Drug:MDM2:MDMXn] -> [Drug:MDM2n]	U_{MDMX}	MDM2 bound MDMX ubiquitination	4.87e-4/s
[Drug:MDM2:MDMXo] -> [Drug:MDM2o]	U_{MDMX}	MDM2 bound MDMX ubiquitination	4.87e-4/s
[MDM2c]+[Drug:MDM2c] -> [MDM2c]+[Drugc]	U_{MDM2}	MDM2 auto ubiquitination	2.38e-6/nMs
[MDM2n]+[Drug:MDM2n] -> [MDM2n]+[Drugn]	U_{MDM2}	MDM2 auto ubiquitination	2.38e-6/nMs
[MDM2o]+[Drug:MDM2o] -> [MDM2o]+[Drugo]	U_{MDM2}	MDM2 auto ubiquitination	2.38e-6/nMs
[MDM2c]+[Drug:MDM2c] -> [Drug:MDM2c]	U_{MDM2}	MDM2 auto ubiquitination	2.38e-6/nMs
[MDM2n]+[Drug:MDM2n] -> [Drug:MDM2n]	U_{MDM2}	MDM2 auto ubiquitination	2.38e-6/nMs
[MDM2o]+[Drug:MDM2o] -> [Drug:MDM2o]	U_{MDM2}	MDM2 auto ubiquitination	2.38e-6/nMs

Reaction	Constant	Description	Value
[Drug:MDM2c]+[Drug:MDM2c] -> [Drug:MDM2c]+[Drugc]	U_{MDM2}	MDM2 auto ubiquitination	2.38e-6/nMs
[Drug:MDM2n]+[Drug:MDM2n] -> [Drug:MDM2n]+[Drugn]	U_{MDM2}	MDM2 auto ubiquitination	2.38e-6/nMs
[Drug:MDM2o]+[Drug:MDM2o] -> [Drug:MDM2o]+[Drugo]	U_{MDM2}	MDM2 auto ubiquitination	2.38e-6/nMs
[Drug:MDM2c]+[MDMXc] -> [Drug:MDM2:MDMXc]	k_{+}	Drugged MDM2 MDMX binding	6e-4/nMs
[Drug:MDM2n]+[MDMXn] -> [Drug:MDM2:MDMXn]	k_{+}	Drugged MDM2 MDMX binding	6e-4/nMs
[Drug:MDM2o]+[MDMXo] -> [Drug:MDM2:MDMXo]	k_{+}	Drugged MDM2 MDMX binding	6e-4/nMs
[Drug:MDM2:MDMXc] -> [Drug:MDM2c]+[MDMXc]	k_{-2x}	Drugged MDM2:MDMX dissociation	0.0506/s
[Drug:MDM2:MDMXn] -> [Drug:MDM2n]+[MDMXn]	k_{-2x}	Drugged MDM2:MDMX dissociation	0.0506/s
[Drug:MDM2:MDMXo] -> [Drug:MDM2o]+[MDMXo]	k_{-2x}	Drugged MDM2:MDMX dissociation	0.0506/s

Table A.6: Additional reactions needed in the MDM2/MDMX dual inhibitor model.

MDM2 MDMX interaction inhibitor species	
Chemical	**Description**
[Drugc]	Free drug in the cytoplasm
[Drugn]	Free drug in the nucleus
[Drugo]	Free drug in the nucleolus
[Drug:MDMXc]	MDMX bound drug in the cytoplasm
[Drug:MDMXn]	MDM2 bound drug in the nucleus
[Drug:MDMXo]	MDM2 bound drug in the nucleolus
[Drug:MDMX:p53c]	drug bound to a MDM2 MDMX heterodimer in the cytoplasm
[Drug:MDMX:p53n]	drug bound to a MDM2 MDMX heterodimer in the nucleus

Table A.7: Chemical species added in the MDM2 MDMX interaction inhibitor model.

MDM2 MDMX interaction inhibitor reactions

Reaction	Constant	Description	Value
[Drugn] -> [Drugc]	E_{Drug}	Nuclear export of drug molecules	0.4/s
[Drug:MDMXn] -> [Drug:MDMXc]	$E_{protein}$	Export of drugged MDMX from the nucleus	0.0136/s
[Drug:MDMX:p53n] -> [Drug:MDMX:p53c]	$E_{protein}$	Export of drugged MDMX:p53 from the nucleus	0.0136/s
[Drug:MDMXn] -> [Drug:MDMXo]	No	Nucleolar sequestration of drugged MDMX	0.00480/s
[Drugn] -> [Drugo]	No_{drug}	Nucleolar drug import	0.1/s
[Drugo] -> [Drugn]	Ne_{drug}	Nucleolar drug export	0.01/s
[Drugc] -> [Drugn]	I_{drug}	Nuclear import of drug molecules	0.1/s
[Drug:MDMXc] -> [Drug:MDMXn]	I_{MDMX}	Import of MDMX to the nucleus	1.73e-7/s
[Drug:MDMX:p53c] -> [Drug:MDMX:p53n]	$0.5*I_{MDMX}+0.5*I_{p53}$	Import of druged MDMX:p53 to the nucleus	0.000107/s
[Drugc]+[MDMXc] -> [Drug:MDMXc]	k_{+Drug}	Drug binding to cytoplasmic MDMX	1e-4/nMs
[Drugn]+[MDMXn] -> [Drug:MDMXn]	k_{+Drug}	Drug binding to nuclear MDMX	1e-4/nMs
[Drugo]+[MDMXo] -> [Drug:MDMXo]	k_{+Drug}	Drug binding to nucleolar MDMX	1e-4/nMs
[Drugc]+[MDMX:p53c] -> [Drug:MDMX:p53c]	k_{+Drug}	Drug binding to cytoplasmic p53 bound MDMX	1e-4/nMs
[Drugn]+[MDMX:p53n] -> [Drug:MDMX:p53n]	k_{+Drug}	Drug binding to nuclear p53 bound MDMX	1e-4/nMs
[Drug:MDMXc] -> [Drugc]+[MDMXc]	k_{-Drug}	Drug dissociation from MDMX	0.1/s
[Drug:MDMXn] -> [Drugn]+[MDMXn]	k_{-Drug}	Drug dissociation from MDMX	0.1/s
[Drug:MDMXo] -> [Drugo]+[MDMXo]	k_{-Drug}	Drug dissociation from MDMX	0.1/s
[Drug:MDMX:p53c] -> [Drugc]+[MDMX:p53c]	k_{-Drug}	Drug dissociation from p53 bound MDMX	0.1/s
[Drug:MDMX:p53n] -> [Drugn]+[MDMX:p53n]	k_{-Drug}	Drug dissociation from p53 bound MDMX	0.1/s

Reaction	Constant	Description	Value
[Drug:MDMXc]+[p53c] -> [MDMX:p53c]	k_+	MDMX binding to p53	6e-4/nMs
[Drug:MDMXn]+[p53n] -> [MDMX:p53n]	k_+	MDMX binding to p53	6e-4/nMs
[Drug:MDMX:p53c] -> [Drug:MDMXc]+[p53c]	k_{-xp}	MDMX:p53 dissociation	41.6/s
[Drug:MDMX:p53n] -> [Drug:MDMXn]+[p53n]	k_{-xp}	MDMX:p53 dissociation	41.6/s
[Drug:MDMXc] -> [Drugc]	H	protein decay, freeing bound drug	1.925e-5/s
[Drug:MDMXn] -> [Drugn]	H	protein decay, freeing bound drug	1.925e-5/s
[Drug:MDMXo] -> [Drugo]	H	protein decay, freeing bound drug	1.925e-5/s

Table A.8: Additional reactions needed in the MDMX MDM2 interaction inhibitor model.

Appendix B: Plots of drug effects on various cell models

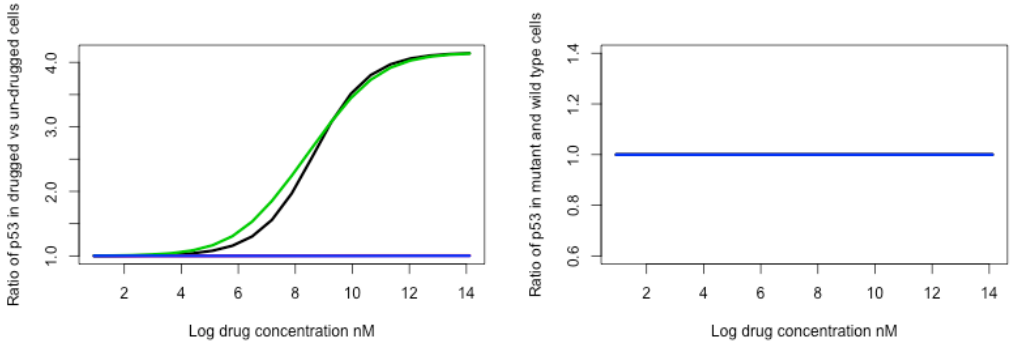

A

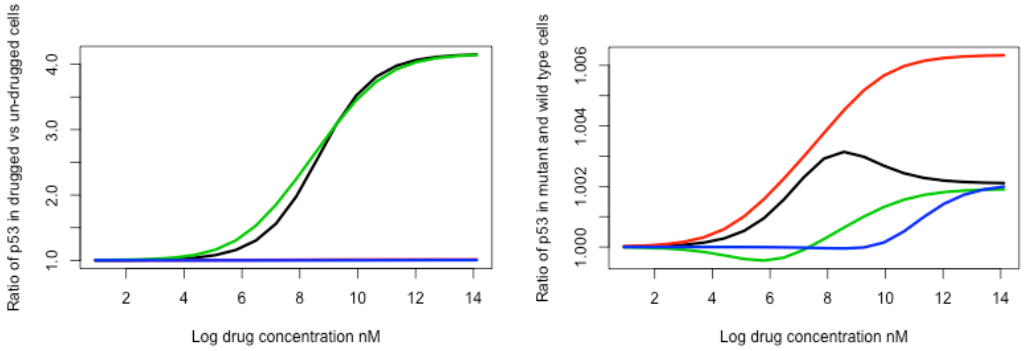

B

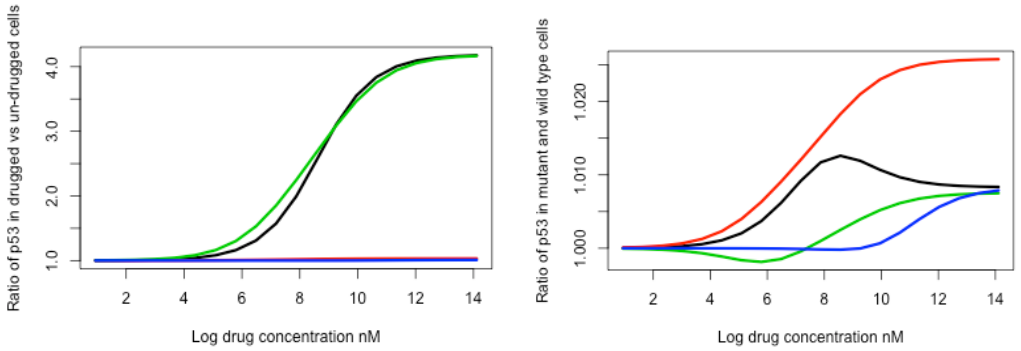

C

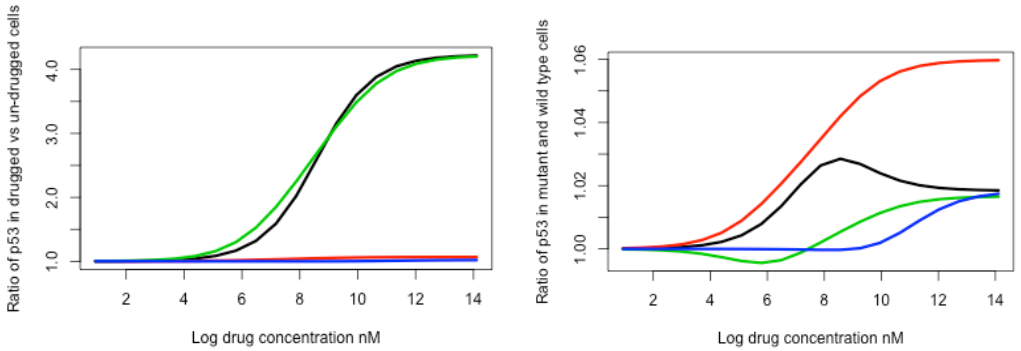
Ratio of p53 in drugged vs un-drugged cells
1.0
2.0
3.0
4.0
2
4
6
8
10
12
14
Log drug concentration nM
Ratio of p53 in mutant and wild type cells
1.00
1.02
1.04
1.06
2
4
6
8
10
12
14
Log drug concentration nM

D

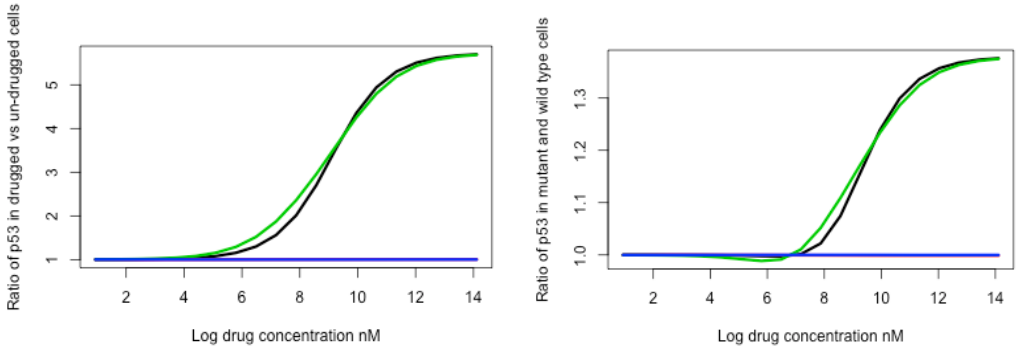
Ratio of p53 in drugged vs un-drugged cells
1
2
3
4
5
2
4
6
8
10
12
14
Log drug concentration nM
Ratio of p53 in mutant and wild type cells
1.0
1.1
1.2
1.3
2
4
6
8
10
12
14
Log drug concentration nM

E

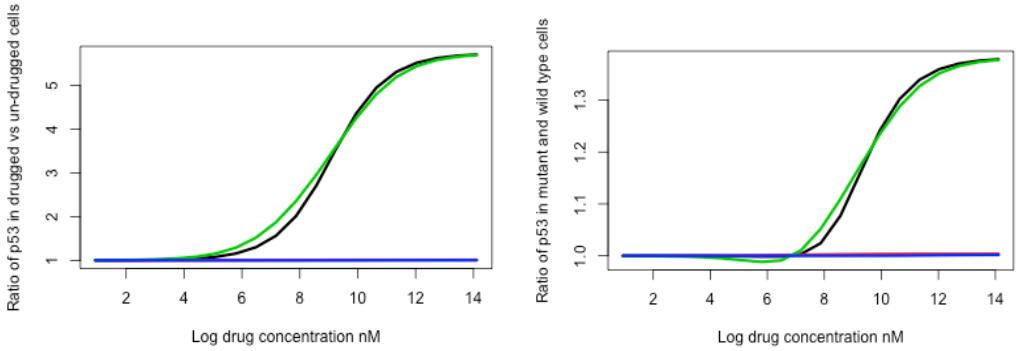
Ratio of p53 in drugged vs un-drugged cells
1
2
3
4
5
2
4
6
8
10
12
14
Log drug concentration nM
Ratio of p53 in mutant and wild type cells
1.0
1.1
1.2
1.3
2
4
6
8
10
12
14
Log drug concentration nM

F

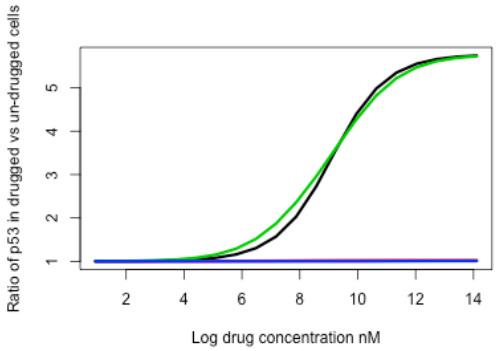
Ratio of p53 in drugged vs un-drugged cells
1
2
3
4
5
2
4
6
8
10
12
14
Log drug concentration nM

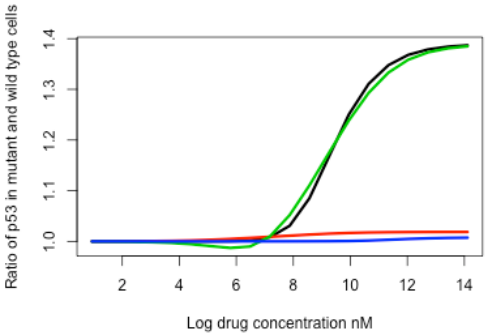
Ratio of p53 in mutant and wild type cells
1.0
1.1
1.2
1.3
1.4
2
4
6
8
10
12
14
Log drug concentration nM

G

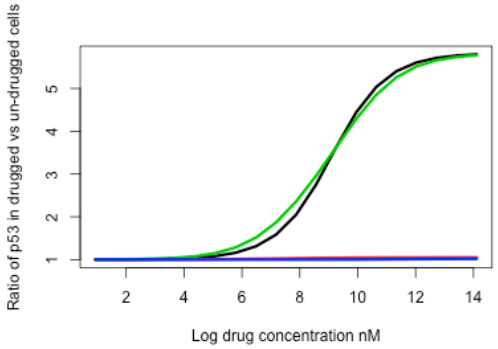
Ratio of p53 in drugged vs un-drugged cells
1
2
3
4
5
2
4
6
8
10
12
14
Log drug concentration nM

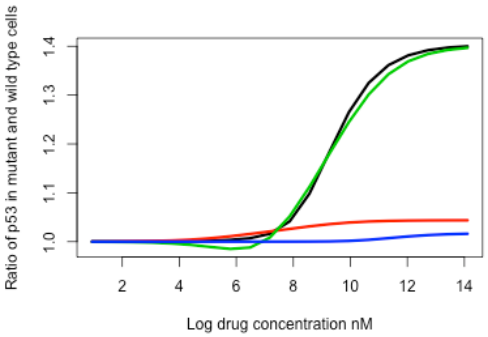
Ratio of p53 in mutant and wild type cells
1.0
1.1
1.2
1.3
1.4
2
4
6
8
10
12
14
Log drug concentration nM

H

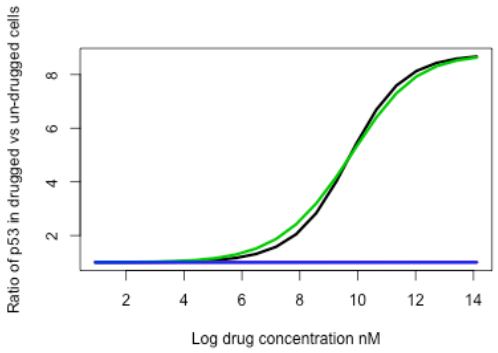
Ratio of p53 in drugged vs un-drugged cells
2
4
6
8
2
4
6
8
10
12
14
Log drug concentration nM

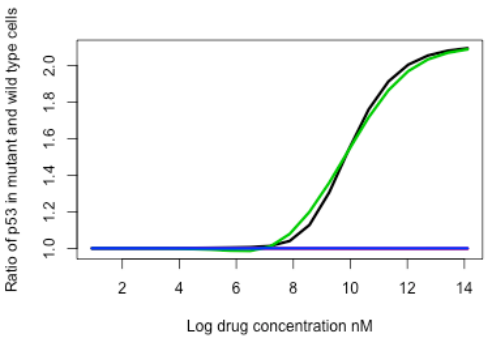
Ratio of p53 in mutant and wild type cells
1.0
1.2
1.4
1.6
1.8
2.0
2
4
6
8
10
12
14
Log drug concentration nM

I

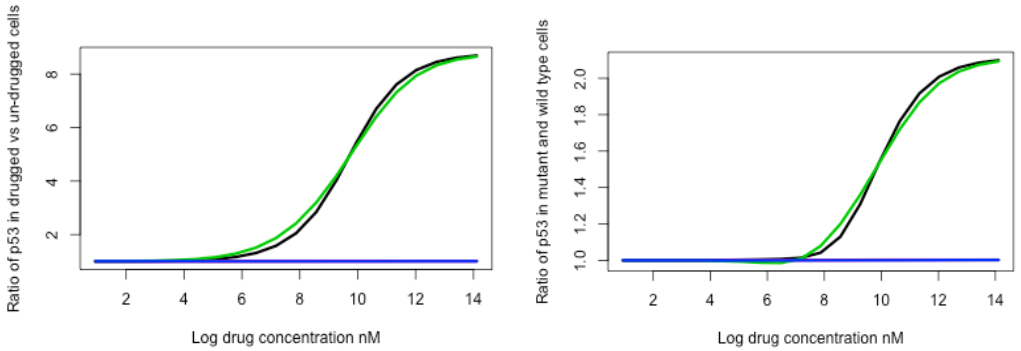
Ratio of p53 in drugged vs un-drugged cells
Log drug concentration nM
Ratio of p53 in mutant and wild type cells
Log drug concentration nM

J

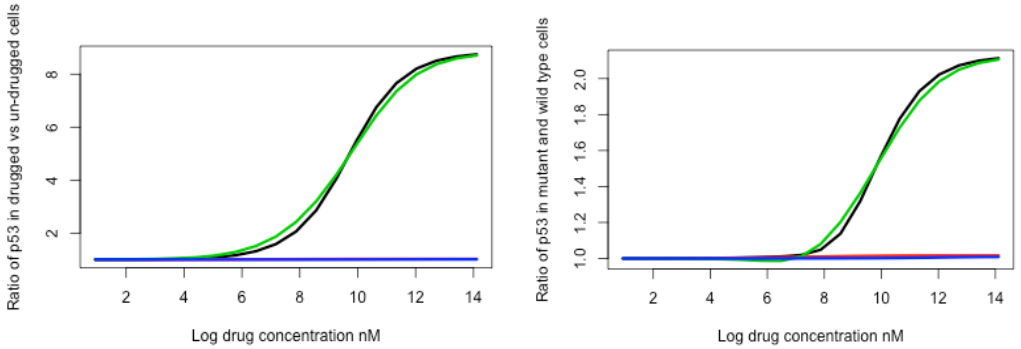
Ratio of p53 in drugged vs un-drugged cells
Log drug concentration nM
Ratio of p53 in mutant and wild type cells
Log drug concentration nM

K

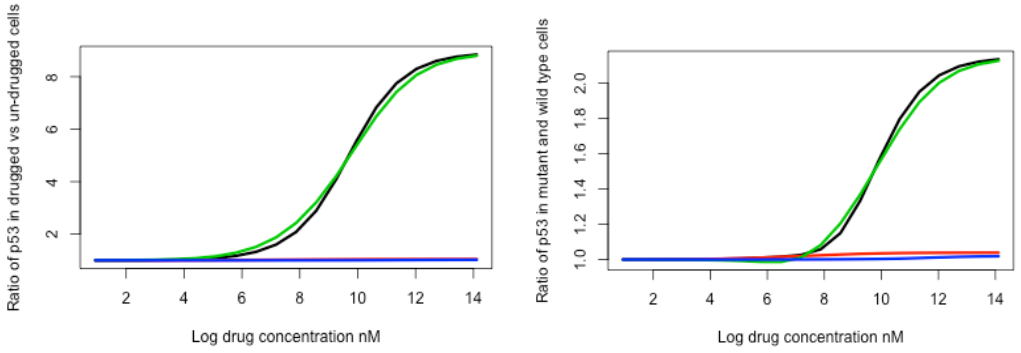
Ratio of p53 in drugged vs un-drugged cells
Log drug concentration nM
Ratio of p53 in mutant and wild type cells
Log drug concentration nM

L

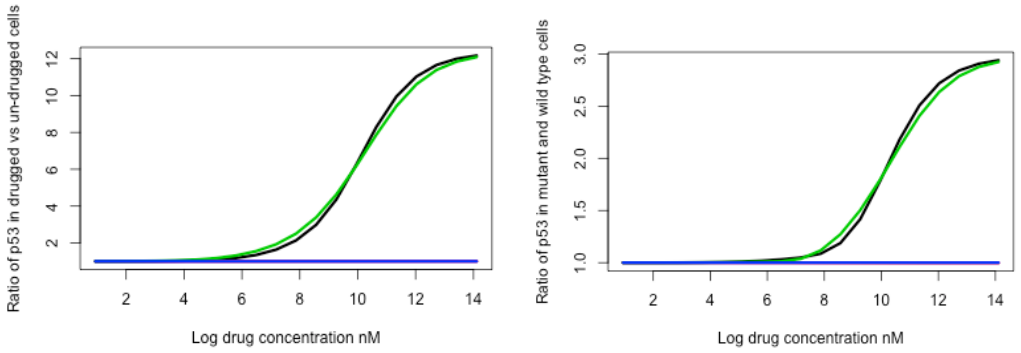
Ratio of p53 in drugged vs un-drugged cells
Log drug concentration nM
Ratio of p53 in mutant and wild type cells
Log drug concentration nM

M

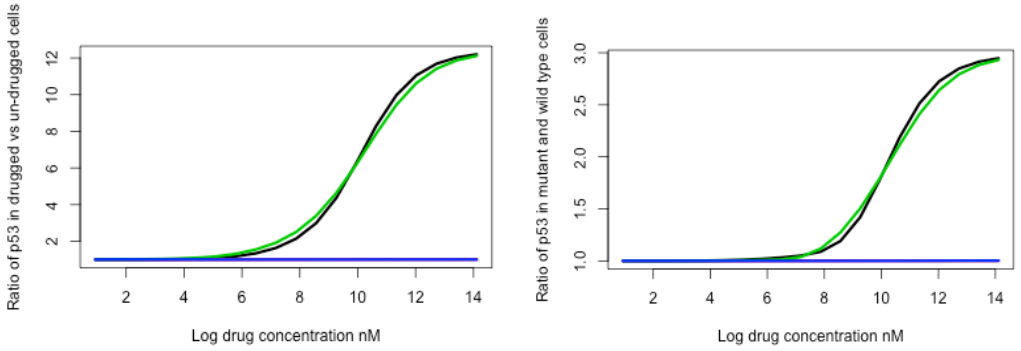
Ratio of p53 in drugged vs un-drugged cells
Log drug concentration nM
Ratio of p53 in mutant and wild type cells
Log drug concentration nM

N

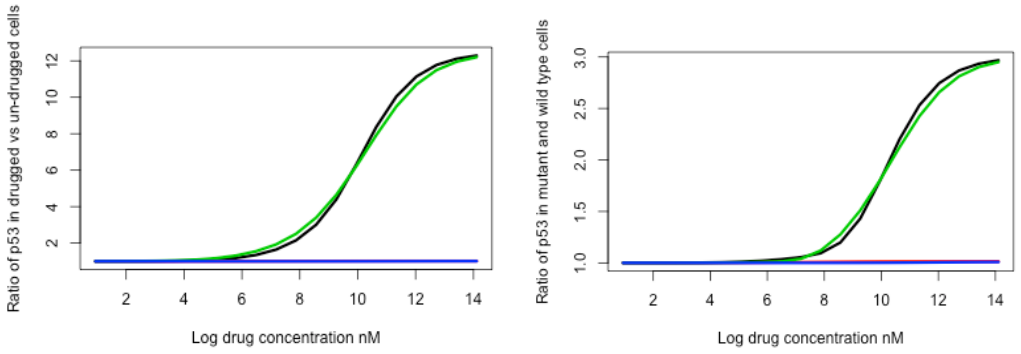
Ratio of p53 in drugged vs un-drugged cells
Log drug concentration nM
Ratio of p53 in mutant and wild type cells
Log drug concentration nM

O

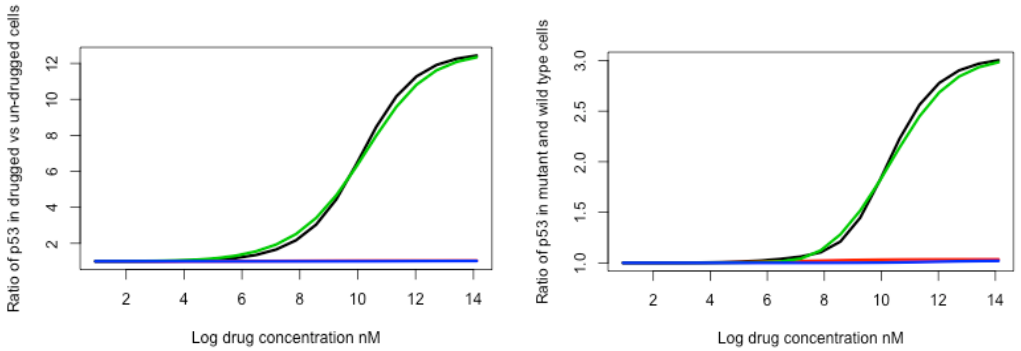

P

Figure B.1: Behaviour of all models of drugged cells. The ratio on the vertical axis is based on an average of p53 concentrations over a 7 hour period. Note that the scale is not the same on all of the vertical axes. The horizontal axis is the natural logarithm of drug concentration in nM. For reference this means that a value of 2 represents a concentration of 7.4nM, a value of 8 means a 3.0μM concentration, and a value of 14 means a 1.2mM concentration. The MDM2 MDMX dual inhibitor is in black, the MDMX p53 binding inhibitor is in red, the MDM2 p53 binding inhibitor is in green and the inhibitor of MDMX binding to MDM2 is in blue. The left column shows the ratio of nuclear p53 in a drugged cell to an un-drugged cell. The right column shows the ratio of nuclear p53 levels in drugged mutated cells to drugged wild type cells. Row A shows wild type cells, B shows cells with 2 times over-expressed MDMX, C shows cells with 5 times over-expressed MDMX, D shows cells with 10 times over-expressed MDMX, E shows cells with 2 times over-expressed MDM2, F shows cells with 2 times over-expressed MDM2 and 2 times over-expressed MDMX, G shows cells with 2 times over-expressed MDM2 and 5 times over-expressed MDMX, H shows cells with 2 times over-expressed MDM2 and 10 times over-expressed MDMX, I shows cells with 5 times over-expressed MDM2, J shows cells with 5 times over-expressed MDM2 and 2 times over-expressed MDMX, K shows cells with 5 times over-expressed MDM2 and 5 times over-expressed MDMX, L shows cells with 5 times over-expressed MDM2 and 10 times over-expressed MDMX, M shows cells with 10 times over-expressed MDM2, N shows cells with 10 times over-expressed MDM2 and 2 times over-expressed MDMX, O shows cells with 10 times over-expressed MDM2 and 5 times over-expressed MDMX, P shows cells with 10 times over-expressed MDM2 and 10 times over-expressed MDMX.